THE UNIVERSITY OF ALBERTA

Release Form

NAME OF AUTHOR Praveer Asthana

TITLE OF THESIS An Inverse Method in One Dimension

DEGREE FOR WHICH THESIS WAS PRESENTED   M.Sc.

YEAR THIS DEGREE GRANTED 1982

THE UNIVERSITY OF ALBERTA

AN INVERSE METHOD IN ONE DIMENSION

BY

Ⓒ PRAVEER ASTHANA

A THESIS

SUBMITTED TO THE FACULTY OF GRADUATE STUDIES AND RESEARCH

IN PARTIAL FULFILMENT OF THE REQUIREMENTS FOR THE DEGREE

OF MASTER OF SCIENCE

DEPARTMENT OF PHYSICS

EDMONTON, ALBERTA

FALL, 1982

THE UNIVERSITY OF ALBERTA

FACULTY OF GRADUATE STUDIES AND RESEARCH

The undersigned certify that they have read, and recommend to
the Faculty of Graduate Studies and Research for acceptance, a thesis
entitled AN INVERSE METHOD IN ONE DIMENSION submitted by PRAVEER ASTHANA
in partial fulfilment of the requirements for the degree of Master of
Science.

ABSTRACT

Given a sequence of bound-state energies, the inverse Gel'fand-Levitan theory for the one-dimensional Schrödinger equation enables us to uniquely construct a symmetric reflectionless potential which supports those bound-states. A question of interest is that if the bound-state energies belong to a symmetric, but not necessarily reflectionless, potential then how closely does the reflectionless potential simulate the actual one?

This method, if reliable, gives us a means of approximately constructing a symmetric 'non-confining well' in one dimension from its bound-state spectrum. With the inclusion of an additional parameter, 'E_0', this technique can also be used for 'locally' approximating a symmetric 'confining' potential in one dimension.

In order to test the reliability of this technique, we apply it to some known symmetric potentials (confining and non-confining) in one dimension. We also calculate the reflection coefficients of the actual potentials (of the 'local' non-confining counterparts in the case of the confining ones) as a function of momentum and look for some 'favourable' (or 'unfavourable') systematics towards this end.

In conclusion, the reflectionless potential simulates the rough qualitative features of the actual potential quite well. Within this perspective, the technique survives the tests.

ACKNOWLEDGEMENTS

It is a great pleasure to thank Dr. A.N. Kamal for suggesting this problem to me and for his immense patience and valuable guidance during the course of this work.

My sincere thanks to Dr. F.A. Baragar (Department of Mathematics, The University of Alberta) who proved a lemma for us (reported in Appendix A of this thesis) and paved the way out of a 'combinatorics' jungle'.

I owe a deep gratitude to Mr. R. Teshima, Programming Analyst at the Theoretical Physics Institute, for his enormous help during the course of this work. Apart from the aspects of computer programming, his striking command over the mathematical functions and quantum mechanical problems was of great help. It is difficult for me to conceive of this work without his ever-willing and ever-smiling help.

I wish to thank my fellow graduate student, Mr. V. Gudmundsson, for showing me a treasure-chest of one-dimensional problems. His familiarity with this topic, though in a different context, led to many fruitful discussions. Thanks to Dr. L. Pandey for his help in detecting some of the typographical errors.

It goes beyond words to express my thanks to Baba, Amma, Neeli and Meeti, for providing me with all the moral strength which I have. It would have been impossible for me to live here and do the work at peace without their constant encouragement.

My earnest thanks to Ms. Georgette Jolicoeur, who kindly consented to undertake the arduous task of typing this thesis. It is by

her grace that this thesis is in a readable form before us.

And, finally, it is imperative for me to register the sweet memories of Dada who left for heavenly abode to join Dadi during the course of this work; and of Nani who, very recently, succumbed to death after having braved it for ten long years - all of them leaving a void of unique affection which will, perhaps, never be filled again.

TABLE OF CONTENTS

LIST OF TABLES

LIST OF FIGURES

1. INTRODUCTION

The 'November revolution', even in the winter of 1974, had made things hum in High-Energy Physics. A new particle ψ/J (with a mass of 3.096 GeV) was discovered at the Brookhaven National Laboratory in the study of the reaction [1]

$$p + Be \rightarrow (e^+e^-) + \text{anything}$$
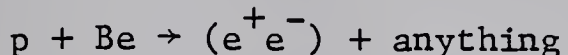
and almost simultaneously at SLAC [2] in the reaction

$$e^+e^- \rightarrow \text{hadrons} .$$
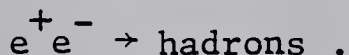
Its companion particle ψ' (3.686 GeV) was almost immediately spotted at SLAC [3]. Amidst growing theoretical expectations, it confirmed the need for the introduction of a fourth 'c(*charm*)-quark' in the description of hadronic matter. It was accepted, almost immediately, that ψ and ψ' were different energy states of a system made up of a c-quark and a $\bar{c}$-antiquark. Since their discovery in November 1974, a rather satisfactory spectrum of $c\bar{c}$ bound-states has been unfolded [4-7]. A recently reported spectrum is being tabulated in Table 1.1 [4,5].

The discovery of $c\bar{c}$ states stimualted the quest for such bound-systems of quarks with still newer 'flavours'. In the spring of 1977, barely two and a half years after the entry of ψ to the hadronic world, another particle 'upsilon (T)' was discovered at Fermilab [8,9] in the reaction

$$p + N \rightarrow (\mu^+ + \mu^-) + \text{anything}.$$
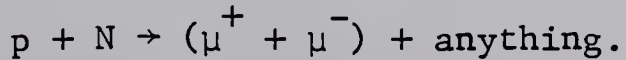
Almost immediately, it was found to be accompanied by another partner T' [10]. It has been a field of intense experimentation since then.

Table 1.1. *Charmonium States*

State	Mass (MeV)
η_c	2978 ± 4
ψ	3096.9 ± 0.1
χ_0	3412 ± 5
χ_1	3508.4 ± 4
χ_2	3553.9 ± 4
η_c'	3592 ± 5
ψ'	3686 ± 0.2

Table 1.2. *Bottomonium States*

State	Mass (MeV)
Υ	9459 ± 10
$\Upsilon' - \Upsilon$	560 ± 3
$\Upsilon'' - \Upsilon$	889 ± 4
$\Upsilon''' - \Upsilon$	1114 ± 5

Note: The numbers tabulated above are being quoted from a very recent paper. The reference is: K.J. Miller and M.G. Olsson, Phys. Rev. D25 *(1982) 2383.*

So far four companions of Υ have been detected experimentally [5,11] as shown in Table 1.2. In much the same way as ψ and ψ', these particles have been interpreted as different energy states of a bound-system of a new quark, 'b(*bottom*)' and its antiquark, $\bar{b}$.

As the $c\bar{c}$ and $b\bar{b}$ systems resemble positronium, in the sense of being a bound state of a particle and its antiparticle, they are known as the "charmonium' and 'bottomonium' respectively. The generic name 'quarkonium' has been assigned to a system of this kind.

It is enough of a testimony of the significance of the $c\bar{c}$- and $b\bar{b}$-systems that they have attracted special attention in a medley of hundreds of mesons. What is so fascinating about them? Let us consider the $c\bar{c}$-system for instance. It is a very heavy meson built up of two very heavy quarks. The binding energy available to the quarks is very small compared to their mass. So, it is a system which can be analyzed using the tools of the usual non-relativistic quantum mechanics, unlike the case of the systems made up of lighter quarks. The situation is still better and more promising in bottomonium as it is still heavier in mass. To highlight this latitude in dealing with these particles, people have called these systems as the "hydrogen-atoms of strong-interaction physics [12]". It is worthwhile to acknowledge another remark [7]: "The discovery of charm marks the beginning of quark chemistry".

At the core of this enthusiasm is the hope to unravel the nature of interquark-potential using simple non-relativistic quantum techniques on these systems. Since the discovery of charmonium in 1974, a

lot of effort has gone into this direction. These efforts were further invigorated by the discovery of bottomonium in 1977. It still remains the motivation for a very active phenomenology.

The majority of the work done in this direction can be broadly classified into two categories. In the first case, guided by theoretical suggestions, one assumes a specific form of spherically symmetric static potential. This consists of some free parameters. One then tries to calculate the level schemes and other known relevant quantities using the Schrödinger equation. Fitting these to the known spectrum and quantitites, one fixes the parameters. There is a whole variety of such potentials which do the job [6,13-21]. With certain forms of potential, e.g. the power law potentials, the Schrödinger equation dictates simple scaling laws for many quantities of interest like level spacings, decay widths, etc. This is the topic of interest in the second category. By comparing the predicted and observed systematics in these quantities one can fix the details of the potential or, at least, establish some bounds on its characteristics. In addition to these, many general quantum mechanical and semi-classical results have also been used to extract information regarding the interquark-potential from the available experimental data [6,20-35].

What one has to realize is that in all such calculations, one has to assume some kind of a potential - no matter how general it may be - to start with. It will be, thus, highly desirable and satisfying to have a method which can give us the 'confining' interquark potential straight from the measured quantities. The measured quantities are the bound-state energies and the square of the bound-state wavefunctions

at origin which are known from the leptonic decay widths [6,20]. This

defines an *inverse quantum-mechanical problem.*

Such aspirations are not very recent in the history of physics.

Determination of a molecular potential from its bound-state spectrum

using WKB inversion techniques dates back to the late 1920's and early

'30's [36-44]. An application of these techniques to the present prob-

lem will require that the bound-state energy E_n be considered as a

continuous function of the principal quantum number 'n' and the deri-

vative (dE_n/dn) be known as an input [20,33,45]. This information is

not available to us. Moreover, the known energy levels are so few in

number that a polynomial fit to E_n as a function of n by the standard

numerical methods will not be highly dependable [33]. In the present

context, therefore, one needs a different method to achieve this goal.

Quigg, Rosner and Thacker (QRT) came forward with an ingenious

suggestion [45-47]. They considered the n^3S_1 levels of the quarkonium.

The well-known correspondence between the radial Schrödinger equation

with $\ell = 0$ and the one-dimensional Schrödinger equation, then, tells us

that these are nothing but the odd-parity levels of a symmetric poten-

tial in one dimension. The square of the n^3S_1 wavefunction at the

origin, $|\Psi_n(o)|^2$, can also be related to the odd-parity wavefunction in

one dimension. ψ_{2n}, by the well-known result [20,46,47]

$$|\Psi_n(o)|^2 = \frac{1}{2\pi} |\psi'_{2n}(o)|^2 \qquad (1.1)$$

where the prime denotes the derivative with respect to 'x'. QRT's idea

was to look for an inverse method for the one-dimensional Schrödinger

equation which can uniquely reconstruct a symmetric potential from its

odd-parity bound-state energies and the slopes of the odd-parity wave-functions at the origin.

In fact, they dug out of the literature, a modest and practicable way. It has been known for a long time that a reflectionless potential can be uniquely constructed in terms of 2N parameters, where N is the number of bound states it can support [45,47,49-56]. N of these parameters are the bound-state energies $E_n{}' = -\kappa_n^2$. If one demands, in addition, that the potential be symmetric, i.e.

$$V(x) = V(-x) \tag{1.2}$$

then the other N parameters A_n also get related to the N bound-state energies in the following way [45,47]

$$\frac{A_n}{2\kappa_n} = \prod_{m \neq n} \left| \frac{\kappa_m + \kappa_n}{\kappa_m - \kappa_n} \right| . \tag{1.3}$$

The symmetric reflectionless potential is given by [45,47,49]

$$V(x) = -2 \frac{d^2}{dx^2} \{\ln \det (I + \hat{A})\} \tag{1.4}$$

I is the N×N unit matrix and $\hat{A}$ is the matrix given by

$$\hat{A} = A_n^{1/2} A_\nu^{1/2} \frac{e^{(\kappa_n + \kappa_\nu)x}}{(\kappa_n + \kappa_\nu)} . \tag{1.5}$$

The normalized bound-state wavefunctions of this potential are given by

$$\psi_n(x) = \frac{1}{A_n^{1/2} e^{\kappa_n x}} \frac{\det(I + \hat{A})^{(n)}}{\det(I + \hat{A})} \tag{1.6}$$

where $(I + \hat{A})^{(n)}$ is the matrix $(I + \hat{A})$ with its nth column differentiated once with respect to 'x'. Thus, we can reconstruct a symmetric reflec-

tionless potential in one dimension only from its bound-state spectrum.

However, this method in its present form, is still not suf-
ficient to serve the purpose in the context of the quarkonium. In a
quarkonium problem, one has to approximate a 'confining' potential
for which the whole edifice of scattering theory breaks down. It has
an infinite number of bound states and no scattering states at all.
The last of QRT's suggestions was to remove this deadlock. According
to them, one should try to construct a N bound-state approximation
$V_N(x)$ to the confining potential $V(x)$, where $[V_N(x) - E_o]$ is a reflec-
tionless potential supporting N bound-states at the energies
$-\kappa_n^2 = -E_o + E_n$. Here E_n is the nth bound state energy of the confining
potential and E_o is a parameter which defines the zero of energy.
There is no physical reasoning which will enable us to fix this para-
meter uniquely. It, thus, gives rise to an E_o - *ambiguity*. However,
it can lie in the range

$$E_N < E_o < E_{N+1} \ .$$ (1.7)

Increasing N in steps from $N = 1$, one can then successively build up
'local approximations' to the confining potential. QRT carried out
such a local construction of the harmonic oscillator, the linear
potential and the infinite square well. Their numerical experiments
by varying E_o in its allowed interval showed that a consistent choice
of

$$E_o = \frac{1}{2} (E_N + E_{N+1})$$ (1.8)

gives extremely good agreement between the confining potential and the
local reflectionless approximation $V_N(x)$. In fact, the approximation

seemed to converge to the actual potential 'locally' as N became
larger [45,47].

In the application of this technique to the actual three-
dimensional inverse problem, the odd parity levels $\kappa_2, \kappa_4, \ldots$ of the
corresponding symmetric potential in one dimension are given by the
energy levels of the three-dimensional potential. A knowledge of the
slopes of the odd-parity wave functions at the origin then yields
simultaneous equations for the 'unphysical' even-parity levels $\kappa_1, \kappa_3, \ldots$
via eqn. (1.6). The solutions can be obtained by numerical methods
[46,47,48]. Thus one has all the bound-states of a symmetric poten-
tial in one-dimension. Using the inverse technique outlined above,
one can then approximate it by a reflectionless potential. Such an
application, in the context of quarkonium, was undertaken in a prac-
tical way by QRT. They were able to obtain the charmonium and the
bottomonium potentials [46]. They also used such a technique to in-
vestigate the 'flavour-independence' of the interquark potential [48].

Quarkonia are not the only systems where such an inversion
might be desired. The most attractive feature of this technique is
that it gives us a direct, though approximate, information regarding
the potential from a few bound-state energies. Such a technique can,
thus, have a much wider applicability. These handsome prospects were
precisely the motivation for further studying this technique in this
thesis. The task undertaken in this thesis is to test the reliability
of this technique by applying it to a larger variety of known symmetric
potentials in one dimension. In Chapter 2 we develop the formal as-
pects of this technique. Chapter 3 is then devoted to the applications.

It was realized that confining potentials are not very clean cases to serve as tests of this technique. There is an inherent, but unavoidable, artificiality involved in translating the pure bound-state problem of a confining potential to a scattering problem. This technique, in its own right, is applicable only to 'local' scattering (non-confining) potentials. Moreover, not all the potentials of interest, in general, are confining. So, one of the tasks undertaken in this thesis is to estimate some local symmetric potentials in one dimension by the corresponding reflectionless potentials using this technique. Since we are, in general, approximating a reflecting potential by a reflectionless one, it would be interesting to calculate its reflection coefficient and look for some systematics in its behaviour as a function of momentum which suggest a close agreement between the actual and the estimated potentials. Section 3.1 is devoted to this task.

In Section 3.2 we estimate some confining potentials using the QRT prescription.

Section 3.3 is devoted to a discussion concerning the convergence of the reflectionless approximation to the actual reflecting potential. Our aim is to try to unravel various factors which affect the convergence, both 'favourably' and 'unfavourably'.

Chapter 4 concludes this work with a critical discussion of the results obtained; it weighs the enthusiasm regarding the prospects of this technique against the skepticism.

2. THE TECHNIQUE AND ITS NUMERICAL TEST

In this chapter, we first briefly review the Gel'fand–Levitan formalism of inverse scattering in one dimension. Then we derive the technique for approximating a symmetric potential by a symmetric reflectionless potential having the same bound-state spectrum. Finally, we test this technique by applying it to a known symmetric reflectionless potential in one dimension.

2.1 (DIRECT) SCATTERING IN ONE DIMENSION

2.1.1 One-dimensional Schrödinger Equation and the Fundamental Solutions.

We start with the one-dimensional Schrödinger equation ($\hbar = 2m = 1$)

$$\frac{d^2 u(x,k)}{dx^2} + [k^2 - V(x)]u(x,k) = 0 \quad . \tag{2.1}$$

Here $u(x,k)$ is the wavefunction, $V(x)$ is the potential and $k^2 (=E)$ is the energy of the particle. The variable x is defined on the infinite interval, $-\infty < x < \infty$.

If the potential is localized, i.e., if

$$V(x) \to 0 \qquad \qquad \text{as } |x| \to \infty \tag{2.2}$$

then the solutions $u(x,k)$ of the Schrödinger equation will reduce to a linear combination of plane waves $e^{\pm ikx}$ at $x = \pm\infty$. It is, therefore, convenient to express all solutions of the Schrödinger equation as linear combinations of the two solutions $f_1(x,k)$ and $f_2(x,k)$ which exhibit the following large x behaviour

$$f_1(x,k) = e^{ikx} \qquad \qquad \text{as } x \to +\infty$$

$$f_2(x,k) = e^{-ikx} \qquad \qquad \text{as } x \to -\infty \tag{2.3}$$

These solutions are commonly referred to as the *fundamental solutions* of the Schrödinger equation.

2.1.2 Integral Equations for the Fundamental Solutions.

It is obvious by looking at eqn. (2.1) that explicit forms of $f_1(x,k)$ and $f_2(x,k)$ cannot be obtained unless we are given the potential $V(x)$. However, if we treat k as a complex variable, their analytic properties in the complex k-plane can be inferred from their integral forms.

Using the Green function for eqn. (2.1), we can immediately get the following integral equations for $f_1(x,k)$ and $f_2(x,k)$

$$f_1(x,k) = e^{ikx} - \frac{1}{k} \int_x^\infty dx' \sin k(x-x') V(x') f_1(x',k) \quad (2.4)$$

$$f_2(x,k) = e^{-ikx} + \frac{1}{k} \int_{-\infty}^x dx' \sin k(x-x') V(x') f_2(x',k) \ . \quad (2.5)$$

If the potential $V(x)$ is real, then we get the following two properties of $f_1(x,k)$ and $f_2(x,k)$ from their integral equations

$$\left. \begin{aligned} f_1^*(x,k) &= f_1(x,-k^*) \\ f_2^*(x,k) &= f_2(x,-k^*) \end{aligned} \right\} . \quad (2.6)$$

If, in addition, k is also real, then we get from eqn. (2.6)

$$\left. \begin{aligned} f_1^*(x,k) &= f_1(x,-k) \\ f_2^*(x,k) &= f_2(x,-k) \end{aligned} \right\} . \quad (2.7)$$

Let us now try to solve these integral equations by iteration. In eqn. (2.4), for example, we first put e^{ikx} for $f_1(x,k)$ and so on.

The resulting integrals would then be found to converge for Imk>0. It is also well-known that the resulting series for Volterra integral equations such as eqn. (2.4) and eqn. (2.5) are always uniformly convergent with respect to k [57.58]. Thus, we conclude that $f_1(x,k)$ is an analytic function in the upper half of the complex k-plane. In exactly the same way, $f_2(x,k)$ will also be an analytic function in the upper half of the complex k-plane.

2.1.3 Definitions of the Reflection and the Transmission Coefficients.

We, now, define the Wronskian of two solutions of the Schrödinger equation as

$$W[u_1;u_2] \equiv u_1'u_2 - u_1u_2' .$$ (2.8)

This definition differs from the conventional one by a minus sign. Here the prime means a differentation with respect to x.

The Schrödinger equation (2.1) does not contain the first derivative of $u(x,k)$. So, the Wronskian of any two linearly independent solutions will be independent of x but it may depend on k [59]. We can exploit this property in calculating the following useful Wronskian relations

$$W[f_1(x,k);f_1(x,-k)] = W[f_1(x,k);f_1(x,-k)]_{x=\infty} = 2ik$$ (2.9)

$$W[f_2(x,k);f_2(x,-k)] = W[f_2(x,k);f_2(x,-k)]_{x=-\infty} = -2ik.$$ (2.10)

These Wronskian relations depend, obviously, only on k. Hence, $\{f_1(x,k),f_1(x,-k)\}$ and $\{f_2(x,k),f_2(x,-k)\}$ form two sets of linearly independent solutions to the Schrödinger equation on the infinite interval. We can, thus, write

$$f_2(x,k) = c_{11}(k) f_1(x,k) + c_{12}(k) f_1(x,-k) \qquad (2.11)$$

$$f_1(x,k) = c_{21}(k) f_2(x,-k) + c_{22}(k) f_2(x,k) \quad . \qquad (2.12)$$

These two equations, as we discuss below, describe two complementary scattering situations in one dimension.

Using the asymptotic forms, eqns. (2.3), of $f_1(x,k)$ and $f_2(x,k)$ we conclude from eqn. (2.11) that it represents a wave e^{-ikx} at $x = -\infty$ and a linear combination $c_{11}(k)e^{ikx} + c_{12}(k)e^{-ikx}$ at $x = +\infty$. Therefore, this represents a scattering situation in which a wave of amplitude $c_{12}(k)$ is incident from the right on the potential $V(x)$. It is re-flected with an amplitude $c_{11}(k)$ and transmitted with an amplitude unity to $x = -\infty$. This has been drawn schematically in Figure 2.1.

Similarly, eqn. (2.12) represents a scattering situation in which a wave of amplitude $c_{21}(k)$ is incident from the left. A part $c_{22}(k)$ is reflected and a wave of unit amplitude is transmitted to $x = +\infty$. Figure 2.2 represents this scattering from the left, schematically.

The familiar *reflection coefficient*, $R(k)$, and the *transmission coefficient*, $T(k)$, for waves of unit incident amplitude can now be de-fined as follows

$$R_R(k) = \frac{c_{11}(k)}{c_{12}(k)} \qquad ; \; T_R(k) = \frac{1}{c_{12}(k)} \qquad (2.13)$$

$$R_L(k) = \frac{c_{22}(k)}{c_{21}(k)} \qquad ; \; T_L(k) = \frac{1}{c_{21}(k)} \qquad (2.14)$$

where the subscripts R and L refer to the scattering of waves incident from the right and the left respectively.
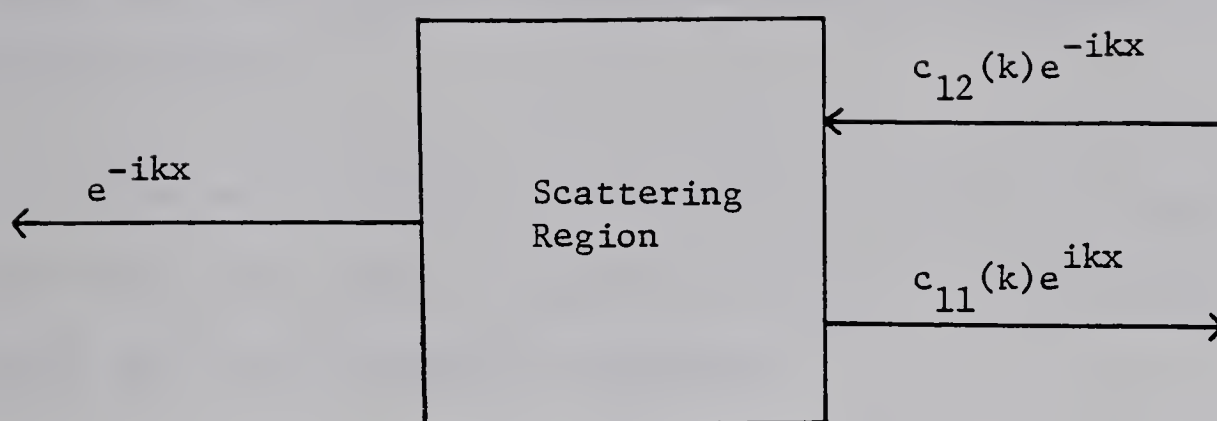
Fig. 2.1. *A wave incident from the right.*
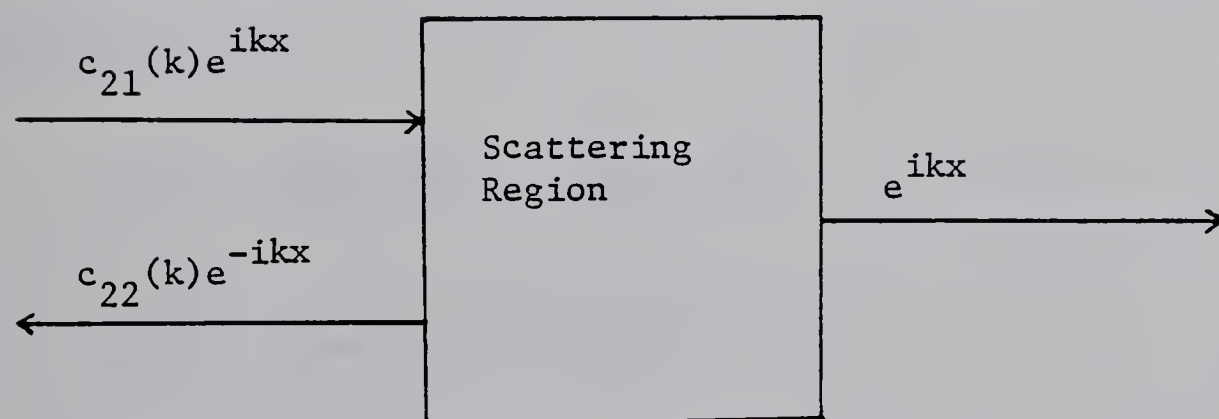
Fig. 2.2. *A wave incident from the left.*

2.1.4 Relationships between these Coefficients.

A number of relationships exist between the various coefficients defined in the previous section. It is particularly illuminating to establish them for some of those relations are statements of important physical realities.

Let us substitute $f_1(x,k)$ from eqn. (2.12) into eqn. (2.11) and equate the coefficients of $f_2(x,k)$ and $f_2(x,-k)$ on both the sides. We finally get the following two relations

$$1 = c_{11}(k)\ c_{22}(k) + c_{12}(k)\ c_{21}(-k)$$

$$0 = c_{11}(k)\ c_{21}(k) + c_{12}(k)\ c_{22}(-k)\ . \tag{2.15}$$

Similarly, if we substitute $f_2(x,k)$ from eqn. (2.11) into eqn. (2.12) and equate the coefficients of $f_1(x,k)$ and $f_1(x,-k)$ on both the sides, we get

$$1 = c_{21}(k)\ c_{12}(-k) + c_{22}(k)\ c_{11}(k)$$

$$0 = c_{21}(k)\ c_{11}(-k) + c_{22}(k)\ c_{12}(k) \qquad . \tag{2.16}$$

Equations (2.9) to (2.12) enable us to establish the following expressions for c_{ij}'s

$$c_{11}(k) = \frac{1}{2ik}\ W[f_2(x,k);f_1(x,-k)] \tag{2.17}$$

$$c_{22}(k) = \frac{1}{2ik}\ W[f_2(x,-k);f_1(x,k)] \tag{2.18}$$

$$c_{12}(k) = c_{21}(k) = \frac{1}{2ik}\ W[f_1(x,k);f_2(x,k)]. \tag{2.19}$$

Combining the expressions for $T_L(k)$ and $T_R(k)$ with eqn. (2.19), we

immediately conclude that

$$T_L(k) = T_R(k) \quad . \tag{2.20}$$

This is commonly referred to as the *reprocity relation*.

In the event when $V(x)$ and k are real i.e. when eqn. (2.7) holds good, one can show that

$$c_{12}(-k) = c_{12}^{*}(k) \tag{2.21}$$

and

$$c_{11}(k) = -c_{22}^{*}(k) = -c_{22}(-k) \quad . \tag{2.22}$$

Using eqn. (2.21) and eqn. (2.22) in eqn. (2.15) and eqn. (2.16), we get

$$\left| c_{12}(k) \right|^2 = 1 + \left| c_{11}(k) \right|^2 = 1 + \left| c_{22}(k) \right|^2 \quad . \tag{2.23}$$

By the definitions of the reflection and transmission coefficients, eqn. (2.23) implies

$$1 = \left| T(k) \right|^2 + \left| R_R(k) \right|^2 = \left| T(k) \right|^2 + \left| R_L(k) \right|^2 \tag{2.24}$$

where, in view of the reciprocity relation (2.20), we have used $T(k)$ for both the left and right transmission coefficients. Eqn. (2.24) is the statement of the *law of conservation of energy*.

If one starts with the definitions (2.13) and (2.14) and uses the relationships (2.21) and (2.22), one gets the following equations

$$R_R(k) \, T(-k) + R_L(-k) \, T(k) = 0 \quad . \tag{2.25}$$

Eqn. (2.25) is commonly referred to as the *phase law*.

It is also a simple matter to verify, using eqn. (2.21) and

eqn. (2.22) that

$$R_L^*(-k) = R_L(k)$$

$$R_R^*(-k) = R_R(k) \tag{2.26}$$

2.1.5. A Bridge between these Coefficients and the S-Matrix in One Dimension.

We have already remarked that remote from a localized potential any solution, $u(x,k)$, of the Schrödinger equation in one dimension, can be written as a linear combination of the plane waves $e^{\pm ikx}$. Therefore, we have [60]

$$\lim_{x \to +\infty} \{A_+ e^{ikx} + B_+ e^{-ikx} - u(x,k)\} = 0 \tag{2.27}$$

and

$$\lim_{x \to -\infty} \{A_- e^{ikx} + B_- e^{-ikx} - u(x,k)\} = 0 \tag{2.28}$$

We define an *incoming wave* as a right moving wave at $x = -\infty$ and a left moving wave at $x = +\infty$. Similarly an *outgoing wave* is a right moving wave at $x = +\infty$ or left moving wave at $x = -\infty$. So, the incoming parts of $u(x,k)$ are $A_- e^{ikx}$ and $B_+ e^{-ikx}$ whereas the outgoing parts of $u(x,k)$ are $A_+ e^{ikx}$ and $B_- e^{-ikx}$.

We can further define a two-dimensional vector space of column vectors. The first component of each vector represents the amplitude of the right moving part and the second represents the left moving part. So, the incoming wave vector is

$$\begin{pmatrix} A_- \\ B_+ \end{pmatrix}$$

whereas the outgoing wave vector is

$$\begin{pmatrix} A_+ \\ B_- \end{pmatrix} .$$

Right from the definitions of the reflection and the transmission co-efficients, it is obvious that a relationship must exist between these two vectors. To establish that, note that the incoming wave vector has a wave of amplitude A_- incident from $x = -\infty$. This will get reflected with an amplitude $R_L(k)A_-$ and transmitted with an amplitude $T_L(k)A_-$. So, this will give rise to an outgoing wave $R_L(k)A_-$ at $x = -\infty$ and another $T_L(k)A_-$ at $x = +\infty$. Similarly, we have a wave of amplitude B_+ incident from the right. This will give rise to an outgoing wave of amplitude $R_R(k)B_+$ to the right and another one of amplitude $T_R(k)B_+$ to the left. So, the outgoing wave vector has a component $[T_L(k)A_- + R_R(k)B_+]$ moving towards $x = +\infty$ and another component $[R_L(k)A_- + T_R(k)B_+]$ moving towards $x = -\infty$. In other words,

$$\begin{pmatrix} A_+ \\ B_- \end{pmatrix} = \begin{pmatrix} T_L(k)A_- + R_R(k)B_+ \\ R_L(k)A_- + T_R(k)B_+ \end{pmatrix}$$

i.e.

$$\begin{pmatrix} A_+ \\ B_- \end{pmatrix} = S \begin{pmatrix} A_- \\ B_+ \end{pmatrix} \qquad (2.29)$$

where S is a 2×2 matrix given by

$$S \equiv \begin{pmatrix} T_L(k) & R_R(k) \\ R_L(k) & T_R(k) \end{pmatrix} . \qquad (2.30)$$

We can alternatively write eqn. (2.29) as

$$u^{(+)}(x,k) = S\, u^{(-)}(x,k) \tag{2.31}$$

where $u^{(+)}(x,k)$ and $u^{(-)}(x,k)$ stand for the outgoing and incoming parts of the wave function respectively. The matrix S is the so-called *S-matrix*.

This establishes the correspondence between the reflection and the transmission coefficients and the more common description of the scattering theory in terms of the S-matrix. It is obvious that the relations (2.24) and (2.25), derived in the previous section, confirm the desired unitarity of the S-matrix.

2.1.6 Bound-State Poles of the Transmission Coefficient.

The potential V(x) can, in general, support bound states. Where does this characteristic of the potential get reflected? This is, clearly, a vital information for the problem we are concerned with. And, in this section, we explore this question.

Let us start by investigating the analytic structure of the transmission coefficient in the complex k-plane. We first prove that the poles of the transmission coefficient in the upper half-plane lie on the positive imaginary axis. By eqn. (2.13) and eqn. (2.14), it is obvious that we are interested in the zeros of $c_{12}(k)$. By eqn. (2.24), which holds only for real k, it is evident that $c_{12}(k)$ can never vanish on the real k-axis, i.e.

$$c_{12}(k) \neq 0 \qquad\qquad \text{if } \mathrm{Im}\,k = 0 \ . \tag{2.32}$$

So, the zero of $c_{12}(k)$ must lie off the real axis.

Let k_o be the location of one of the poles. The Schrödinger equation gives

$$u'' + k_o^2 u = V(x)u \qquad (2.33)$$

and its complex conjugate dictates

$$u^{*''} + k_o^{*2} u^* = V(x)u^* \qquad (2.34)$$

where we have *assumed* that $V(x)$ is real. $u(x,k)$ may be either of the two fundamental solutions $f_1(x,k)$ or $f_2(x,k)$ and $u^*(x,k)$ is the corresponding complex conjugate. Multiplying eqn. (2.33) by u^* and eqn. (2.34) by u, and subtracting

$$(u^* u'' - u^{*''} u) + (k_o^2 - k_o^{*2})u^* u = 0 . \qquad (2.35)$$

Integrating over all x

$$-(k_o^2 - k_o^{*2}) \int_{-\infty}^{\infty} dx \ |u|^2 = |(u^* u' - uu^{*'})|_{-\infty}^{\infty} . \qquad (2.36)$$

The right hand side of eqn. (2.36) is either of the two Wronskians in eqn. (2.10), both of which are independent of x. So, it is zero. Therefore,

$$(k_o^2 - k_o^{*2}) \int_{-\infty}^{\infty} dx \ |u|^2 = 0 . \qquad (2.37)$$

If we write

$$k_o = k_{or} + ik_{oi} \qquad (2.38)$$

then eqn. (2.37) becomes

$$k_{or} k_{oi} \int_{-\infty}^{\infty} dx \ |u|^2 = 0 . \qquad (2.39)$$

Thus, if $k_{oi} \neq 0$, then $k_{or} = 0$, because the integral is a positive and

finite quantity (we prove this claim below) when $\text{Im} k > 0$.

If $c_{12}(k_o) = 0$, then from eqn. (2.11) and eqn. (2.12)

$$f_2(x,k_o) = c_{11}(k_o) \, f_1(x,k_o)$$

$$f_1(x,k_o) = c_{22}(k_o) \, f_2(x,k_o) \quad . \tag{2.40}$$

Hence, $c_{11}(k_o)$ and $c_{22}(k_o)$ are related by

$$c_{11}(k_o) = \frac{1}{c_{22}(k_o)} \quad . \tag{2.41}$$

So, the two solutions are linearly dependent. From the asymptotic forms of $f_1(x,k)$ and $f_2(x,k)$ we infer that if $\text{Im} k_o > 0$, then $f_1(x,k_o)$ exponentially decreases at $x = +\infty$ while the solution $f_2(x,k_o)$ behaves likewise at $x = -\infty$. Thus, for $k_o = i\kappa_o$, we have a solution which is quadratically integrable on the entire axis [55]. The characteristic exponential decay shows that $f_1(x,i\kappa_o)$, or equivalently $f_2(x,i\kappa_o)$, corresponds to a bound-state solution.

2.1.7. The Bound-State Wavefunctions and their Normalizations.

With the results of the preceding section at our disposal, we know that if the potential $V(x)$ supports N bound states at $k = i\kappa_n$ ($n = 1,2,\ldots,N$), then the transmission coefficient has N poles on the positive imaginary axis at $k_n = i\kappa_n$ ($n = 1,2,\ldots,N$). The nth bound-state wavefunction is given by $f_1(x,i\kappa_n)$ or $f_2(x,i\kappa_n)$ with the relation

$$f_2(x,i\kappa_n) = c_{11}(i\kappa_n) \, f_1(x,i\kappa_n) \tag{2.42}$$

where $c_{11}(i\kappa_n)$ and $c_{22}(i\kappa_n)$ are related by

$$c_{11}(i\kappa_n) = \frac{1}{c_{22}(i\kappa_n)} \tag{2.43}$$

Let us now try to derive expressions for the normalization constants

of $f_1(x,i\kappa_n)$ and $f_2(x,i\kappa_n)$.

As the first step, we calculate $\dot{c}_{12}(k_n)$ defined by

$$\dot{c}_{12}(k_n) \equiv \frac{dc_{12}(k)}{dk}\bigg|_{k=k_n} . \tag{2.44}$$

Using eqn. (2.19), we get

$$\dot{c}_{12}(k) = -\frac{1}{2ik^2} W[f_1(x,k);f_2(x,k)] + \frac{1}{2ik} \{W[\dot{f}_1;f_2] + W[f_1;\dot{f}_2]\} .$$

By virtue of eqn. (2.42), the first term on the right-hand side vanishes

at $k = k_n$ and the second reduces to

$$\dot{c}_{12}(k_n) = \frac{1}{2ik_n} \{c_{11}(k_n) W[\dot{f}_1;f_1] + c_{22}(k_n) W[f_2;\dot{f}_2]\}. \tag{2.45}$$

We have to now evaluate the Wronskians on the right-hand side of eqn.

(2.45). Towards this end, we start by writing the Schrödinger equa-

tions corresponding to $f_1(x,k)$ and $f_1(x,k_n)$

$$f_1''(x,k) + k^2 f_1(x,k) = V(x) f_1(x,k) \tag{2.46}$$

$$f_1''(x,k_n) + k_n^2 f_1(x,k_n) = V(x) f_1(x,k_n) . \tag{2.47}$$

Multiplying eqn. (2.46) by $f_1(x,k_n)$ and eqn. (2.47) by $f_1(x,k)$ and then

subtracting one equation from the other

$$\frac{d}{dx} [f_1'(x,k_n)f_1(x,k) - f_1'(x,k)f_1(x,k_n)] - (k^2 - k_n^2)f_1(x,k)f_1(x,k_n)=0. \tag{2.48}$$

Differentiating eqn. (2.48) with respect to k and then putting $k = k_n$,

$$\frac{d}{dx} W[f_1(x,k_n);\dot{f}_1(x,k_n)] = 2k_n[f_1(x,k_n)]^2 . \tag{2.49}$$

Integrating eqn. (2.49) from x to $+\infty$, we get

$$W[f_1(x',k_n);\dot{f}_1(x',k_n)]\Big|_x^\infty = 2k_n \int_x^\infty dx' [f_1(x',k_n)]^2 \quad . \quad (2.50)$$

It is obvious from eqn. (2.3) that for $\mathrm{Im}k_n > 0$, $f_1(x,k_n) \to 0$ as $x \to +\infty$.
Hence, the Wronskian in eqn. (2.50) will vanish at $x = +\infty$ yielding

$$W[f_1(x,k_n);\dot{f}_1(x,k_n)] = -2k_n \int_x^\infty dx' [f_1(x',k_n)]^2 \quad . \quad (2.51)$$

Following exactly the same reasoning for $f_2(x,k_n)$, we get

$$W[f_2(x,k_n);\dot{f}_2(x,k_n)] = 2k_n \int_{-\infty}^x dx' [f_2(x',k_n)]^2 \quad . \quad (2.52)$$

Substituting eqn. (2.51) and eqn. (2.52) into eqn. (2.45), we get

$$\dot{c}_{12}(k_n) = \frac{1}{i} \int_{-\infty}^\infty dx\, \dot{f}_1(x,k_n) \dot{f}_2(x,k_n) \quad . \quad (2.53)$$

As an immediate corollary to eqn. (2.53), we can see that the
zeros of $c_{12}(k)$ for a real potential can only be simple. First of all,
from the integral equations for $f_1(x,k)$ and $f_2(x,k)$ we see that for
real potential and $\mathrm{Im}k_n > 0$, $f_1(x,k_n)$ and $f_2(x,k_n)$ are real. Now, eqn.
(2.53) can be written as,

$$\dot{c}_{12}(k_n) = -ic_{11}(k_n) \int_{-\infty}^\infty dx [f_1(x,k_n)]^2 \quad .$$

Since $f_1(x,k_n)$ is real, the integrand on the right hand side is positive
and the integral is non-zero. As we will see below, the normalization
constant of $f_1(x,k_n)$ is proportional to $c_{11}(k_n)$. So, $c_{11}(k_n) \neq 0$. Hence,
$\dot{c}_{12}(k_n) \neq 0$. This implies that the zeros of $c_{12}(k)$, or equivalently, the
poles of the transmission coefficient, have to be simple for a real po-
tential.

Eqn. (2.53) leads us to the residue of the transmission coefficient at $k = k_n$, viz.

$$i\gamma_n \equiv \text{Residue of } \left[\frac{1}{c_{12}(k)}\right]_{k=k_n} = \frac{1}{\dot{c}_{12}(k_n)} = \frac{i}{\int_{-\infty}^{\infty} dx\, f_1(x,k_n) f_2(x,k_n)} \quad . \tag{2.54}$$

Using eqn. (2.42) and eqn. (2.43), we obtain from eqn. (2.54), the following two relations

$$\gamma_n \int_{-\infty}^{\infty} dx\, f_1(x,k_n) f_2(x,k_n) = 1 = \int_{-\infty}^{\infty} dx\, \gamma_n c_{11}(k_n)[f_1(x,k_n)]^2 \tag{2.55}$$

and

$$\gamma_n \int_{-\infty}^{\infty} dx\, f_1(x,k_n) f_2(x,k_n) = 1 = \int_{-\infty}^{\infty} dx\, \gamma_n c_{22}(k_n)[f_2(x,k_n)]^2 \tag{2.56}$$

It is evident from eqn. (2.55) and eqn. (2.56) that $[\gamma_n c_{11}(k_n)]^{1/2}$ and $[\gamma_n c_{22}(k_n)]^{1/2}$ are the normalization constants for the bound-state wavefunctions $f_1(x,k_n)$ and $f_2(x,k_n)$, respectively.

Also, since $f_1(x,k_n)$ and $f_2(x,k_n)$ are real, it follows from eqn. (2.54) that γ_ℓ is real. We can write the normalization constants as:

$$A_{Rn} \equiv \gamma_n c_{11}(k_n) = -i \frac{c_{11}(k_n)}{\dot{c}_{12}(k_n)} = \left[\int_{-\infty}^{\infty} dx[f_1(x,k_n)]^2\right]^{-1} \tag{2.58}$$

and

$$A_{Ln} \equiv \gamma_n c_{22}(k_n) = -i \frac{c_{22}(k_n)}{\dot{c}_{12}(k_n)} = \left[\int_{-\infty}^{\infty} dx[f_2(x,k_n)]^2\right]^{-1} \quad . \tag{2.59}$$

As $f_1(x,k_n)$ and $f_2(x,k_n)$ are real, A_{Rn} and A_{Ln} are also real and positive. Using the results obtained above, one can immediately prove the following [55]

$$\gamma_n^2 = A_{Rn} A_{Ln} \quad . \qquad\qquad (2.60)$$

Proof of eqn. (2.60): We have remarked above that $c_{11}(k_n) \neq 0$ due to the normalization condition. So:

$$\text{L.H.S.} = \gamma_n^2$$

$$= \gamma_n c_{11}(k_n) \cdot \frac{\gamma_n}{c_{11}(k_n)}$$

$$= [\gamma_n c_{11}(k_n)][\gamma_n c_{22}(k_n)] \quad , \text{ from eqn. (2.40)}$$

$$= A_{Rn} A_{Ln} = \text{R.H.S.} \qquad\qquad QED.$$

2.2 INVERSE SCATTERING IN ONE DIMENSION

2.2.1. The Prelude: A Representation of the Fundamental Solutions and the Potential in terms of a Function K(x,y) Characterizing the Scattering.

We have been considering the time-independent Schrödinger equation so far. The solutions of this equation are monochromatic waves. The scattering of an incident pulse can then be constructed by a Fourier synthesis of the results of steady-state calculations. However, there are some advantages of considering the scattering of pulses directly in the time domain [56,60]. Firstly, we are led to a new representation for the fundamental solutions, $f_1(x,k)$ and $f_2(x,k)$, in terms of a function $K(x,y)$ characterizing the scattering and secondly, we are able to relate the scattering potential $V(x)$ to the function $K(x,y)$. This is the main aim of this section.

The Fourier transform $u(x,t)$ of $u(x,k)$ is a transient wave

solution of the equation

$$\frac{\partial^2 u(x,t)}{\partial x^2} - \frac{1}{c^2} \frac{\partial^2 u(x,t)}{\partial t^2} - V(x) \, u(x,t) = 0 \quad . \tag{2.61}$$

Obviously, if the potential is zero or if it is localized, then remote

from the potential, eqn. (2.61), looks like

$$\frac{\partial^2 u(x,t)}{\partial x^2} - \frac{1}{c^2} \frac{\partial^2 u(x,t)}{\partial t^2} = 0 \quad . \tag{2.62}$$

An exact solution of eqn. (2.62) is $\delta(t \pm \frac{x}{c})$. However, since there is

a scattering potential $V(x)$, we would expect this delta function pulse to be

partly scattered and thus leave some sort of disturbance behind a sharp

leading edge. We, thus, write a solution to eqn. (2.61) as

$$u_2(x,t) = \delta(t + \frac{x}{c}) + c\theta(t + \frac{x}{c}) \, K_L(x,-ct) \quad . \tag{2.63}$$

Here $\theta(x)$ is the unit step function and $K_L(x,-ct)$ is the function which

carries the scattering information. Factor c is just a constant (but

has dimensions).

If we take the Fourier transform of eqn. (2.63) we get, with

$ct = x'$ and $k = \frac{\omega}{c}$,

$$U_2(x,\omega) = \int_{-\infty}^{\infty} dt \, e^{i\omega t} \, u_2(x,t)$$

$$= e^{-ikx} + \int_{-\infty}^{x} dx' \, e^{-ikx'} \, K_L(x,x'); \quad x' < x \quad . \tag{2.64}$$

It can be easily shown that $U_2(x,\omega)$ is a solution to the following equa-

tion

$$\frac{\partial^2 U_2(x,\omega)}{\partial x^2} + \left[\left(\frac{\omega}{c}\right)^2 - V(x) \right] U_2(x,\omega) = 0 \quad . \tag{2.65}$$

Also, it is obvious from eqn. (2.64) that

$$\lim_{x \to -\infty} [e^{ikx} U_2(x,\omega)] = 1 . \tag{2.66}$$

Remembering that $(\omega/c) = k$, we see that eqn. (2.65) is nothing but the time-independent Schrödinger equation (2.1). We know that $f_2(x,k)$ is a unique solution eqn. (2.65) or equivalently eqn. (2.1), with the same asymptotic form as in eqn. (2.66). Hence, it follows that $U_2(x,\omega)$ is another representation of $f_2(x,k)$

$$U_2(x,\omega) = f_2(x,k) = e^{-ikx} + \int_{-\infty}^{x} dx' \, K_L(x,x') e^{-ikx'} ; \quad x' < x . \tag{2.67}$$

Similarly, the other solution to eqn. (2.61) is

$$u_1(x,t) = \delta(t - \frac{x}{c}) + c\theta(t - \frac{x}{c}) \, K_R(x,ct) . \tag{2.68}$$

Its Fourier transform is given by

$$U_1(x,\omega) = e^{ikx} + \int_{x}^{\infty} dx' \, K_R(x,x') e^{ikx'} ; \qquad x' > x . \tag{2.69}$$

Eqn. (2.69) is again a solution of the time-independent Schrodinger equation with the asymptotic property

$$\lim_{x \to \infty} [e^{-ikx} U_1(x,\omega)] = 1 . \tag{2.70}$$

Therefore, $U_1(x,\omega)$ must be another representation of $f_1(x,k)$

$$U_1(x,\omega) = f_1(x,k) = e^{ikx} + \int_{x}^{\infty} dx' \, K_R(x,x') e^{ikx'} ; \quad x' > x. \tag{2.71}$$

These alternative representations of the fundamental solutions will be extremely useful in our discussion of the inverse problem.

As we remarked above, all scattering information is stored in the

function $K_L(x,y)$ or $K_R(x,y)$ for the left and right scattering situations respectively. We now show that the scattering potential $V(x)$ is related to $K_L(x,x')$ or $K_R(x,x')$ by a simple relation. Substituting eqn. (2.63) into eqn. (2.61), we get

$$-\delta(t+\frac{x}{c})\left[-\frac{2\partial K_L(x,-ct)}{\partial x}+\frac{2}{c}\cdot\frac{\partial K_L(x,-ct)}{\partial t}+V(x)\right]$$

$$+ c\theta(t+\frac{x}{c})\left[\frac{\partial^2 K_L(x,-ct)}{\partial x^2}-\frac{1}{c^2}\cdot\frac{\partial^2 K_L(x,-ct)}{\partial t^2}-V(x)K_L(x,-ct)\right]=0 \ .$$

$$(2.72)$$

Let us integrate eqn. (2.72) from $t=-\frac{x}{c}-\varepsilon$ to $t=-\frac{x}{c}+\varepsilon$. As $\varepsilon \to 0$, the second term on the left hand side makes no contribution. The delta function in the first term gives the following non-zero contribution

$$-2\left.\frac{\partial K_L(x,-ct)}{\partial x}\right|_{-ct=x} -2\left.\frac{\partial K_L(x,-ct)}{\partial(-ct)}\right|_{-ct=x} +V(x) = 0 \ . \quad (2.73)$$

And, obviously this relates $V(x)$ with $K_L(x,x')$ by

$$V(x) = 2\frac{d}{dx}K_L(x,x). \quad (2.74)$$

Similarly, if we substitute eqn. (2.68) in eqn. (2.61) and carry out the same calculation as above, we will get

$$V(x) = -2\frac{d}{dx}K_R(x,x) \ . \quad (2.75)$$

Thus, if we have a means of calculating $K_L(x,y)$ or $K_R(x,y)$ from the S-matrix elements, we can get the scattering potential via eqn. (2.74) or eqn. (2.75) respectively. It has been shown [55] that the potential must satisfy the following criterion for the validity of this procedure.

$$\int_{-\infty}^{\infty} dx(1+|x|)|V(x)| < \infty \ . \quad (2.76)$$

This procedure is inapplicable if the above integral diverges. So, this excludes the cases where the potential is either too singular such as $V(x) = \delta'(x)$, or too slowly converging for large values of x [56]. And, if the above criterion holds good then potentials obtained from each of the two equations (2.74) and (2.75) coincide. In fact, if we are confident about the validity of eqn. (2.76) then we need to know only $K_L(x,x')$ or $K_R(x,x')$ for the inverse procedure.

The final step in establishing an inverse technique is, therefore, to look for a relationship which can give us $K_L(x,y)$ or $K_R(x,y)$ in terms of the reflection and the transmission coefficients. This is, in fact, the *Gel'fand-Levitan Equation*.

2.2.2. The Finale: The Gel'fand-Levitan Equation for K(x,y).

This *integral equation* can be derived in a number of ways [51-53, 55,56,60]. We prefer the one using a dispersion technique [45,50]. We start by considering an analytic function

$$
u(x,k) = \begin{cases} \dfrac{1}{c_{12}(k)}\, f_1(x,k)e^{-ikx} \; ; & \mathrm{Im}\,k > 0 & (2.77a) \\[4mm] f_2^*(x,k^*)e^{-ikx} \; ; & \mathrm{Im}\,k < 0 \; . & (2.77b) \end{cases}
$$

The form in eqn. (2.77a) is dictated by the fact that $[1/c_{12}(k)]f_1(x,k)$ gives the desired scattering boundary conditions. As discussed in Section (2.1.3), this represents an incoming wave from the left with amplitude unity and transmitted and reflected waves with amplitudes $T_L(k)$ and $R_L(k)$ respectively.

Obviously, by construction, $u(x,k)$ has poles on the positive

imaginary axis corresponding to the bound-state poles of the transmission coefficient. Apart from these $u(x,k)$ has a discontinuity along the real axis. The discontinuity can be easily calculated and it turns out to be

$$\lim_{\varepsilon \to 0}[u(x,k+i\varepsilon) - u(x,k-i\varepsilon)] = R_L(k)f_2(x,k)e^{-ikx} \equiv \rho(x,k). \quad (2.78)$$

The discontinuity across the cut along the real axis is, therefore, proportional to the reflection coefficient. In fact, this was the motivation for choosing the form in eqn. (2.77b).

From the integral forms (2.4) and (2.5) for $f_1(x,k)$ and $f_2(x,k)$, we have

$$f_1(x,k) = e^{ikx} \qquad ; \; k = \pm\infty$$

$$f_2(x,k) = e^{-ikx} \qquad ; \; k = \pm\infty \qquad . \qquad (2.79)$$

Using this in eqn. (2.19), we get

$$c_{12}(k) = 1 \qquad ; \; k = \pm\infty \qquad . \qquad (2.80)$$

Therefore, it follows from eqn. (2.77) that

$$u(x,k) = 1 \qquad ; \; k = \pm\infty \qquad . \qquad (2.81)$$

We will thus construct $u(x,k)$ from its singularities using a dispersion relation normalized to unity at a subtraction point at ∞.

Let us consider $u(x,k)$ in the upper-half of the complex k-plane. We can write the dispersion integral

$$\frac{u(x,k)}{[\text{Im}\,k>0]} = \frac{1}{2\pi i} \oint_C \frac{u(x,k')dk'}{k'-k} \qquad (2.82)$$

where C is the contour shown in Figure 2.3. In the upper half-plane $u(x,k)$ has simple poles on the positive imaginary axis at $i\kappa_n (n=1,2,..,N)$ corresponding to the N bound states. Assuming, as justified above, that $u(x,k)$ goes to zero at large k, we can deform the contour C in the way shown in Figure 2.4. We can, thus, write

$$\begin{matrix} u(x,k) \\ [\text{Im}k>0] \end{matrix} = \frac{1}{2\pi i} \int_{-\infty}^{\infty} \frac{u(x,k')dk'}{k'-k} + \frac{1}{2\pi i} \oint_{\gamma} \frac{u(x,k')dk'}{k'-k} . \qquad (2.83)$$

The contribution to the second integral on the right-hand side comes from the bound-state poles. It is, in fact, the sum of the residues of (2.77a) at the bound-state poles with an overall minus sign coming from the clockwise direction of the contour γ. This calculation yields

$$\frac{1}{2\pi i} \oint_{\gamma} \frac{u(x,k')dk'}{k'-k} = \sum_{n=1}^{N} \frac{f_1(x,i\kappa_n)e^{\kappa_n x}}{\dot{c}_{12}(i\kappa_n)(k-i\kappa_n)} . \qquad (2.84)$$

Substituting eqn. (2.84) in eqn. (2.83), we get

$$\begin{matrix} u(x,k) \\ [\text{Im}k>0] \end{matrix} = \sum_{n=1}^{N} \frac{f_1(x,i\kappa_n)e^{\kappa_n x}}{\dot{c}_{12}(i\kappa_n)(k-i\kappa_n)} + \frac{1}{2\pi i} \int_{-\infty}^{\infty} \frac{u(x,k')dk'}{k'-k} \qquad (2.85)$$

$u(x,k)$ is, by construction, an analytic function in $\text{Im}k<0$. So, if we close the contour C' as in Figure 2.5, we have

$$0 = \frac{1}{2\pi i} \oint_{C'} \frac{u(x,k')dk'}{k'-k} = \frac{1}{2\pi i} \oint_{C'} \frac{u(x,k')dk'}{k'-k} \qquad (2.86)$$

as the point k is outside the contour. Since the contribution from the semi-circle is zero eqn. (2.86) gives us

$$0 = \frac{1}{2\pi i} \int_{-\infty}^{\infty} \frac{u(x,k')dk'}{k'-k} . \qquad (2.87)$$

In eqn. (2.85), k' is at the upper lip of the cut along the real axis whereas in eqn. (2.87), it is at the lower lip of the cut. If we

Fig. 2.3.
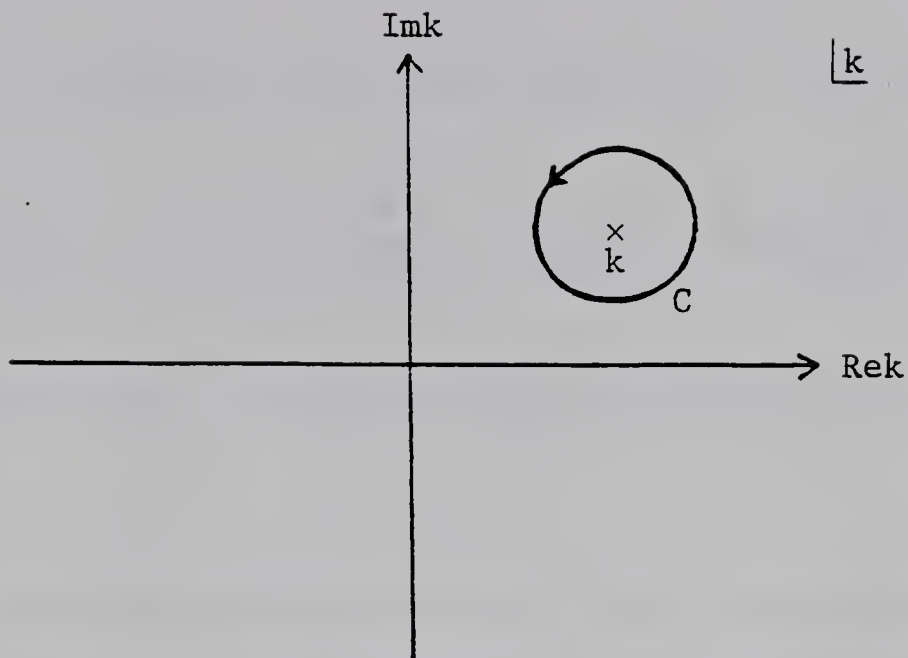
Fig. 2.4.
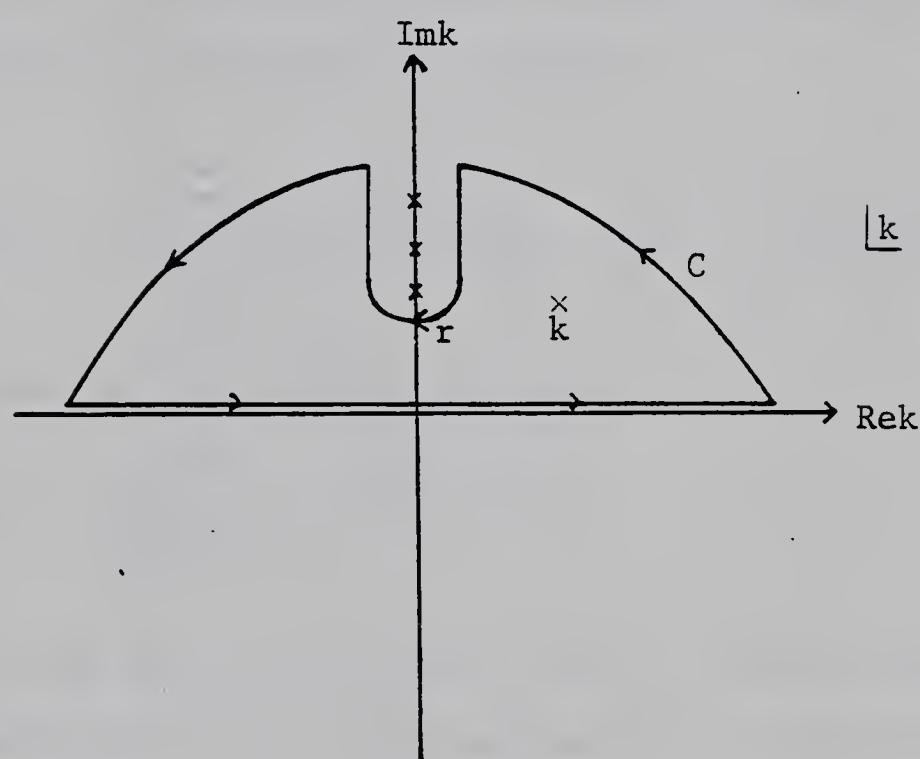
Fig. 2.5.
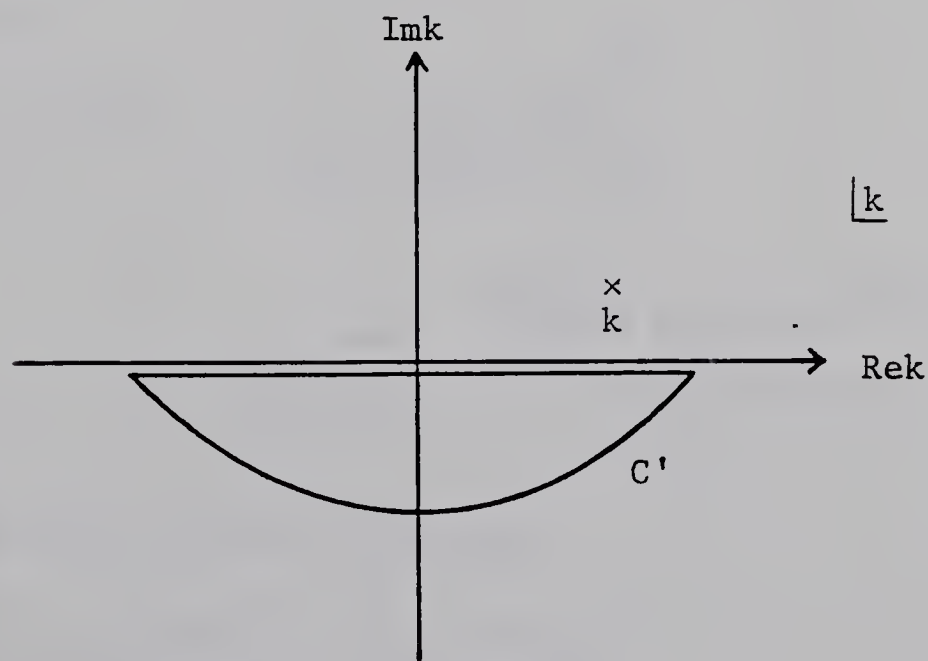
remember this and subtract eqn. (2.87) from eqn. (2.85), we have

$$\frac{u(x,k)}{[\text{Im}k>0]} = \sum_{n=1}^{N} \frac{f_1(x,i\kappa_n)e^{\kappa_n x}}{\dot{c}_{12}(i\kappa_n)(k-i\kappa_n)} + \frac{1}{2\pi i} \int_{-\infty}^{\infty} \frac{\rho(x,k')dk'}{k'-k} \qquad (2.88)$$

where we have used eqn. (2.78) for the discontinuity in $u(x,k)$ across the cut.

The dispersion relation in eqn. (2.88) holds also for the case $\text{Im}k < 0$. In order to normalize $u(x,k)$ to unity at infinity we write eqn. (2.88) with one subtraction at infinity

$$u(x,k) = 1 + \sum_{n=1}^{N} \frac{e^{\kappa_n x}f_1(x,i\kappa_n)}{\dot{c}_{12}(i\kappa_n)(k-i\kappa_n)} + \frac{1}{2\pi i} \int_{-\infty}^{\infty} \frac{\rho(x,k')dk'}{k'-k}. (2.89)$$

Using eqn. (2.14) in eqn. (2.78), one gets

$$\rho(x,k') = \frac{c_{22}(k')}{c_{12}(k')} f_2(x,k')e^{-ik'x} \quad .$$

Evaluating the left hand side of eqn. (2.89) for $\text{Im}k < 0$ using eqn. (2.77b) and substituting the above expression for $\rho(x,k')$ on the right hand side, we get

$$f_2(x,-k)e^{-ikx} = 1 + \sum_{n=1}^{N} \frac{f_1(x,i\kappa_n)e^{\kappa_n x}}{\dot{c}_{12}(i\kappa_n)(k-i\kappa_n)}$$

$$+ \frac{1}{2\pi i} \int_{-\infty}^{\infty} dk' \frac{\dfrac{c_{22}(k')}{c_{12}(k')} f_2(x,k')e^{-ik'x}}{k'-k}. \qquad (2.90)$$

For $\text{Im}k < 0$, one can write the following,

$$\frac{e^{-ik'x}}{k'-k} = -i \, e^{-ikx} \int_{-\infty}^{x} e^{i(k-k')y} \, dy \qquad (2.91)$$

and

$$\frac{e^{\kappa_n x}}{k-i\kappa_n} = i\, e^{-ikx} \int_{-\infty}^{x} e^{i(k-i\kappa_n)y}\, dy \quad . \tag{2.92}$$

Multiplying both the sides of eqn. (2.90) by e^{ikx} and using eqn. (2.91) and eqn. (2.92), one gets after a slight rearrangement,

$$f_2(x,-k) = e^{ikx} + \int_{-\infty}^{x} K_L(x,y)e^{iky}\, dy \tag{2.93}$$

where

$$K_L(x,y) = i \sum_{n=1}^{N} \frac{f_1(x,i\kappa_n)}{\dot{c}_{12}(i\kappa_n)} e^{\kappa_n y}$$

$$- \frac{1}{2\pi} \int_{-\infty}^{\infty} dk'\, \frac{c_{22}(k')}{c_{12}(k')}\, f_2(x,k')e^{-ik'y} \quad . \tag{2.94}$$

Using the representation for $f_2(x,k)$ derived in Section (2.2.1), we have

$$f_2(x,k') = e^{-ik'x} + \int_{-\infty}^{x} K_L(x,y)e^{-ik'y}\, dy \quad ; \ y < x$$

and, hence

$$f_2(x,i\kappa_n) = e^{\kappa_n x} + \int_{-\infty}^{x} K_L(x,y)e^{\kappa_n y}\, dy \quad . \tag{2.95}$$

Using these two relations and remembering eqn. (2.42), we get from eqn. (2.94)

$$\Omega_L(x+y) + K_L(x,y) + \int_{-\infty}^{x} K_L(x,z)\Omega_L(z+y)\, dz = 0 \quad ; \ y < x \tag{2.96}$$

where

$$\Omega_L(z) = \int_{-\infty}^{\infty} \frac{dk}{2\pi}\, \frac{c_{22}(k)}{c_{12}(k)}\, e^{-ikz} - i \sum_{n=1}^{N} \frac{c_{22}(i\kappa_n)}{\dot{c}_{12}(i\kappa_n)} e^{\kappa_n z}$$

$$= \int_{-\infty}^{\infty} \frac{dk}{2\pi}\, R_L(k)e^{-ikz} + \sum_{n=1}^{N} A_{Ln} e^{\kappa_n z} \quad . \tag{2.97}$$

We have used eqn. (2.14) and eqn. (2.59) in writing down the final step.

Equation (2.96) is the Gel'fand-Levitan equation. Obviously, it enables us to obtain the function $K_L(x,y)$ in terms of the informations on the reflection and the transmission coefficients.

We have considered, in the above derivation, the situation in which a wave of unit amplitude is incident from the left. The complementary problem, in which a wave of unit amplitude incident from the right is scattered, can be dealt with in a similar manner.

Instead of eqn. (2.77), one starts with an analytic function

$$u(x,k) = \begin{cases} \dfrac{1}{c_{12}(k)} \, f_2(x,k) e^{ikx} & ; \ \mathrm{Im}\, k > 0 & (2.98a) \\[3ex] f_1^*(x,k^*) e^{ikx} & ; \ \mathrm{Im}\, k < 0 \ . & (2.98b) \end{cases}$$

Then one follows the derivation outlined above. Finally, one gets the Gel'fand-Levitan equation for $K_R(x,y)$, viz.,

$$\Omega_R(x+y) + K_R(x,y) + \int_x^\infty K_R(x,z)\Omega_R(z+y)\,dz = 0 \quad ; \ y > x \quad (2.99)$$

where

$$\Omega_R(z) = \int_{-\infty}^\infty \frac{dk}{2\pi} \frac{c_{11}(k)}{c_{12}(k)} e^{ikz} - i \sum_{n=1}^N \frac{c_{11}(i\kappa_n)}{\dot{c}_{12}(i\kappa_n)} e^{-\kappa_n z}$$

$$= \int_{-\infty}^\infty \frac{dk}{2\pi} R_R(k) e^{ikz} + \sum_{n=1}^N A_{Rn} e^{-\kappa_n z} \ . \qquad (2.100)$$

We have used eqn. (2.13) and eqn. (2.58) in writing down the final expression.

With this, we conclude the discussion of the generalities of the inverse problem in one-dimensional quantum scattering.

2.3. RECONSTRUCTION OF A SYMMETRIC, REFLECTIONLESS POTENTIAL IN ONE DIMENSION FOLLOWING THE GEL'FAND-LEVITAN PROCEDURE.

Once the reflection and the transmission coefficients are known one can, in principle, solve the Gel'fand-Levitan equation for $K_L(x,y)$ or $K_R(x,y)$ and then obtain $V(x)$ by the prescription given in Section (2.2.1). In general, however, it is not an easy task to get a solution of the Gel'fand-Levitan equation in a closed form. Only for a very restricted class of reflection coefficients, the Gel'fand-Levitan equation is known to have simple looking solutions [55,56,60]. The simplest of the solvable cases is, perhaps, the one where the scattering potential is reflectionless for all energies. It is this simple case which is the subject of our investigation.

In what follows, we will discuss, in detail, only that problem where a wave of unit amplitude is incident from the left. The results for the complementary scattering problem, where a wave of unit amplitude is incident from the right, will only be quoted.

2.3.1 Expression for the Potential

When the reflection coefficient $R_L(k)$ has the simple form

$$R_L(k) \equiv 0 \qquad \forall \text{ real } k \qquad (2.101)$$

then $\Omega_L(x,y)$ in eqn. (2.97) reduces to the simple form

$$\Omega_L(x,y) = \sum_{n=1}^{N} A_n e^{\kappa_n(x+y)} . \qquad (2.102)$$

Here we have omitted the subscript L from A_{Ln} for convenience.

The left Gel'fand-Levitan equation (2.96) then reads

$$\sum_{n=1}^{N} A_n e^{\kappa_n(x+y)} + K_L(x,y) + \sum_{n=1}^{N} A_n \int_{-\infty}^{x} K_L(x,z) e^{\kappa_n(y+z)} dz$$

$$(2.103)$$

where we have interchanged the summation and integration on the right-hand side. This integral equation will accept solutions of the form

$$K_L(x,y) = \sum_{n=1}^{N} g_n(x) e^{\kappa_n y} \quad .$$

$$(2.104)$$

where the functions $g_n(x)$ are to be found. Substituting eqn. (2.104) into eqn. (2.103), dividing the resulting equation throughout by $e^{\kappa_n y}$ and carrying out the integration, we get

$$\sum_{n=1}^{N} \left\{ A_n e^{\kappa_n x} \sum_{\nu=1}^{N} \left[\frac{e^{\kappa_\nu x}}{(\kappa_n + \kappa_\nu)} \right] g_\nu(x) + g_n(x) + A_n e^{\kappa_n x} \right\} = 0. \quad (2.105)$$

Hence, the functions $g_n(x)$ are the solutions of the following system of N linear algebraic equations

$$A_n e^{\kappa_n x} \sum_{\nu=1}^{N} \left(\frac{e^{\kappa_\nu x}}{\kappa_n + \kappa_\nu} \right) g_\nu(x) + g_n(x) + A_n e^{\kappa_n x} = 0 \quad (2.106)$$

where $n = 1,2,\ldots,N$. This can be conveniently written in the form of a matrix equation

$$(I + A)g = C$$

$$(2.107)$$

where,

$$I = \| \delta_{n\nu} \|$$

$$(2.108)$$

$$A = \| A_n \frac{e^{(\kappa_n + \kappa_\nu)x}}{(\kappa_n + \kappa_\nu)} \|$$

$$(2.109)$$

$$g = \begin{pmatrix} g_1(x) \\ g_2(x) \\ \vdots \\ g_N(x) \end{pmatrix}$$

(2.110)

and

$$C = \begin{pmatrix} -A_1 e^{\kappa_1 x} \\ -A_2 e^{\kappa_2 x} \\ \vdots \\ -A_N e^{\kappa_N x} \end{pmatrix}$$

(2.111)

*We claim that the coefficient matrix of eqn. (2.106) viz. (I+A)
is non-singular and has a positive determinant for all x* [49]. *Proof*:
Towards this aim, it is advantageous to cast (I+A) in a symmetric form.
Writing eqn. (2.106) in a vector form and applying the diagonal trans-
formation

$$D = \| A_n^{-1/2} \delta_{n\nu} \|$$

(2.112)

we get the following set of equations

$$(I + \hat{A})\hat{g} = \hat{C}$$

(2.113)

where I is again the N×N unit matrix, and

$$\hat{A} = \| A_n^{1/2} A_\nu^{1/2} \frac{e^{(\kappa_n + \kappa_\nu)x}}{(\kappa_n + \kappa_\nu)} \|$$

(2.114)

$$\hat{g} = \begin{pmatrix} \hat{g}_1(x) \\ \hat{g}_2(x) \\ \vdots \\ \hat{g}_N(x) \end{pmatrix}$$

(2.115)

and

$$\hat{C} = \begin{pmatrix} -A_1^{1/2} \ e^{\kappa_1 x} \\ -A_2^{1/2} \ e^{\kappa_2 x} \\ \vdots \\ -A_N^{1/2} \ e^{\kappa_N x} \end{pmatrix} \ .$$

(2.116)

The function $\hat{g}_n(x)$ is related to $g_n(x)$ by a simple relation

$$\hat{g}_n(x) = A_n^{-1/2} \ g_n(x) \ .$$

(2.117)

It can be immediately checked that

$$DAD^{-1} = \hat{A}$$

(2.118)

and, hence

$$D(I + A)D^{-1} = I + DAD^{-1} = (I + \hat{A}) \ .$$

(2.119)

Obviously, then

$$\det(I + A) = \det(I + \hat{A}) \ .$$

(2.120)

So, it is equivalent to proving that $\det(I + \hat{A})$ is positive definite.

It is, for obvious reasons, sufficient to prove that $\det \hat{A} > 0$. Since $\hat{A}$ is a real symmetric matrix, we know that it can always be diagonalized [57] i.e. we can find an orthogonal matrix 0 such that

$$0^{-1}\hat{A}0 = \hat{A}_d$$

(2.121)

where $\hat{A}_d$ stands for the diagonal counterpart of $\hat{A}$. Obviously,

$$\det \hat{A}_d = \det \hat{A}$$

So, if we can prove that $\det \hat{A}_d > 0$, our initial claim will be established.

It is well-known that if a matrix B is similar to a diagonal

matrix M then the diagonal elements of M are the eigenvalues of B [57].

Using this result

$$
\hat{A}_d = \begin{pmatrix} \lambda_1 & & & 0 \\ & \lambda_2 & & \\ & & \ddots & \\ & & & \ddots \\ 0 & & & \lambda_N \end{pmatrix}
$$

(2.122)

where $\lambda_1, \lambda_2, \ldots, \lambda_N$ are the eigenvalues of $\hat{A}$. Clearly,

$$
\det \hat{A}_d = \lambda_1 \lambda_2, \ldots \lambda_N \quad .
$$

(2.123)

So, $\det \hat{A}_d > 0$ if all the eigenvalues of $\hat{A}$ are positive definite i.e. $\hat{A}$ is a positive definite matrix. This is our concern now.

We know that a quadratic form $Q = Y'\hat{A}Y$ is positive-definite [57] if all the eigenvalues of $\hat{A}$ are positive. Hence $\hat{A}$ is positive-definite if

$$
Q = Y'\hat{A}Y > 0 \qquad \text{unless } Y = 0
$$

(2.124)

Here Y is a N-dimensional column vector and $Y' = Y^{*T}$. So, eqn. (2.124) implies that

$$
\sum_{n,\nu} Y'_\nu \hat{A}_{\nu n} Y_n > 0
$$

i.e.

$$
\sum_{n,\nu} y_n \bar{y}_\nu A_n^{1/2} A_\nu^{1/2} \frac{e^{(\kappa_n + \kappa_\nu)x}}{(\kappa_n + \kappa_\nu)} > 0
$$

i.e.

$$
\int_{-\infty}^{x} \left| \sum_{n=1}^{N} A_n^{1/2} y_n e^{\kappa_n z} \right|^2 dz > 0 \quad .
$$

(2.125)

This is always positive unless

$$
\sum_{n=1}^{N} A_n^{1/2} y_n e^{\kappa_n z} = 0
$$

(2.126)

for all z between $-\infty$ and x. So, (2.125) is always positive unless all y_n are zero. $Q.E.D.$

With this result, it is obvious that the system of equations (2.106) has a unique solution, i.e. $g_n(x)$ are unique. The same is true for eqns. (2.113) and $\hat{g}_n(x)$.

Applying Cramer's rule to the system of equation (2.106), we immediately get the solution $g_n(x)$.

$$g_n(x) = \frac{\det(I+A)_R}{\det(I+A)} \quad ; \qquad n = 1,2,\ldots,N \tag{2.127}$$

where $(I+A)_R$ is the matrix with its nth column replaced by the vector C in (2.111). Substituting this value of $g_n(x)$ in eqn. (2.104) we get the solution for $K_L(x,y)$.

For writing down an expression for the potential, we need $K_L(x,x)$. From eqn. (2.104)

$$K_L(x,x) = \sum_{n=1}^{N} g_n(x) e^{K_n x} . \tag{2.128}$$

Obviously,

$$g_n(x) e^{K_n x} = -\frac{\det(I+A)^{(n)}}{\det(I+A)} \tag{2.129}$$

where $(I+A)^{(n)}$ is the matrix $(I+A)$ with its nth column replaced by its first derivative with respect to x. Substituting eqn. (2.129) in eqn. (2.128) and recalling the rule for differentiating a determinant, we get

$$K_L(x,x) = -\frac{d}{dx} \{\ell n \det(I+A)\}. \tag{2.130}$$

Then from eqn. (2.74), we have the potential

$$V(x) = -2 \frac{d^2}{dx^2} \{\ell n \det(I+A)\} . \tag{2.131}$$

We can write eqn. (2.131) in a more symmetric form using eqn. (2.120), viz.

$$V(x) = -2 \frac{d^2}{dx^2} \{\ln \det(I+\hat{A})\} . \qquad (2.132)$$

Had we started with $R_R(k)$ and the right Gel'fand-Levitan equation, we would have got [45]

$$V(x) = -2 \frac{d^2}{dx^2} \{\ln \det(I+\hat{A}')\} \qquad (2.133)$$

where, now

$$\hat{A}' = \| A_n^{1/2} A_\nu^{1/2} \frac{e^{-(\kappa_n+\kappa_\nu)x}}{(\kappa_n+\kappa_\nu)} \| . \qquad (2.134)$$

Strictly speaking, the A's in eqn. (2.134) must have a subscript R. The A_{Ln} (the ones in eqn. (2.132)) and A_{Rn} are related by eqn. (2.60) and under these conditions eqn. (2.132) and eqn. (2.133) will give us the same potential [55]. However, in the case of a symmetric potential, which is of interest to us, A_{Ln} and A_{Rn} are equal and so, we prefer to drop the subscripts R and L.

Having got the potential, we turn our attention towards some of its properties.

Properties of V(x).

1. V(x) are the only potentials for which there is no reflection.

Proof: We proved above that the solutions $g_n(x)$ of eqn. (2.106) are unique. So is, also, $K_L(x,y)$. As a result V(x) is unique for the kind of $\Omega_L(x,y)$ chosen. And, for the reflection coefficient satisfying eqn. (2.101), this is the only kind possible. This, therefore proves our claim.

2. V(x) is negative for all finite x.

Proof: Let us write

$$\Delta = \det(\hat{A}+I) \ . \tag{2.135}$$

The potential $V(x)$ is, then, given by

$$V(x) = - \frac{2(\Delta\Delta'' - \Delta'^2)}{\Delta^2} \ . \tag{2.136}$$

It is, therefore, sufficient to show that

$$\Delta\Delta'' - \Delta'^2 > 0 \qquad \forall \text{ finite } x \ . \tag{2.137}$$

For this purpose, let us start by considering $\det \hat{A}$. If we take out $A_i^{1/2} e^{\kappa_i x}$ from each of the ith column in $\det \hat{A}$ and similarly $A_i^{1/2} e^{\kappa_i x}$ from each of the ith row, we immediately get

$$\det \hat{A} = \left(\prod_{n=1}^{N} A_n \right) e^{2 \sum_{n=1}^{N} \kappa_n x} \left(\det \left\| \frac{1}{\kappa_n + \kappa_\nu} \right\| \right) \tag{2.138}$$

$\det \left\| \frac{1}{\kappa_n + \kappa_\nu} \right\|$ is always positive as it has the same form as $\det \hat{A}$. Hence, we can write

$$\det \hat{A} = \alpha e^{\beta x}$$

where α and β are positive constants. Their exact appearance is not of our concern now. The characteristic polynomial of $\hat{A}$ is given by

$$\det\{\hat{A} + \lambda I\} = \lambda^N + a_1 \lambda^{N-1} + \dots + a_N$$

where a_r is the sum of the principal minors of $\hat{A}$ of order r. Putting $\lambda = 1$ and realizing that each of the principal minors of $\hat{A}$ has again the same form as $\det \hat{A}$, we immediately get that

$$\Delta = \det\{\hat{A} + I\} = 1 + \sum_n \alpha_n e^{\beta_n x} \tag{2.139}$$

where α_n and β_n are positive constants. Using this form for Δ, we immediately get

$$\Delta\Delta'' - \Delta'^2 = \sum_n \beta_n^2 \alpha_n \exp(\beta_n x) + \frac{1}{2} \sum_{n,\nu} \alpha_n \alpha_\nu (\beta_n - \beta_\nu)^2 \exp[(\beta_n + \beta_\nu)x]$$

$$(2.140)$$

α_n and β_n being positive, this gives us the required result.

3. $V(x)$ approaches zero exponentially as x approaches either $+\infty$ or $-\infty$.

Proof: Again using the form (2.139) for $\Delta(x)$ and (2.140) for $\Delta\Delta'' - \Delta'^2$

write down the potential as

$$V(x) = \frac{-2\{\sum_n \beta_n^2 \alpha_n \exp(\beta_n x) + \frac{1}{2} \sum_{n,\nu} \alpha_n \alpha_\nu (\beta_n - \beta_\nu)^2 \exp[(\beta_n + \beta_\nu)x]\}}{\{1 + 2\sum_n \alpha_n \exp(\beta_n x) + \sum_{n,\nu} \alpha_n \alpha_\nu \exp[(\beta_n + \beta_\nu)x]\}}.$$

$$(2.141)$$

As $x \to -\infty$, obviously, the numerator goes towards zero whereas

the denominator tends towards unity. Therefore,

$$V(x) \to 0 \qquad ; x \to -\infty \ . \qquad (2.142)$$

The behaviour as $x \to +\infty$ is implicit. Suppose β_μ is the largest

of the constants β_n. The fastest growing term in the denominator, as

$x \to +\infty$, is the one for which $n = \nu = \mu$ i.e. the one with an exponent

$e^{2\beta_\mu x}$. However, this term is absent from the numerator due to the pre-

sence of the factor $(\beta_n - \beta_\nu)$. So, the denominator grows faster than

the numerator as $x \to +\infty$. We have then

$$V(x) \to 0 \qquad ; x \to +\infty \ . \qquad (2.143)$$

2.3.2. Expressions for the Bound-State Wavefunctions.

The simplest way to get the expressions for the normalized

bound-state wavefunctions is the one starting with the dispersive form

of $u(x,k)$ viz. (2.89). For the reflectionless case, the last term on

the right hand side of eqn. (2.89) is identically zero. Using the form

(2.77b) for $u(x,k)$ in the lower half-plane and using eqn. (2.6), we get

$$f_2(x,-k)e^{-ikx} = 1 + \sum_{n=1}^{N} \frac{f_1(x,i\kappa_n)}{\dot{c}_{12}(i\kappa_n)} \frac{e^{\kappa_n x}}{k-i\kappa_n} \quad . \tag{2.144}$$

Evaluating (2.144) at $k = -i\kappa_\nu$ and using eqn. (2.42) and eqn. (2.59), we get

$$f_2(x,i\kappa_\nu) = e^{\kappa_\nu x} - \sum_{n=1}^{N} A_n \frac{e^{(\kappa_n+\kappa_\nu)x}}{(\kappa_n+\kappa_\nu)} f_2(x,i\kappa_n) \tag{2.145}$$

where we have again omitted the subscript L from A_{Ln} for reasons already mentioned. Multiplying eqn. (2.145) through by $A_\nu^{1/2}$ and remembering that the normalized bound-state wavefunction ψ_n is related to $f_2(x,i\kappa_n)$ by

$$\psi_n = A_n^{1/2} f_2(x,i\kappa_n) \tag{2.146}$$

we have the following set of N algebraic equations for the N bound-state wavefunctions.

$$\sum_{n=1}^{N} A_n^{1/2} A_\nu^{1/2} \frac{e^{(\kappa_n+\kappa_\nu)x}}{(\kappa_n+\kappa_\nu)} \psi_n(x) + \psi_\nu(x) = A_\nu^{1/2} e^{\kappa_\nu x} \tag{2.147}$$

for $\nu = 1,2,\ldots,N$. If we remember, this is the same set of equations as for $\hat{g}_n(x)$ except the absence of a negative sign on the right hand side. Applying Cramer's rule again

$$\psi_n(x) = \frac{\det(I+\hat{A})_R}{\det(I+\hat{A})} \quad ; \quad n = 1,2,\ldots,N \tag{2.148}$$

where $(I+\hat{A})_R$ is the matrix $(I+\hat{A})$ with its nth column replaced by the column on the right hand side of eqn. (2.147). If we multiply this column by $A_n^{1/2} e^{\kappa_n x}$ we get its derivative. Realizing that

$$\psi_n(x) = \frac{1}{A_n^{1/2} e^{\kappa_n x}} \frac{\det(I+\hat{A})^{(n)}}{\det(I+\hat{A})} \quad ; \quad n = 1,2,\ldots,N \tag{2.149}$$

where $(I+\hat{A})^{(n)}$ is the matrix $(I+\hat{A})$ with its nth column differentiated once with respect to x.

Similarly, for the complementary scattering problem, where a wave of unit amplitude is incident from the right, the expression for $\psi_n(x)$ is [45]

$$\psi_n(x) = - \frac{1}{A_n^{1/2} e^{-\kappa_n x}} \frac{\det(I+\hat{A}')^{(n)}}{\det(I+\hat{A}')}$$ (2.150)

where the matrix $\hat{A}'$ was introduced in eqn. (2.134). $(I+\hat{A}')^{(n)}$ carries the same meaning as $(I+\hat{A})^{(n)}$. Again, we have dropped the subscript R from A_{Rn} in eqn. (2.150) for reasons already discussed.

2.3.3. Imposing Symmetry on the Potential.

We have been able to derive, so far, the expressions for cal-
culating a transparent potential V(x) and the corresponding bound-
state wave functions $\psi_n(x)$ in terms of 2N parameters, N being the
number of bound-states. The N κ_i's are the bound-state energies. The
other N parameters, viz., the A_i's, have to be fixed by some explicit
information regarding the bound-state wavefunctions or some desired
constraint on the potential V(x). We are specifically interested in
a potential which is symmetric about the origin, i.e.

$$V(x) = V(-x) .$$ (2.151)

We *claim* that the condition (2.151) is guaranteed provided that the
A_i's are given by

$$\frac{A_n}{2\kappa_n} = \prod_{m \neq n} \left| \frac{\kappa_m + \kappa_n}{\kappa_m - \kappa_n} \right| \qquad ; \qquad m = 1, 2, \ldots, N$$ (2.152)

Proof: We have already seen that

$$\det\{\hat{A} + I\} = 1 + a_1 + \ldots + a_{N-1} + a_N \tag{2.153}$$

where a_r is the sum of the principal minors of $\hat{A}$ of order r. Also, det $\hat{A}$ is given by eqn. (2.138). All the principal minors of $\hat{A}$ have the same form as (2.138) except that one or more (n, ν) are missing depending upon the order r.

Let us take out a factor $e^{\sum_{n=1}^{N} \kappa_n x}$ on the right hand side of eqn. (2.153) yielding

$$\det\{\hat{A} + I\} = e^{\sum_{n=1}^{N} \kappa_n x} \left\{ e^{-\sum_{n=1}^{N} \kappa_n x} + e^{-\sum_{n=1}^{N} \kappa_n x} a_1 + \ldots \right.$$

$$\left. + e^{-\sum_{n=1}^{N} \kappa_n x} a_{N-1} + e^{-\sum_{n=1}^{N} \kappa_n x} a_N \right\} . \tag{2.154}$$

Here, for example,

$$a_1 = \text{tr } \hat{A} = \sum_{p=1}^{N} \frac{A_p}{2\kappa_p} e^{2\kappa_p} \tag{2.155}$$

$$a_{N-1} = \det\left(\left\| \frac{1}{\kappa_n + \kappa_\nu} \right\| \right)_{\substack{(n,\nu)=p \\ \text{missing}}} \left(\prod_{\substack{n=1 \\ n \neq p}}^{N} A_n \right) e^{2 \sum_{\substack{n=1 \\ n \neq p}}^{N} \kappa_n x} \tag{2.156}$$

and

$$a_N = \det \hat{A} . \tag{2.157}$$

From eqn. (2.132) it is clear that the overall exponential in eqn. (2.154) does not contribute to the potential. A symmetric potential then requires that the quantity in the braces of eqn. (2.154) be symmetric. It is important to note that the only dependence on x

is in the exponents. So, the coefficients of exponents differing only in an overall sign have to be the same.

Let us consider the first term in the braces in eqn. (2.154). The exponent is

$$e^{-\sum_{n=1}^{N} \kappa_n x}$$

with a factor of unity. So, unity must also be the coefficient of

$$e^{\sum_{n=1}^{N} \kappa_n x}$$

for symmetry. This comes from a_N. We must have, then

$$\det \left(\left\| \frac{1}{\kappa_n + \kappa_\nu} \right\| \right)_{\substack{\text{all} \\ n,\nu}} \left(\prod_{n=1}^{N} A_n \right) = 1 \quad . \tag{2.158}$$

According to Lemma 1 in Appendix A, the condition (2.158) becomes,

$$\left\{ \prod_{n=1}^{N} \left(\frac{A_n}{2\kappa_n} \right) \right\} \frac{\displaystyle\sum_{j>1}^{N} (\kappa_1 - \kappa_j)^2 \; \sum_{j>2}^{N} (\kappa_2 - \kappa_j)^2 \cdots \sum_{j>N-1}^{N} (\kappa_{N-1} - \kappa_j)^2}{\displaystyle\sum_{j>1}^{N} (\kappa_1 + \kappa_j)^2 \; \sum_{j>2}^{N} (\kappa_2 + \kappa_j)^2 \cdots \sum_{j>N-1}^{N} (\kappa_{N-1} + \kappa_j)^2} = 1 \tag{2.159}$$

Similarly, the $p = i$ term in a_1 gives us the

coeff. of $e^{(-\kappa_1 - \kappa_2 - \cdots - \kappa_{i-1} + \kappa_i - \kappa_{i+1} - \cdots - \kappa_N)x} = \frac{A_i}{2\kappa_i}$. (2.160)

Its symmetric counterpart in a_{N-1} gives us the

coeff. of $e^{(\kappa_1 + \kappa_2 + \cdots + \kappa_{i-1} - \kappa_i + \kappa_{i+1} + \cdots + \kappa_N)x}$

$$= \det \left(\left\| \frac{1}{\kappa_n + \kappa_\nu} \right\| \right)_{\substack{(n,\nu)=i \\ \text{missing}}} \left(\prod_{\substack{n=1 \\ n \neq i}}^{N} A_n \right) \quad . \tag{2.161}$$

Again using the Lemma mentioned above, the equality of these two

coefficients dictates to us

$$\left(\frac{A_i}{2\kappa_i}\right) = \left\{\prod_{\substack{n=1\\n\neq i}}^{N}\left(\frac{A_n}{2\kappa_n}\right)\right\} \times$$

$$\times \left\{\frac{\prod\limits_{j>1}'(\kappa_1-\kappa_j)^2 \ldots \prod\limits_{j>i-1}'(\kappa_{i-1}-\kappa_j)^2 \prod\limits_{j>i+1}(\kappa_{i+1}-\kappa_j)^2 \ldots \prod\limits_{j>N-1}(\kappa_{N-1}-\kappa_j)^2}{\prod\limits_{j>1}'(\kappa_1+\kappa_j)^2 \ldots \prod\limits_{j>i-1}'(\kappa_{i-1}+\kappa_j)^2 \prod\limits_{j>i+1}(\kappa_{i+1}+\kappa_j)^2 \ldots \prod\limits_{j>N-1}(\kappa_{N-1}+\kappa_j)^2}\right\}$$

(2.162)

where Π' implies that the factor with $j=i$ is to be excluded in the product.

Multiplying both the sides of eqn. (2.162) by

$$\left(\frac{A_i}{2\kappa_i}\right)\frac{(\kappa_1-\kappa_i)^2}{(\kappa_1+\kappa_i)^2}\frac{(\kappa_2-\kappa_i)^2}{(\kappa_2+\kappa_i)^2}\cdots\frac{(\kappa_{i-1}-\kappa_i)^2}{(\kappa_{i-1}+\kappa_i)^2}\frac{\prod\limits_{j>i}^{N}(\kappa_i-\kappa_j)^2}{\prod\limits_{j>i}^{N}(\kappa_i+\kappa_j)^2}$$

(2.163)

and using condition (2.159) on the right-hand side of the resulting

equation, we get

$$\left(\frac{A_i}{2\kappa_i}\right)^2 \prod_{j\neq i}^{N}\left|\frac{\kappa_i-\kappa_j}{\kappa_i+\kappa_j}\right|^2 = 1$$

(2.164)

Remembering that A_i's have to be positive, eqn. (2.164) gives

$$\left(\frac{A_i}{2\kappa_i}\right) = \prod_{j\neq i}^{N}\left|\frac{\kappa_i+\kappa_j}{\kappa_i-\kappa_j}\right| \quad ; \quad j,i = 1,2,\ldots,N$$

which is the desired result.

Let us now try to prove the *converse*. i.e., if eqn. (2.152)

holds good then $V(x)$ is symmetric [47]. For this purpose, let us cast

eqn. (2.153) in a slightly different form. We observed earlier that

all the principal minors of det $\hat{A}$ have the same form as det $\hat{A}$ except

that some of the rows and columns are missing. If we define by s, all

the subsets of $\{1,2,\ldots,N\}$ including the null set and the full set, we

can rewrite eqn. (2.153) as

$$\det\{\hat{A}+I\} = \sum_s a_s \qquad (2.165)$$

where a_s is a principal monor of $\hat{A}$ with only those rows and columns which belong to s. We realize that a_s corresponding to the null set is just unity. Obviously, then

$$a_s = \left(\sum_{p\epsilon s} A_p\right)\left(e^{2\sum_{p\epsilon s} \kappa_p x}\right) \det\left(\left\|\frac{1}{\kappa_n+\kappa_m}\right\|\right)_{n,m\epsilon s} \qquad (2.166)$$

Using Lemma 1 of Appendix A again, the determinant on the right hand side of eqn. (2.166) can be written as

$$a_s = \left(\sum_{p\epsilon s} A_p\right)\left(e^{2\sum_{p\epsilon s} \kappa_p x}\right)\left\{\prod_{p\epsilon s} \frac{1}{2\kappa_p}\right\}$$

$$\left(\frac{\prod\limits_{j>1}^{N}(\kappa_1-\kappa_j)^2 \prod\limits_{j>2}^{N}(\kappa_2-\kappa_j)^2 \cdots \prod\limits_{j>N-1}^{N}(\kappa_{N-1}-\kappa_j)^2}{\prod\limits_{j>1}^{N}(\kappa_1+\kappa_j)^2 \prod\limits_{j>2}^{N}(\kappa_2+\kappa_j)^2 \cdots \prod\limits_{j>N-1}^{N}(\kappa_{N-1}+\kappa_j)^2}\right)_{\text{all } \kappa_p\text{'s}\epsilon s} \qquad (2.167)$$

The factor in brackets contains only those κ_p's in the product which are in S. Others are missing. Supplementing this with Lemma 2 in Appendix A, we can write it in a more intelligible form

$$a_s = \left(\sum_{p\epsilon s} \frac{A_p}{2\kappa_p}\right) e^{2\sum_{p\epsilon s} \kappa_p x} \prod_{(n\neq m)\epsilon s} \left|\frac{\kappa_n-\kappa_m}{\kappa_n+\kappa_m}\right| \qquad (2.168)$$

Substituting eqn. (2.168) in eqn. (2.165), we have

$$\det\{\hat{A}+I\} = \sum_s e^{2\sum_{p\epsilon s} \kappa_p x}\left(\prod_{p\epsilon s} \frac{A_p}{2\kappa_p}\right)\prod_{(n\neq m)\epsilon s}\left|\frac{\kappa_n-\kappa_m}{\kappa_n+\kappa_m}\right| . \qquad (2.169)$$

If we now substitute the assumed conditions for $(A_p/2\kappa_p)$, we get

$$\det\{\hat{A}+I\} = \sum_s e^{2\sum_{p\in s}\kappa_p x} \left(\prod_{\substack{p\in s \\ n\in \text{whole set}}} \left|\frac{\kappa_p+\kappa_n}{\kappa_p-\kappa_n}\right| \right) \left(\prod_{\substack{m\in s \\ n\in s}} \left|\frac{\kappa_n-\kappa_m}{\kappa_n+\kappa_m}\right| \right). \quad (2.170)$$

Obviously, those terms in the first parentheses which have $n\in s$ cancel out with the ones in the second parentheses. We are, thus, left with

$$\det\{\hat{A}+I\} = \sum_s e^{2\sum_{p\in s}\kappa_p x} \Pi(s,\bar{s}) \quad (2.171)$$

where

$$\Pi(s,\bar{s}) = \prod_{\substack{m\in s \\ n\in\bar{s}}} \left|\frac{\kappa_m+\kappa_n}{\kappa_m-\kappa_n}\right| \quad (2.172)$$

and $\bar{s}$ stands for the complement of s. It is clear that $\Pi(s,\bar{s})$ is symmetric under the interchange of s and $\bar{s}$, i.e.,

$$\Pi(s,\bar{s}) = \Pi(\bar{s},s). \quad (2.173)$$

We can write eqn. (2.171) as:

$$\det\{\hat{A}+I\} = e^{\sum_{p=1}^{N}\kappa_p x} \sum_s \left\{ e^{-\sum_{n\in\bar{s}}\kappa_n x + \sum_{m\in s}\kappa_m x} \right\} \Pi(s,\bar{s})$$

$$= e^{\sum_{p=1}^{N}\kappa_p x} \left\{ \sum_s \frac{1}{2}\left(e^{-\sum_{n\in\bar{s}}\kappa_n x + \sum_{m\in s}\kappa_m x} \right) \Pi(s,\bar{s}) \right.$$

$$\left. + \sum_s \frac{1}{2}\left(e^{-\sum_{n\in\bar{s}}\kappa_n x + \sum_{m\in s}\kappa_m x} \right) \Pi(s,\bar{s}) \right\}. \quad (2.174)$$

Since $\Pi(s,\bar{s})$ is symmetric under the interchange $s\to\bar{s}$ and the sum runs over all possible subsets, we can write

$$\det\{\hat{A}+I\} = e^{\sum_{p=1}^{N} \kappa_p x} \left[\left\{ \sum_s \frac{1}{2} \left(e^{-\sum_{n\in\bar{s}} \kappa_n x + \sum_{m\in s} \kappa_m x} \right) \right. \right.$$

$$\left. \left. + \sum_s \frac{1}{2} \left(e^{-\sum_{n\in s} \kappa_n x + \sum_{m\in\bar{s}} \kappa_m x} \right) \right\} \Pi(s,\bar{s}) \right]$$

$$= e^{\sum_{p=1}^{N} \kappa_p x} \sum_s \Pi(s,\bar{s}) \cosh\left(\sum_{m\in s} \kappa_m x - \sum_{n\in\bar{s}} \kappa_n x \right) . \quad (2.175)$$

The first term, as before, does not affect the potential and the second term is manifestly symmetric in x. So, the potential is symmetric. *QED*.

2.3.4. <u>A Numerical Test of the Technique</u>.

As a numerical test of the above technique, let us consider the Pöschl-Teller potential

$$V(x) = -\frac{\lambda(\lambda-1)}{\cosh^2 x} \quad (2.176)$$

with $\lambda > 1$. This is, obviously, a symmetric potential. This potential has been studied and is known to be an exquisite example of a reflectionless potential for certain values of λ [61]. The bound-state energies of (2.176) are

$$E_n = -(\lambda - 1 - n)^2 \quad ; \; n \leq \lambda - 1 \quad (2.177)$$

and n can take the values 0,1,2,.... Also the reflection coefficient is known to be

$$|R_L(k)|^2 = \cos^2(\phi_e - \phi_o) \quad (2.178)$$

where

$$\phi_e - \phi_o = \tan^{-1}\{\frac{\sinh\pi k}{\sin \pi\lambda}\} . \quad (2.179)$$

Obviously, for all integer values of $\lambda(=1,2,3,...)$ the reflection co-efficient identically vanishes for all real k.

So, this is obviously the perfect case for a test of our method. Our technique should reconstruct potential (2.176) for integer values of λ if we use the bound-state energies given by eqn. (2.177). And, in fact, it does. We reconstructed the Pöschl-Teller potentials with $\lambda = 2,3,4,5$ and 6. It was exact in each case. We display the result for $\lambda = 6$ in Figure 2.6.

That proves the uniqueness and credibility of the technique outlined in this chapter.

(b)

(a)
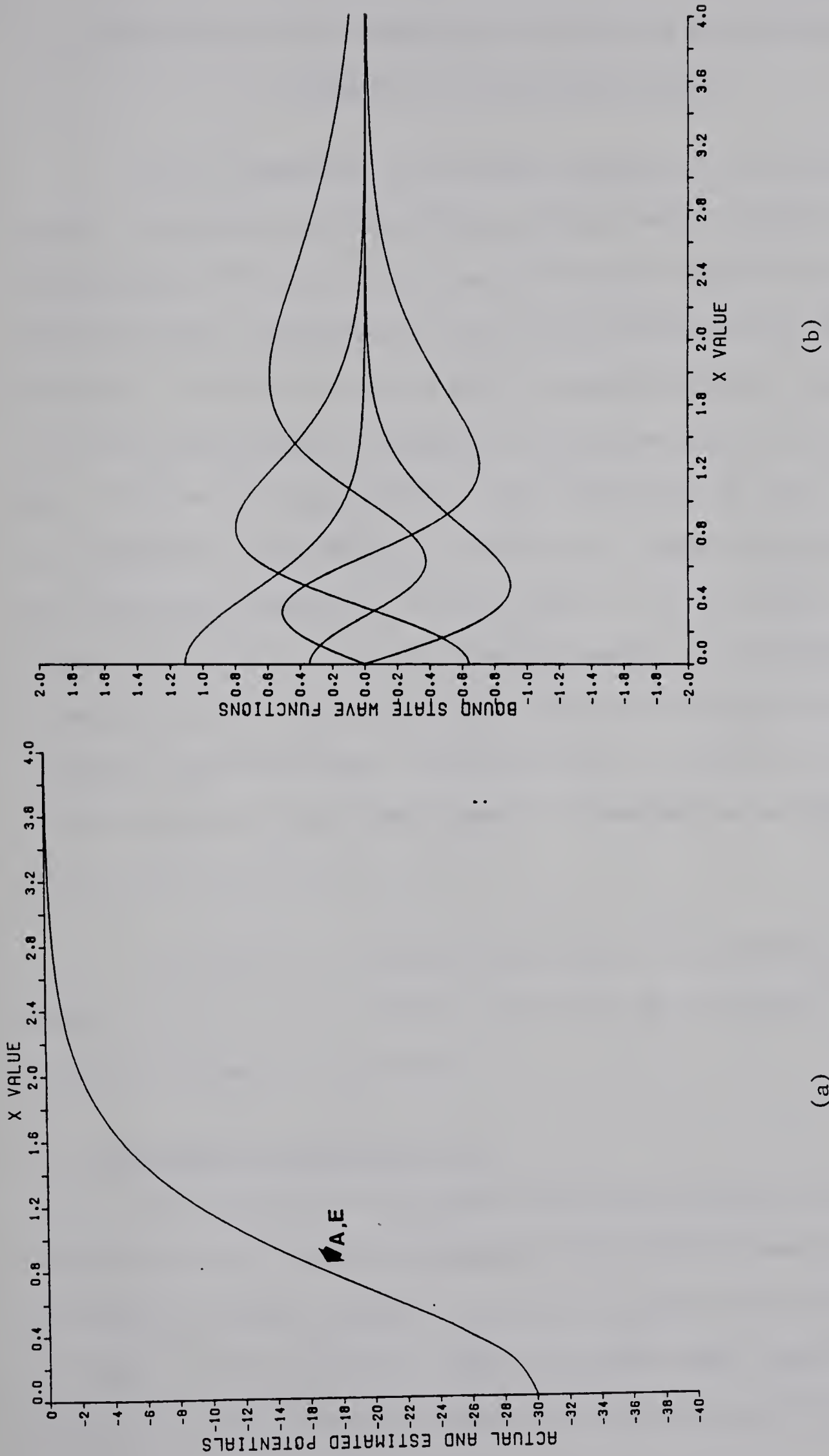
Fig. 2.6. Results for the Pöschl-Teller potential ($\lambda = 6$):
(a) Actual (A) and the reflectionless (E) potentials: exact agreement.
(b) Bound-state wavefunctions.

3. APPLICATIONS TO SOME SYMMETRIC POTENTIALS IN ONE DIMENSION: RELIABILITY OF THE APPROXIMATION.

Given a sequence of bound-state energies, we can uniquely construct a symmetric, reflectionless potential which supports those bound-states. This technique does not have much appeal as an *exact* inverse method. There are not very many reflectionless potentials of interest. Moreover, we do not know, a priori, whether a given sequence of bound-state energies corresponds to a reflectionless potential or not. What we are interested in is the reliability of this technique as a method for *approximately* constructing a symmetric potential from its bound-state energies. In other words, if we are given the bound-state energies of a symmetric potential, which is not necessarily reflectionless, then how closely the constructed reflectionless potential resembles the actual one. The obvious way to check this is to apply this technique to some known symmetric potentials in one dimension. This is the aim of this chapter.

Section 3.1 is devoted exclusively to non-confining potential wells, Section 3.2 to confining potentials and in Section 3.3 we discuss the problem of convergence.

3.1 Non-Confining Potential Wells

In this class, we consider only those symmetric potential wells which are negative and non-singular on the infinite interval $(-\infty < x < \infty)$ and which decay fast enough, as $x = \pm\infty$, to support only a finite number of bound states. In all the cases, we use the exact bound-state energies to construct the corresponding reflectionless potential and the

estimated bound-state wavefunctions. We also calculate the reflection coefficient and plot it as a function of the momentum 'k'.

3.1.1. Pöschl-Teller Potentials with Non-Integer λ's.

The Pöschl-Teller potential given by eqn. (2.176) is not reflectionless for a non-integer value of λ. This potential satisfies all the properties listed above and its reflection coefficient displays a very simple behaviour with increasing momentum k.

Using the exact bound-state energies, reflectionless potentials corresponding to Pöschl-Teller potentials with λ = (2.1 to 2.9) and λ = (3.1 to 3.9) were calculated. In Figure 3.1 to Figure 3.5, we have summarized the calculations for λ = 3.1 to 3.5. These five cases suffice to elucidate the features of the reflectionless approximation.

As we see from eqn. (2.178) and eqn. (2.179), the reflection coefficient for a non-integer λ decays monotonically with increasing k. At a value λ = (n + 0.5); n = 1, 2, ..., the rate of decay is the slowest. The reflection coefficient being periodic in λ, as λ varying both ways from (n + 0.5) to an integer value i.e. towards n or (n + 1), the reflection coefficient shows exactly the same behaviour. The closer λ is to the integer value, the faster the reflection coefficient decays. And, as is obvious from the results, the faster the reflection coefficient decays with increasing k the better is the agreement between the reflectionless approximation and the actual potential.

To further elucidate this behaviour the Pöschl-Teller potential with λ = 3.0001 was reconstructed. As we see in Figure 3.6, the reflection coefficient is equal to unity at k = 0 and practically zero every-

(a)

(b)

(c)
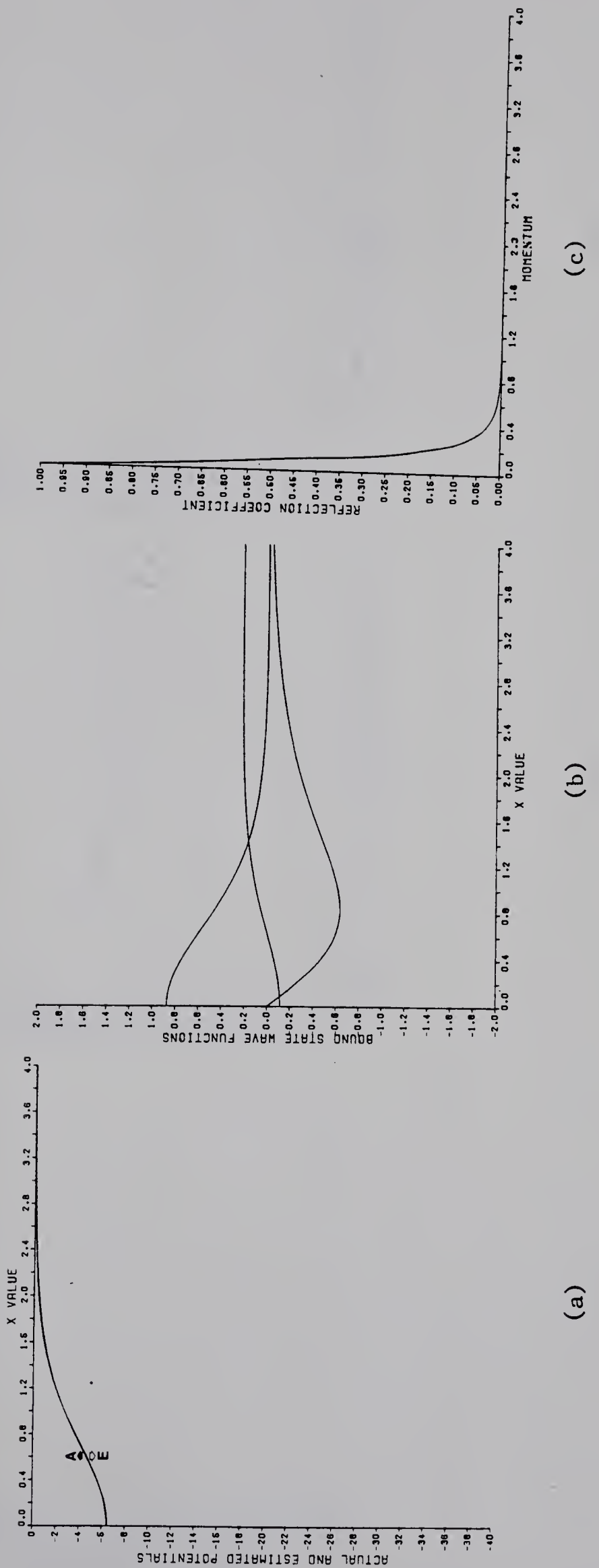
Fig. 3.1. Results for the Pöschl-Teller Potential ($\lambda = 3.1$):
(a) Actual (A) and the reflectionless (E) potential.
(b) Bound-state wavefunctions of the reflectionless potential.
(c) The reflection coefficient.
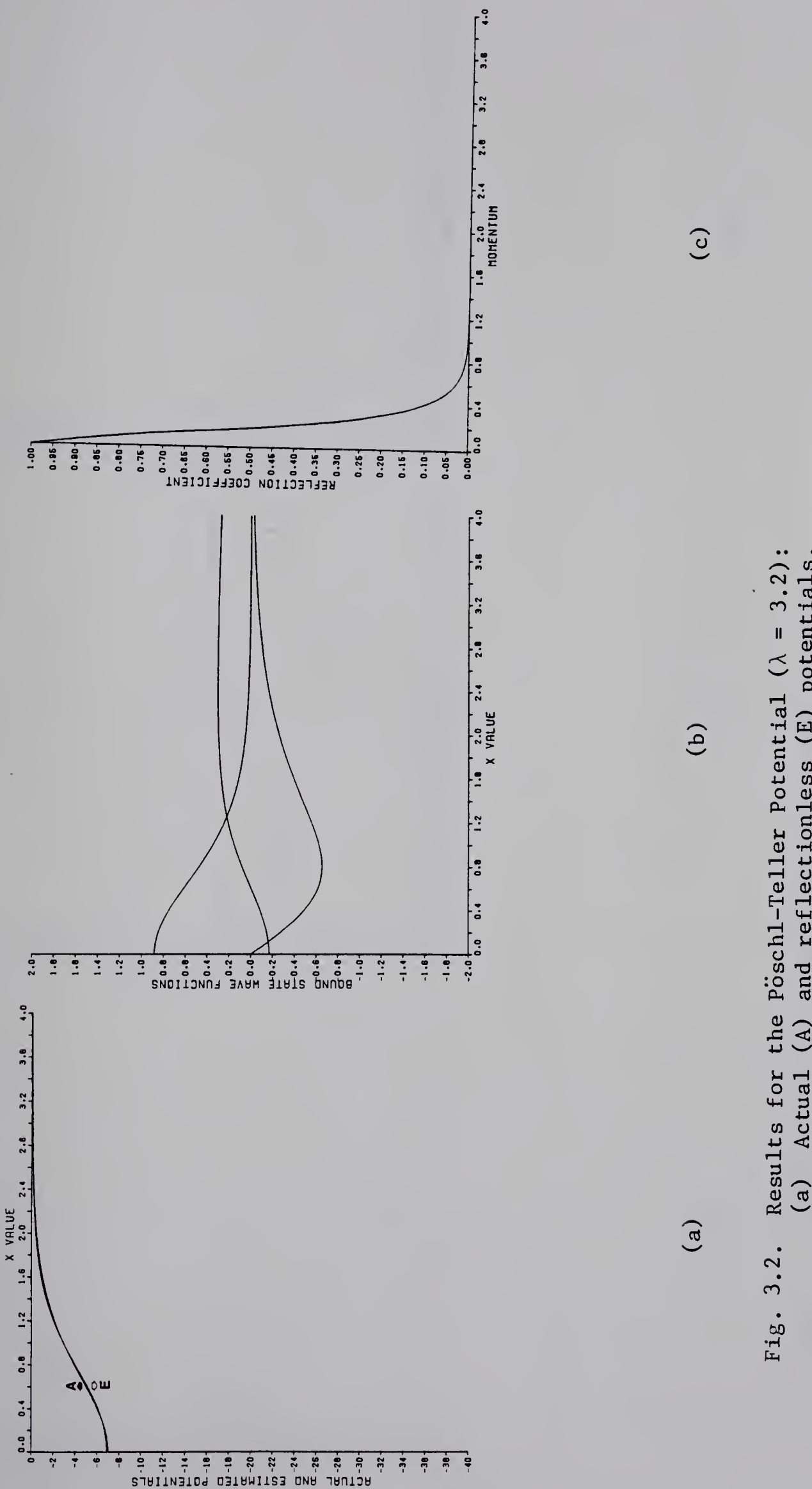
Fig. 3.2. Results for the Pöschl-Teller Potential ($\lambda = 3.2$):
(a) Actual (A) and reflectionless (E) potentials.
(b) Bound-state wavefunctions of the reflectionless potential.
(c) The reflection coefficient.

(a)

(b)

(c)
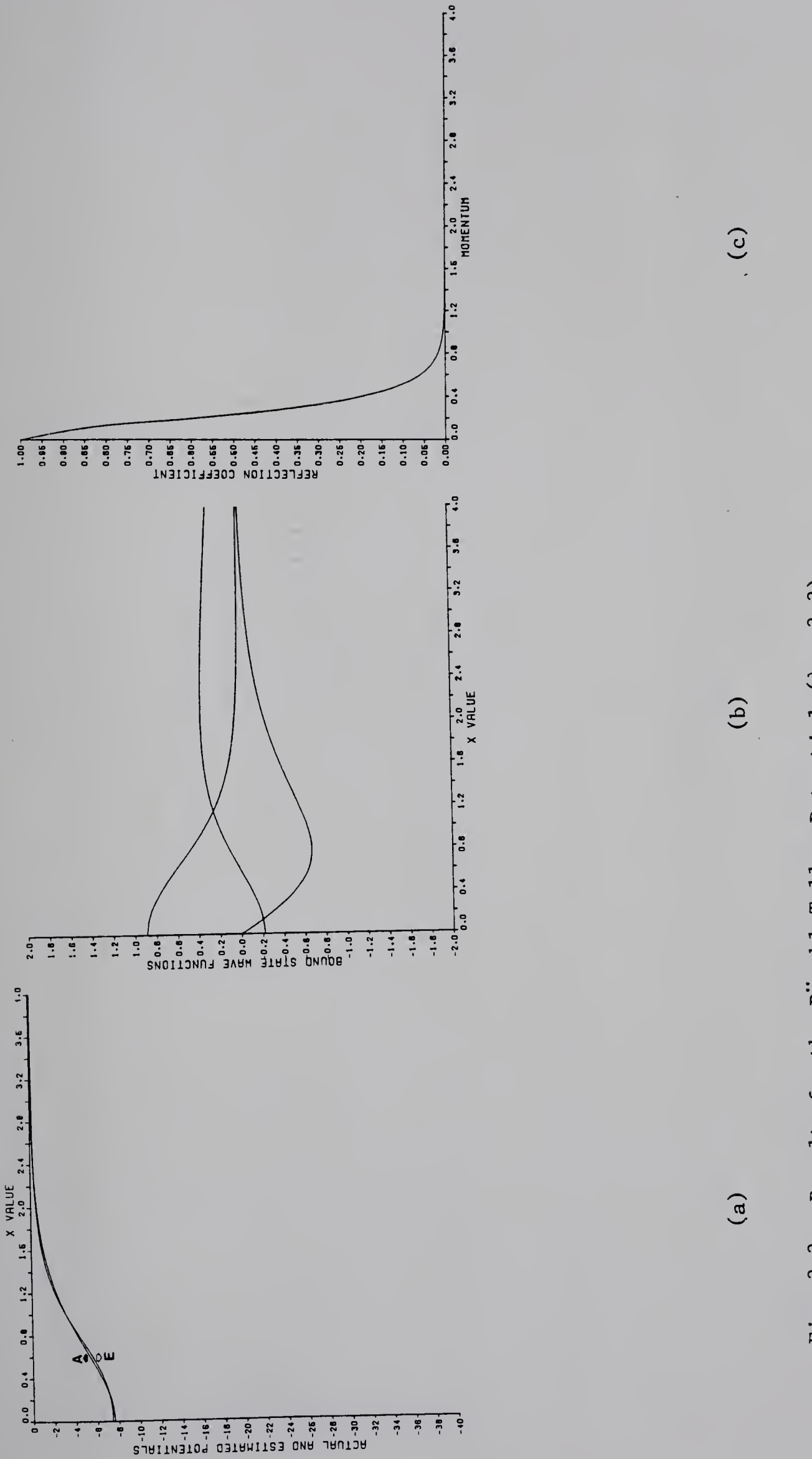
Fig. 3.3   Results for the Pöschl-Teller Potential ($\lambda = 3.3$):
(a)   Actual (A) and reflectionless (E) potentials.
(b)   Bound-state wavefunctions of the reflectionless potential.
(c)   The reflection coefficient.

(a)

(b)

(c)
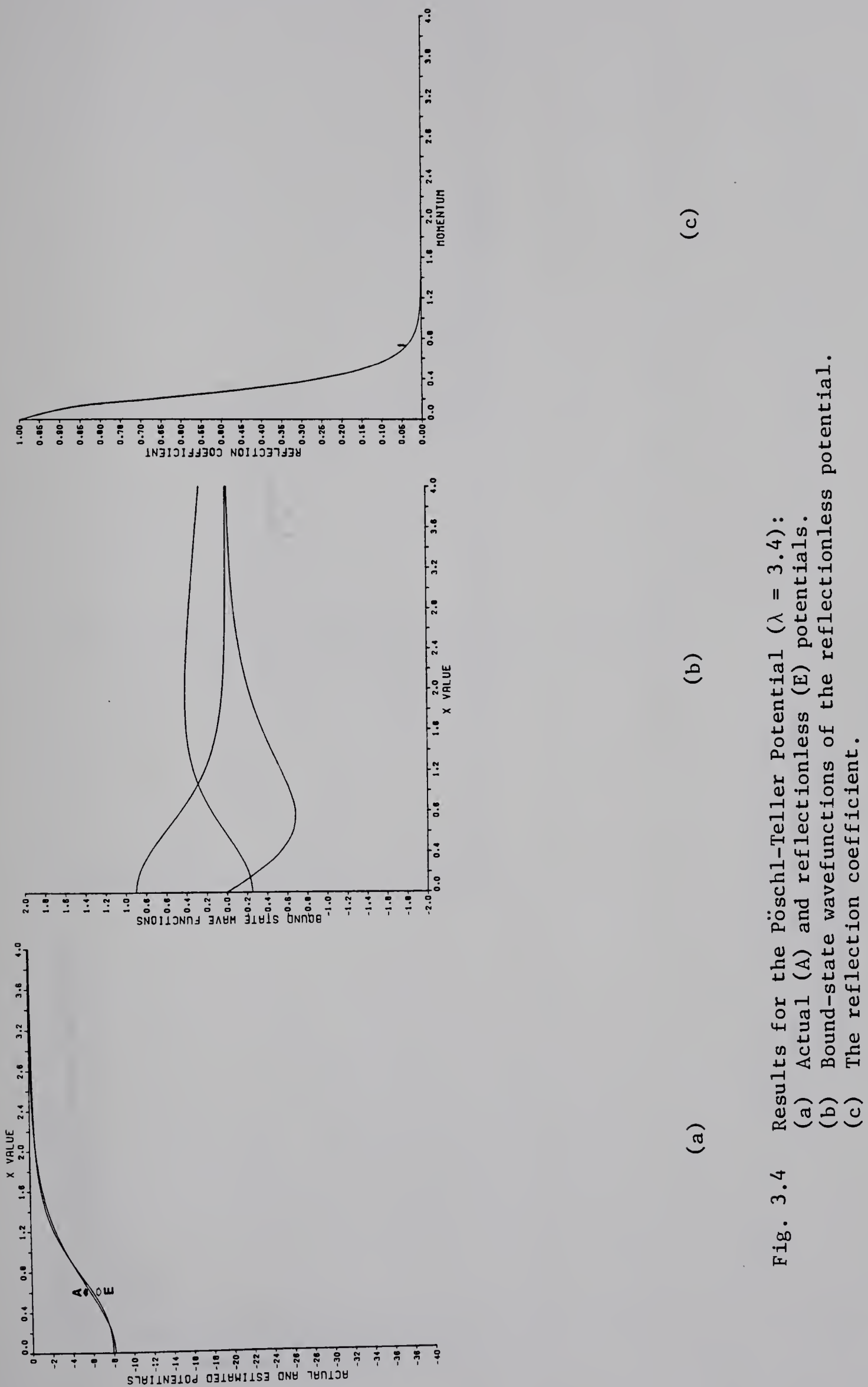
Fig. 3.4   Results for the Pöschl-Teller Potential (λ = 3.4):
(a) Actual (A) and reflectionless (E) potentials.
(b) Bound-state wavefunctions of the reflectionless potential.
(c) The reflection coefficient.

61

(a)

(b)

(c)
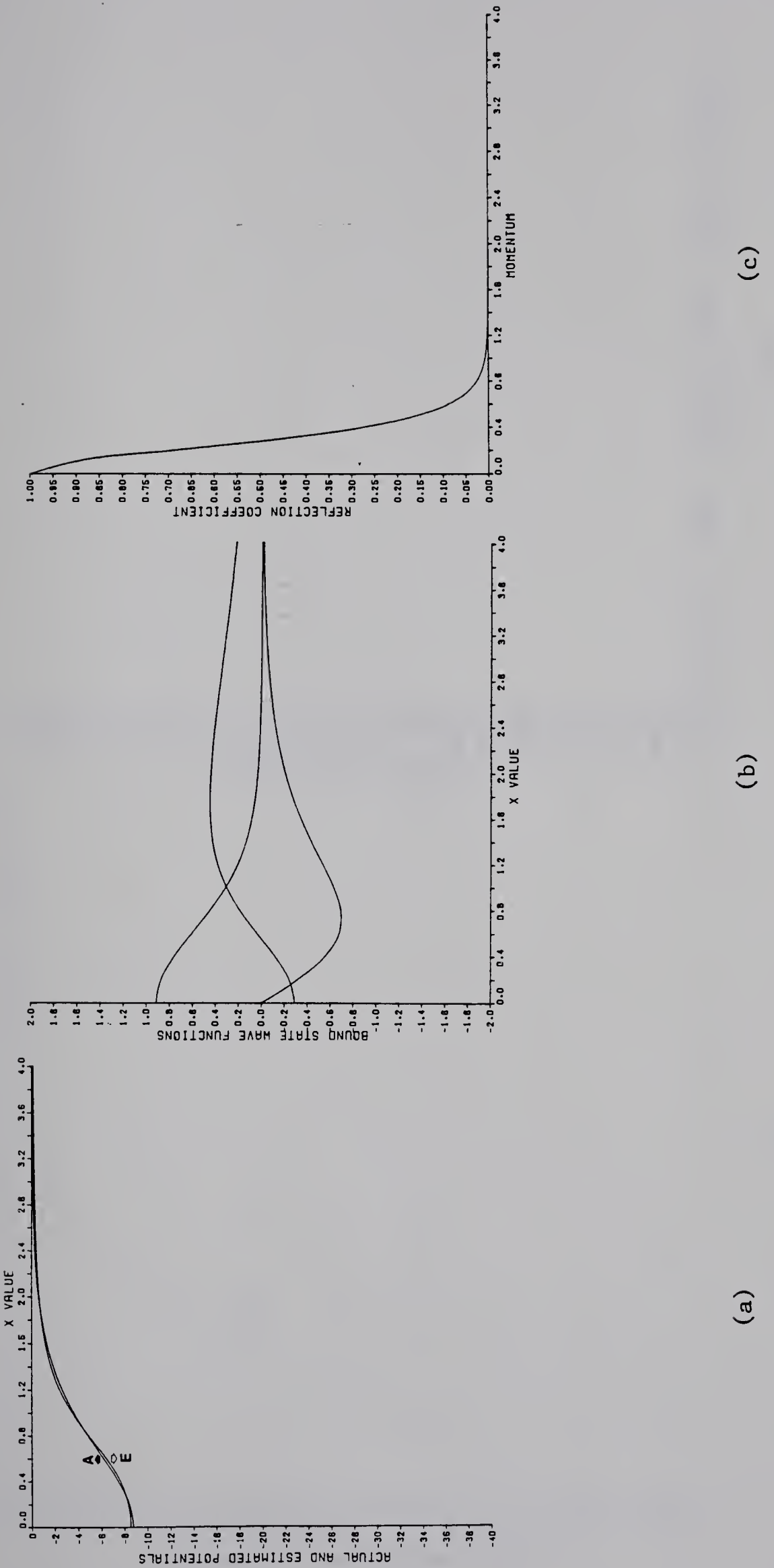
Fig. 3.5. Results for the Pöschl-Teller Potential ($\lambda = 3.5$):
(a) Actual (A) and reflectionless (E) potentials.
(b) Bound-state wavefunctions of the reflectionless potential.
(c) The reflection coefficient.
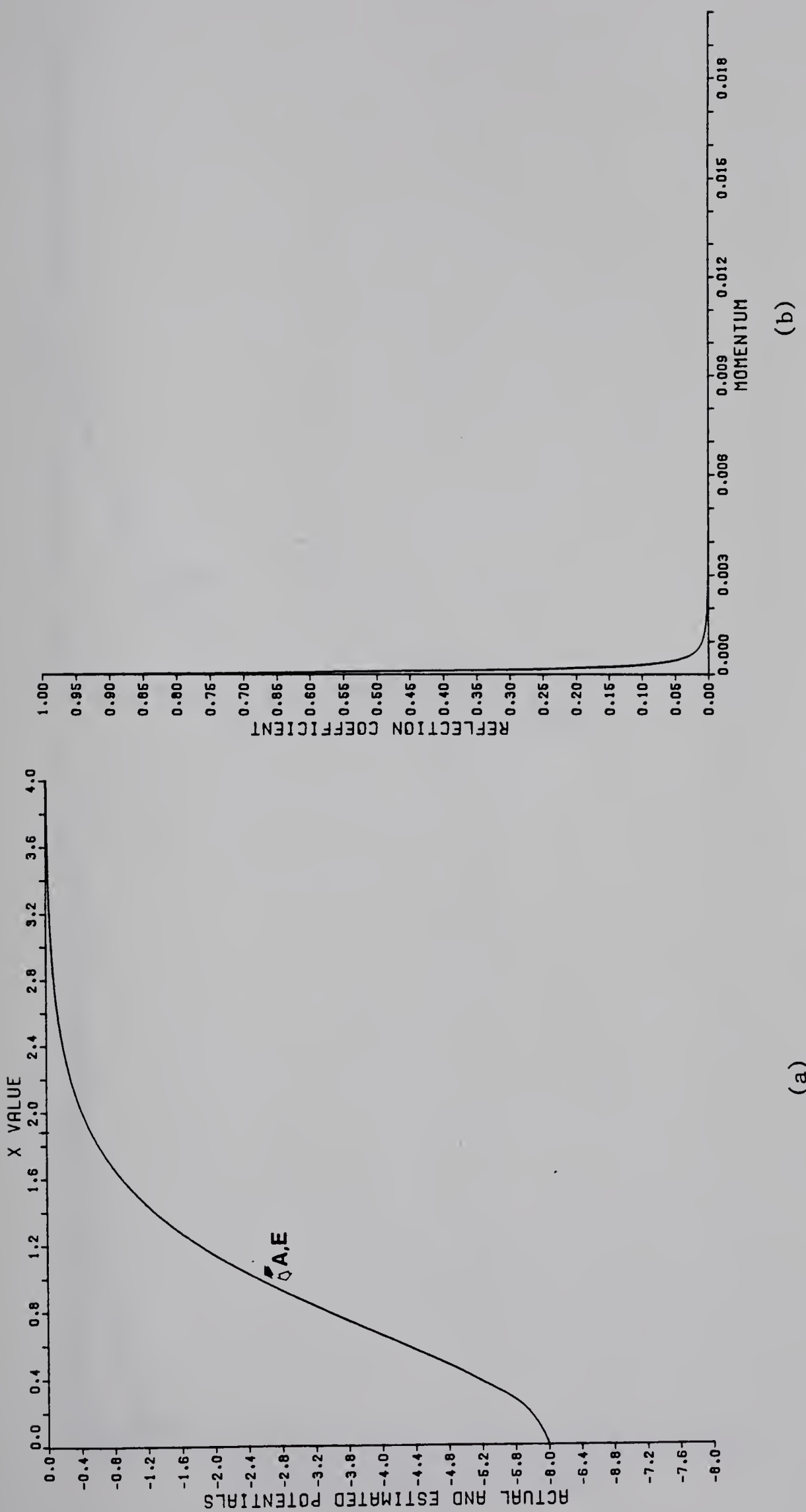
Fig. 3.6.   Results for the Pöschl-Teller Potential ($\lambda = 3.0001$):
(a) Excellent agreement between the actual (A) and the reflectionless (E) potential.
(b) The reflection coefficient of the actual potential.

(a)

(b)
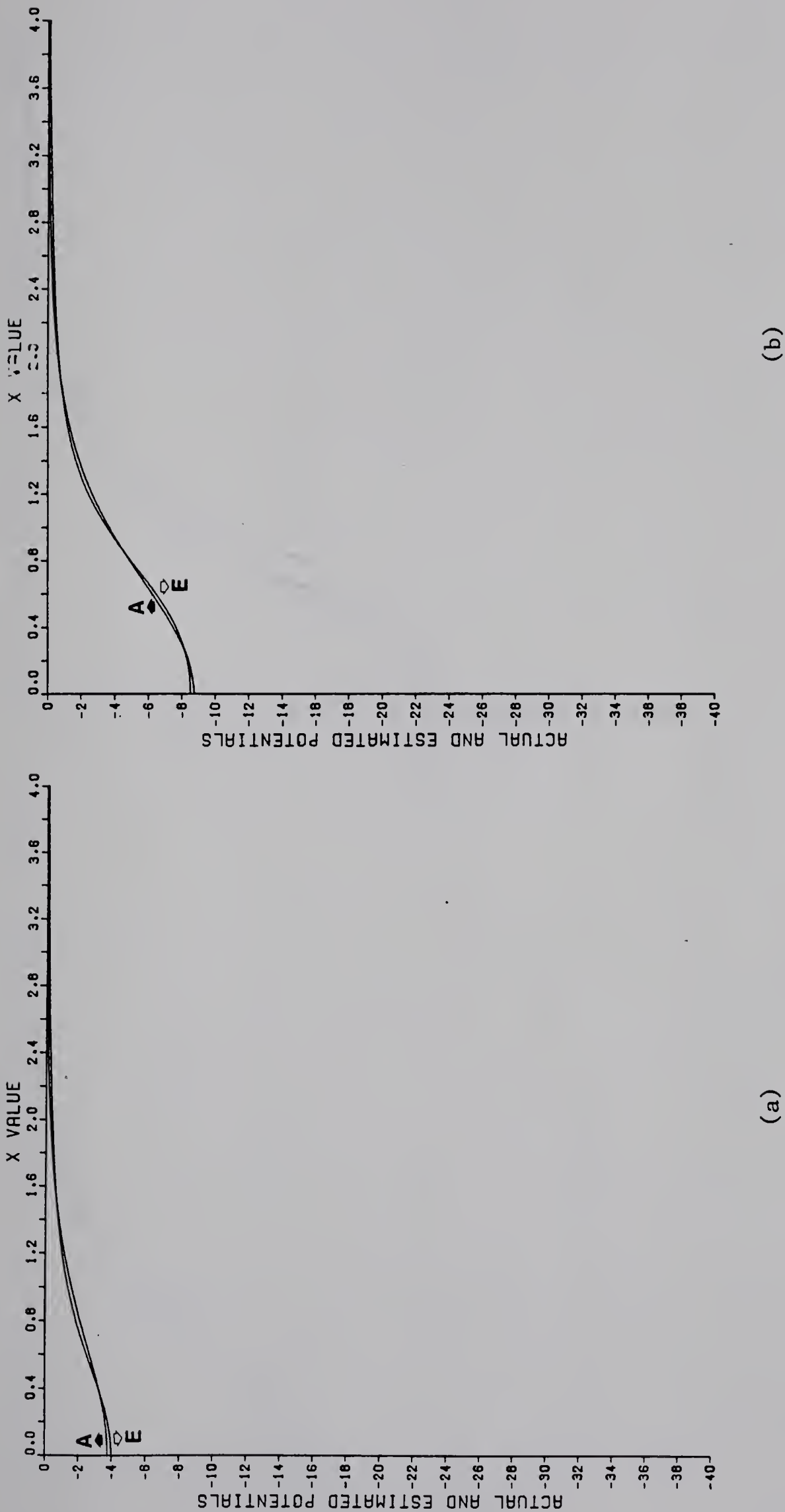
Fig. 3.7. Reflectionless approximation for potentials with the same reflection coefficient but different depths:

(a) Pöschl-Teller potential with $\lambda = 2.5$ (A) and the corresponding reflectionless approximation (E).

(b) Pöschl-Teller potential with $\lambda = 3.5$ (A) and the corresponding reflectionless approximation (E).

(a)

(b)
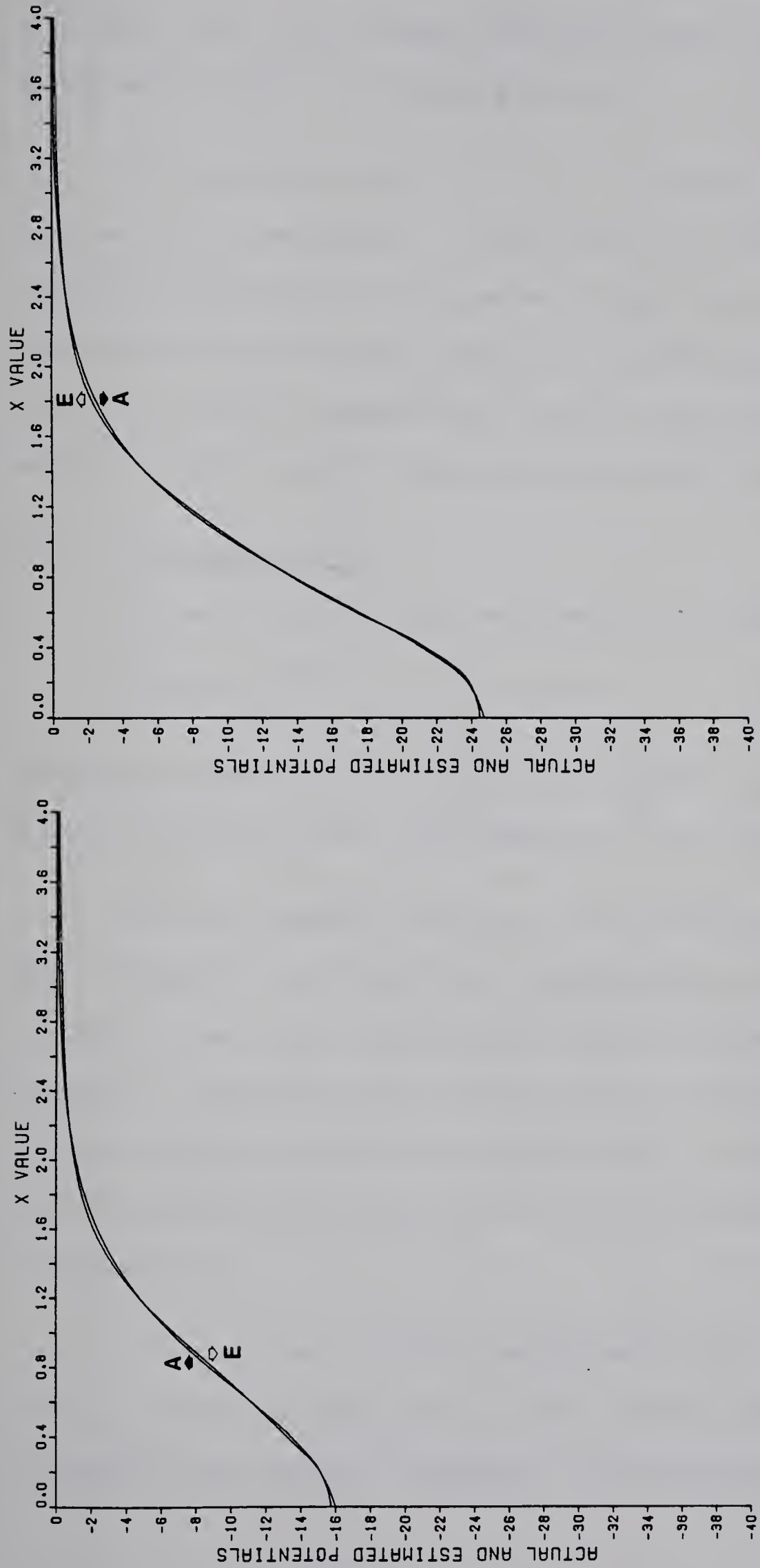
Fig. 3.8. Reflectionless approximation for potentials with the same reflection coefficient but different depths:

(a) Pöschl-Teller potential with $\lambda = 4.5$ (A) and the corresponding reflectionless approximation (E).

(b) Pöschl-Teller potential with $\lambda = 5.5$ (A) and the corresponding reflectionless approximation (E).

where else. The reflectionless potential, though not the same exactly, is extremely close to the actual potential.

The potentials with λ = 2.5, 3.5, 4.5 and 5.5 have exactly the same reflection coefficient. It was, therefore, interesting to see if there is a difference in the agreement between the reflectionless and the actual potential in these cases. We see from Figure 3.7 and Figure 3.8 that the overall agreement gets better as the potential gets deeper despite the fact that the reflection coefficient remains the same.

3.1.2. The Gaussian Well.

Second in this category was a well of the kind

$$V(x) = -V_o \, e^{-x^2} \, , \qquad -\infty < x < \infty \, . \tag{3.1}$$

For obvious reasons, we call it a Gaussian Well. V_o is the depth of the well. Five such wells with different V_o were considered.

Since the analytic solution to the Schrödinger equation with such a potential is not known, the eigenvalues and the reflection co-efficient in each case were calculated using the numerical methods of Appendix B. Eigenvalues and the zeros of the reflection coefficients have been tabulated in Table 3.1 and Table 3.2. Reflection coefficients and the results of the inverse calculations are displayed in Figure 3.9 to Figure 3.13.

A zero of the reflection coefficient is that value of momentum where the reflection coefficient is zero to five places. Since we were interested in the general systematics of the reflection coefficient,

Table 3.1 Eigenvalues of the Gaussian Well

$$V(x) = -V_o e^{-x^2}; \quad -\infty < x < +\infty$$

Depth V_o (Eigenvalues in ascending order)	$E_1 = -\kappa_1^2$	$E_2 = -\kappa_2^2$	$E_3 = -\kappa_3^2$	$E_4 = -\kappa_4^2$	$E_5 = -\kappa_5^2$
2.0	$(-0.955)^*$ $(-0.954)^\dagger$				
8.0	$(-5.549)^*$ $(-5.549)^\dagger$	$(-1.568)^*$ $(-1.568)^\dagger$			
18.0	$(-14.135)^*$ $(-14.135)^\dagger$	$(-7.256)^*$ $(-7.256)^\dagger$	$(-2.278)^*$ $(-2.278)^\dagger$		
30.00	$(-24.900)^*$ $(-24.900)^\dagger$	$(-15.525)^*$ $(-15.525)^\dagger$	$(-7.918)^*$ $(-7.919)^\dagger$	$(-2.429)^*$ $(-2.430)^\dagger$	
46.0	$(-39.595)^*$ $(-39.594)^\dagger$	$(-27.592)^*$ $(-27.592)^\dagger$	$(-17.289)^*$ $(-17.290)^\dagger$	$(-8.901)^*$ $(-8.903)^\dagger$	$(-2.809)^*$ $(-2.810)^\dagger$

Note: * Corresponds to the numerical solution of the eigenvalue equation.

† Corresponds to the matrix method.

These symbols carry the same meaning in the following tables of eigenvalues, too.

Table 3.2 Zeros of the Reflection Coefficient: The Gaussian Well

$$V(x) = -V_o e^{-x^2} \; ; \quad -\infty < x < \infty$$

Momentum at which R is zero / Depth V_o	1st	2nd
2.0	1.04	3.46
8.0	0.82	3.52
18.0	3.54	
30.0	0.28	3.80
46.0	3.92	

(a)

(b)

(c)
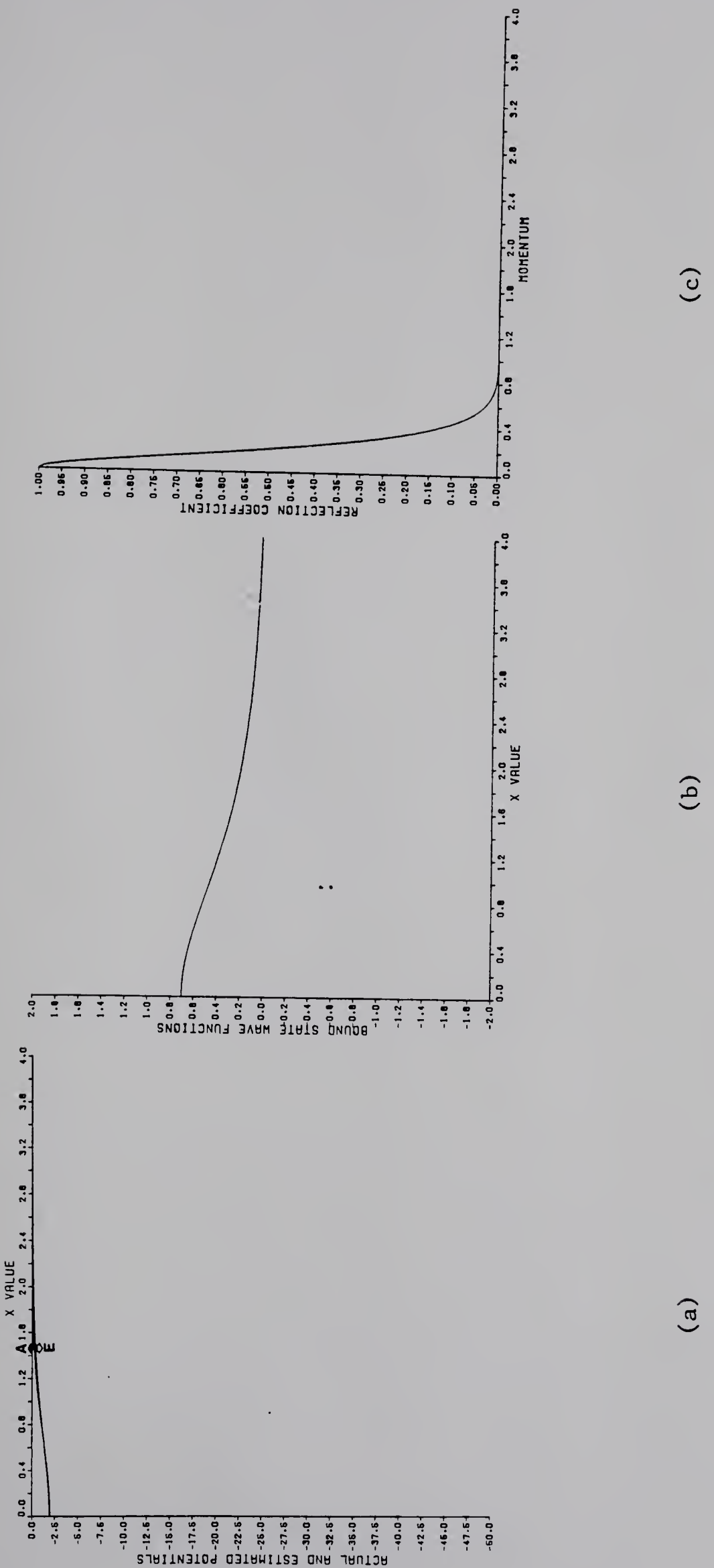
Fig. 3.9.   Results for the Gaussian Well ($V_0 = 2.0$):
(a) Actual (A) and reflectionless (E) potentials.
(b) Bound-state wavefunction of the reflectionless potential.
(c) The reflection coefficient.
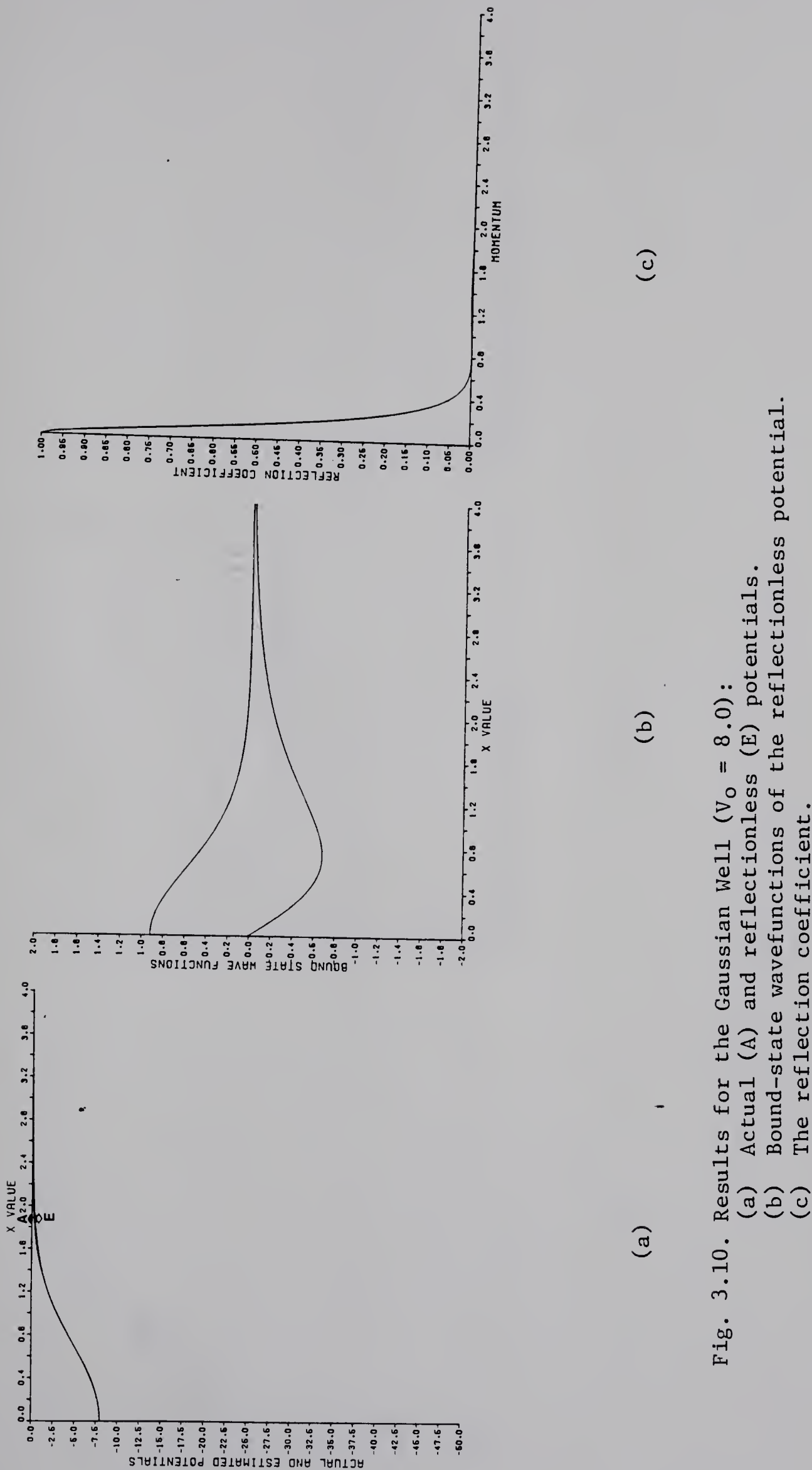
Fig. 3.10. Results for the Gaussian Well ($V_O = 8.0$):
(a) Actual (A) and reflectionless (E) potentials.
(b) Bound-state wavefunctions of the reflectionless potential.
(c) The reflection coefficient.

(a)

(b)

(c)
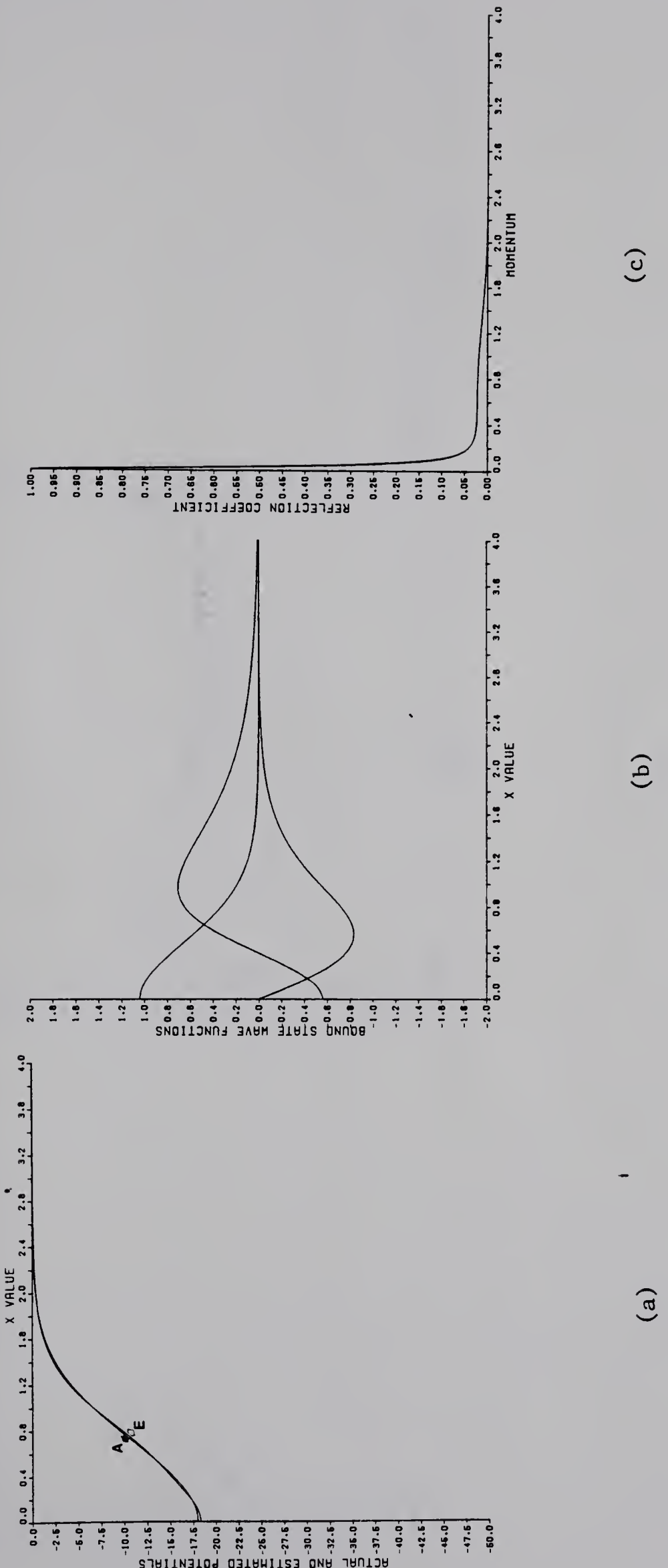
Fig. 3.11. Results for the Gaussian Well ($V_O = 18.0$):
    (a) Actual (A) and reflectionless (E) potentials.
    (b) Bound-state wavefunctions of the reflectionless potential.
    (c) The reflection coefficient.

(a)

(b)

(c)
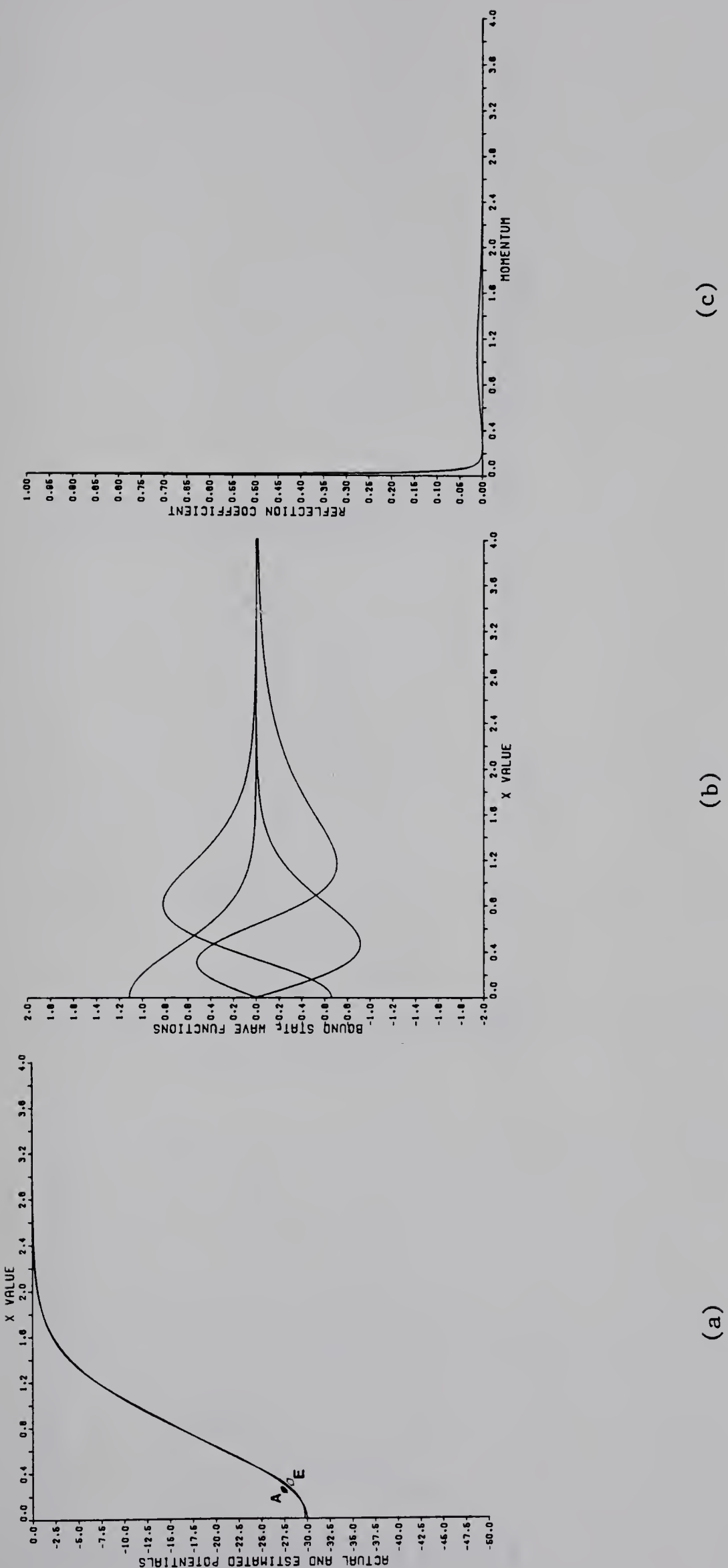
Fig. 3.12. Results for the Gaussian Well ($V_O = 30.0$):
  (a) Actual (A) and reflectionless (E) potentials.
  (b) Bound-state wavefunctions of the reflectionless potential.
 (c) The reflection coefficient.

(a)

(b)

(c)
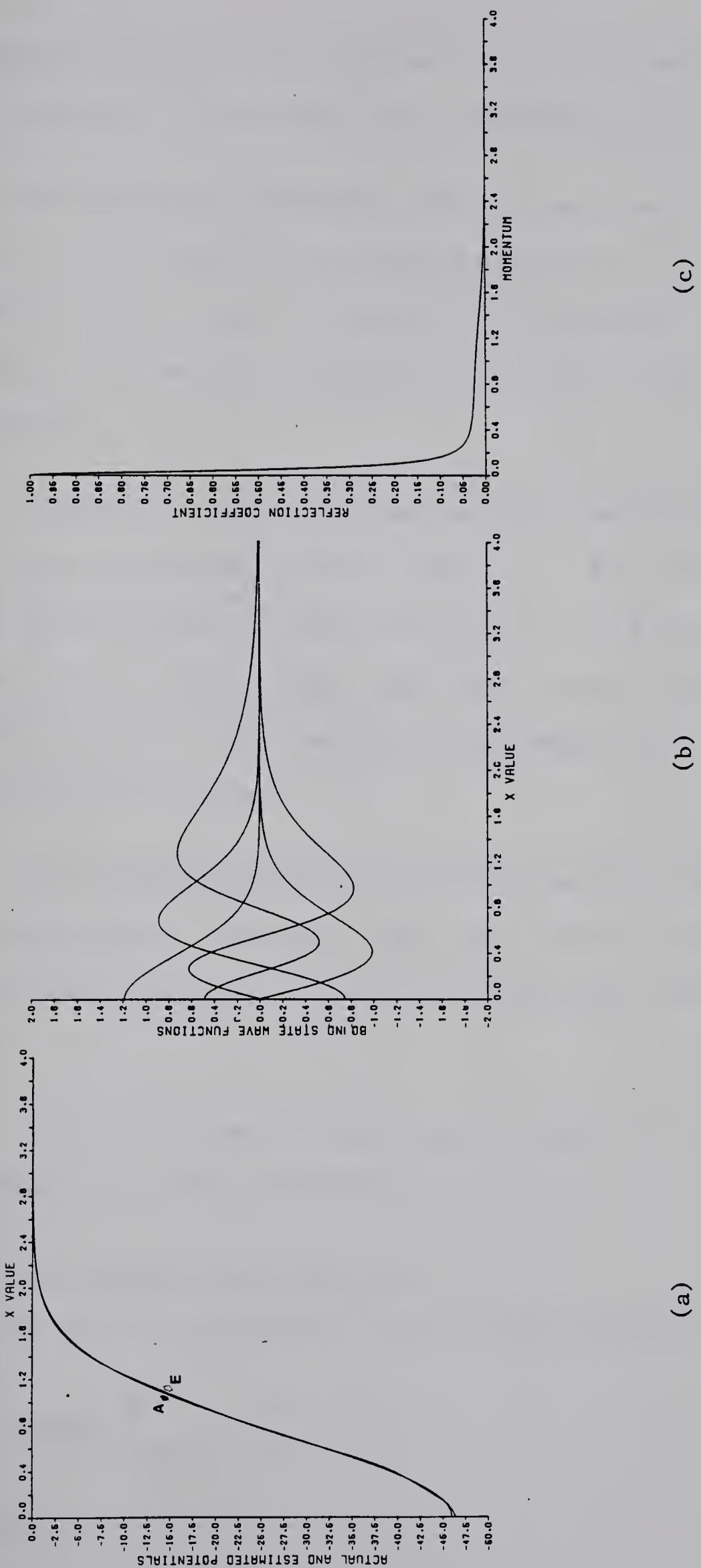
Fig. 3.13. Results for the Guassian Well ($V_O = 46.0$):
(a) Actual (A) and reflectionless (E) potentials.
(b) Bound-state wavefunctions of the reflectionless potential.
(c) The reflection coefficient.

no attempt was made to obtain the zeros to a higher accuracy. As we shall see shortly, these values prove sufficient for our purpose.

The reflection coefficient, in this case, has a complex behaviour. In the absence of an analytic form for it, it is difficult to predict anything about its behaviour for a general 'k'. However, in the range of momentum considered, viz. $k = 0.0$ to 5.0, it shows some regularities.

Firstly, it decays very fast and has a few zeros. Secondly, it shows certain periodicity with increase in V_o. For instance, the behaviour of the reflection coefficient for $V_o = 2.0$, 8.0 and 30.0 are similar - in each case, it has a zero close to $k = 0$. However, for $V_o = 18.0$ and 46.0, it has a zero at a very large k where its amplitude is practically zero anyway.

The agreement between the reflectionless approximation and the actual potential is, once again, very good. The fast decay of the reflection coefficient with increase in k again seems to be a favourable factor.

Within the scope of these numerical results, it seems difficult to go beyond these naive observations.

3.1.3. The Harmonic Oscillator Well.

As the next application, the following potential was considered

$$V(x) = \begin{cases} 0 & ; \ |x| \geq \alpha \\ -E_o + x^2 & ; \ |x| \leq \alpha \ . \end{cases} \qquad (3.2)$$

Obviously,

$$E_o = \alpha^2 \ . \tag{3.3}$$

An increase in E_o, thus, increases both the depth and the range of the potential. Five such potentials with different E_o were considered.

The eigenvalue equations for such potentials have already been derived in Appendix B. In order to calculate the eigenvalues of this potential using eqn. (B.10) and eqn. (B.11) we just need to know the even and odd solutions of the Schrödinger equation in the region $-\alpha \leq x \leq \alpha$. The Schrödinger equation in this region looks like

$$\frac{d^2\psi}{dx^2} + [E + \alpha^2 - x^2]\psi = 0 \ . \tag{3.4}$$

If we change the variable to

$$y = \sqrt{2}\ x$$

this equation is transformed into

$$\frac{d^2\psi}{dy^2} - (\frac{1}{4}\ y^2 + a)\psi = 0 \tag{3.6}$$

where

$$a = -\frac{1}{2}\ (E + \alpha^2) \ . \tag{3.7}$$

Equation (3.6) is the parabolic cylinder equation [62]. The even and odd solutions are given by [62]

$$\psi_e(x,k) = A_1 e^{-\frac{1}{2}x^2} M(\frac{1}{2}\ a + \frac{1}{4}, \frac{1}{2}, x^2) \tag{3.8}$$

and

$$\psi_o(x,k) = A_2 x e^{-\frac{1}{2}x^2} M(\frac{1}{2}\ a + \frac{3}{4}, \frac{3}{2}, x^2) \tag{3.9}$$

where A_1 and A_2 are the normalization constants and $M(a,b,x)$ is the

confluent hypergeometric function.

These solutions, for E < 0, were substituted in eqn. (B.10) and eqn. (B.11) of Appendix B to obtain the eigenvalue equations for this particular problem. The resulting equations were, then, numerically solved by the Regula-Falsi technique to obtain the bound-state energies [63].

Similarly, for E > 0, these solutions were used in eqn. (B.14) of Appendix B to calculate the reflection coefficient for various energies.

In both of these calculations, values of some confluent hypergoemetric functions $M(a,b,x)$ were required for some values of the parameters a, b and x. They were calculated by summing their respective infinite series [62] to a sufficient number of terms.

Table 3.3 and Table 3.4 list the eigenvalues and zeros of the reflection coefficient, respecitvely, for each of the five potentials of this kind which were considered. The inverse calculations and the reflection coefficients are plotted in Figure 3.14 to Figure 3.18.

The behaviour of the reflection coefficient as a function of k is reminiscent of the diffraction pattern in optics. Borrowing the terminology from there, the reflection coefficient shows a principal maximum and some pronounced secondary maxima. The agreement between the reflectionless and the actual potential, though tolerable, is not as good as in the case of Pöschl-Teller potentials or the Gaussian wells.

The secondary maxima and the overall amplitude of the reflection

Table 3.3 Eigenvalues of the Harmonic Oscillator Well

$$V(x) = \begin{cases} 0 & ; \ |x| \geq \alpha \\ -E_o + x^2 & ; \ |x| \leq \alpha \end{cases} \text{ with } E_o = \alpha^2$$

E_o \ Eigenvalues in Ascending order	$E_1 = -\kappa_1^2$	$E_2 = -\kappa_2^2$	$E_3 = -\kappa_3^2$	$E_4 = -\kappa_4^2$	$E_5 = -\kappa_5^2$
2.0	-1.069 (-1.069)* (-1.069)†				
4.0	-3.006 (-3.006)* (-3.005)†	-1.092 (-1.092)* (-1.091)†			
6.0	-5.001 (-5.001)* (-5.000)†	-3.011 (-3.011)* (-3.011)†	-1.106 (-1.106)* (-1.106)†		
8.0	-7.000 (-7.000)* (-7.000)†	-5.002 (-5.002)* (-5.001)†	-3.016 (-3.016)* (-3.016)†	-1.117 (-1.117)* (-1.117)†	
10.0	-9.000 (-9.000)* (-9.000)†	-7.000 (-7.000)* (-7.000)†	-5.002 (-5.002)* (-5.003)†	-3.020 (-3.020)* (-3.021)†	-1.125 (-1.125)* (-1.126)†

Note: The numbers without parentheses correspond to the calculation where the confluent hypergeometric functions were used in the eigenvalue equations.

Table 3.4 Zeros of the Reflection Coefficient: The Harmonic Oscillator Well.

$$V(x) = \begin{cases} 0 & ; \quad |x| \geq \alpha \\ -E_o + x^2 & ; \quad |x| \leq \alpha \end{cases} \text{ with } E_o = \alpha^2$$

E_o \ Momentum at which R is zero	1st	2nd	3rd	4th	5th	6th
2.0	0.7405	2.425	3.65	4.85		
4.0	0.7027	2.12	3.10	3.95	4.80	
6.0	0.6854	1.9992	2.867	3.65	4.35	
8.0	0.6748	1.9318	2.75	3.45	4.15	4.75
10.00	0.6673	1.8876	2.6638	3.329	3.95	4.55

(a)

(b)

(c)
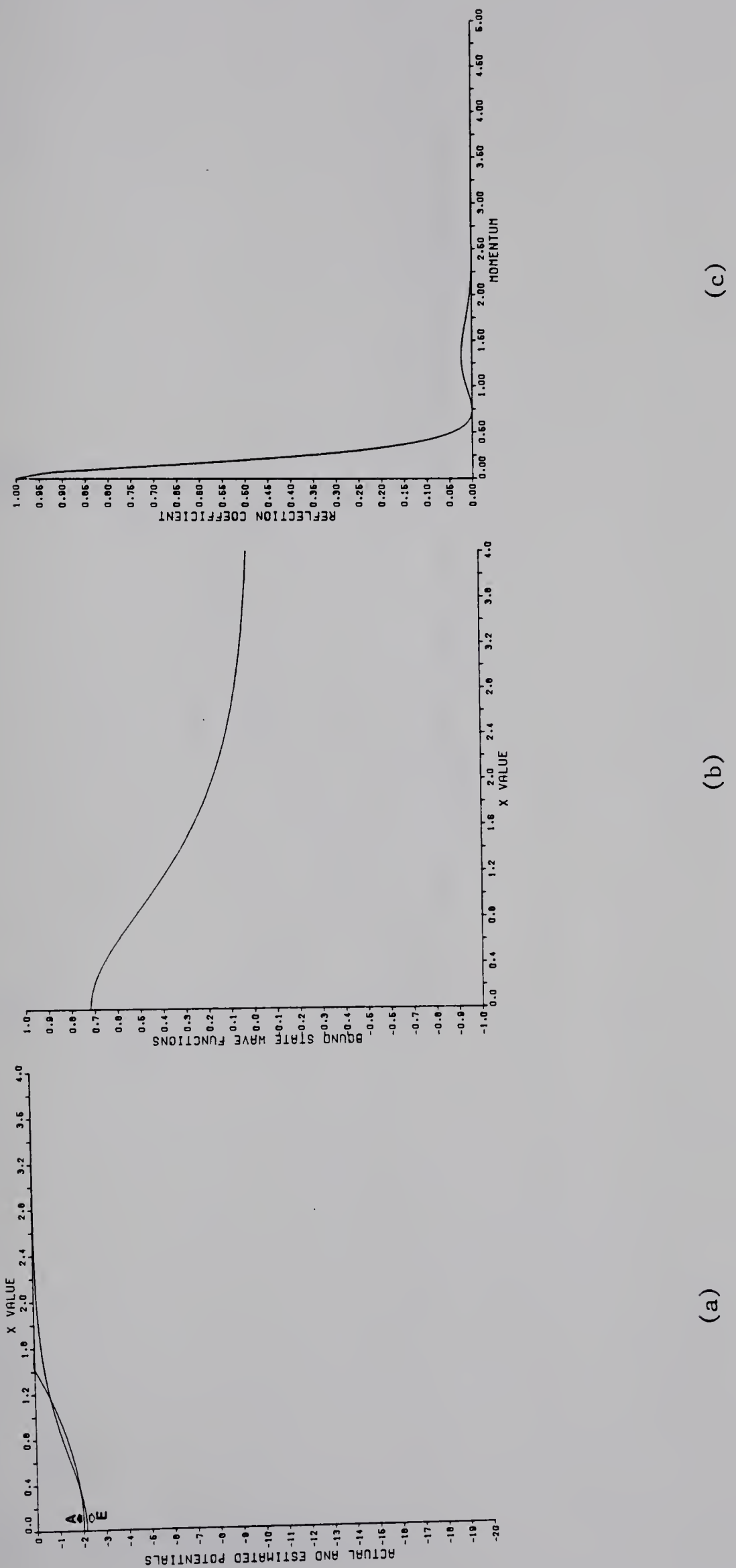
Fig. 3.14. Results for the Harmonic Oscillator Well (E_0 = 2.0):
(a) Actual (A) and reflectionless (E) potentials.
(b) Bound-state wavefunction of the reflectionless potential.
(c) The reflection coefficient.

(a)

(b)

(c)
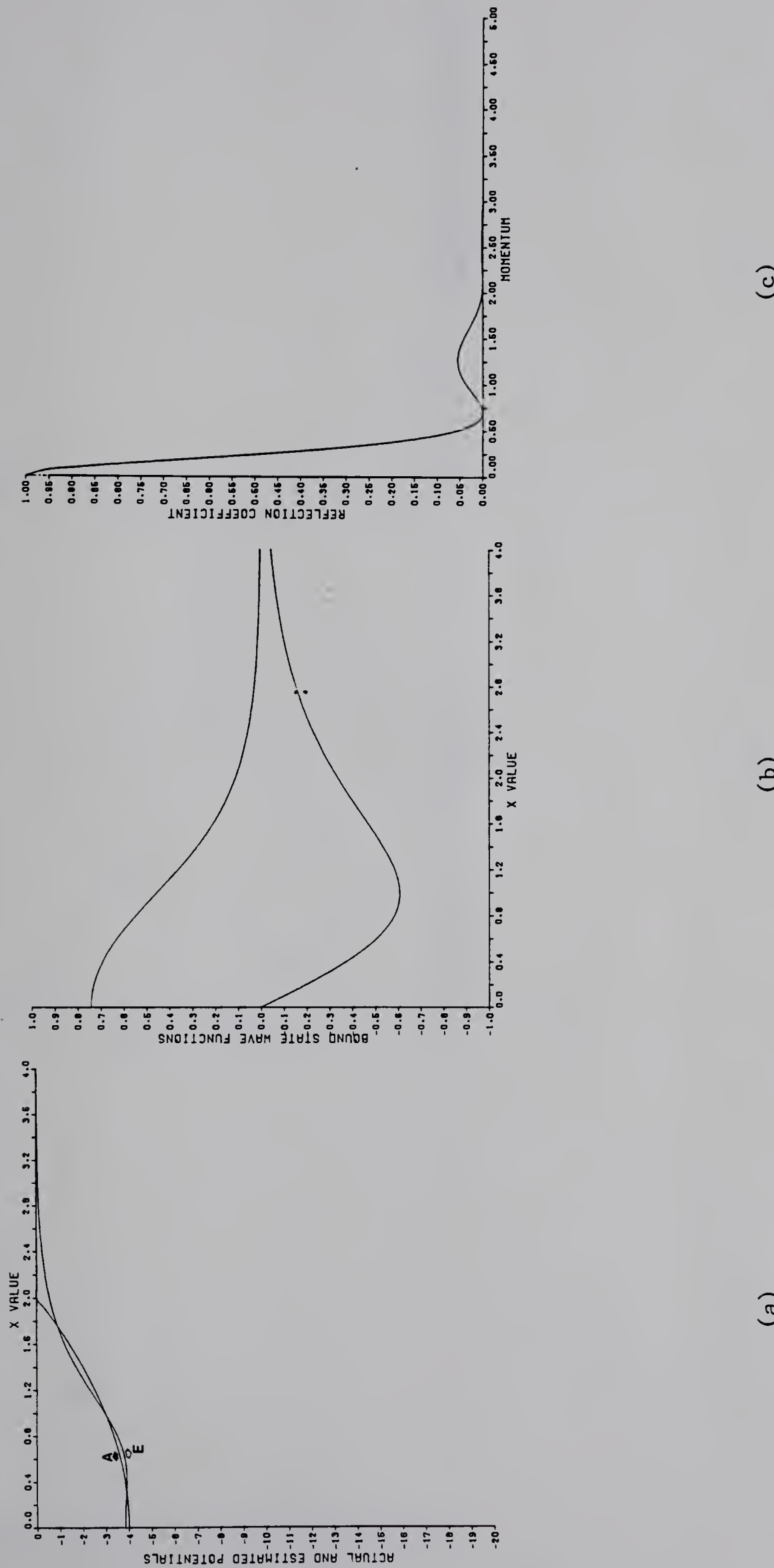
Fig. 3.15. Results for the Harmonic Oscillator Well ($E_O = 4.0$):
(a) Actual (A) and reflectionless (E) potentials.
(b) Bound-state wavefunctions of the reflectionless potential.
(c) The reflection coefficient.

(a)

(b)

(c)
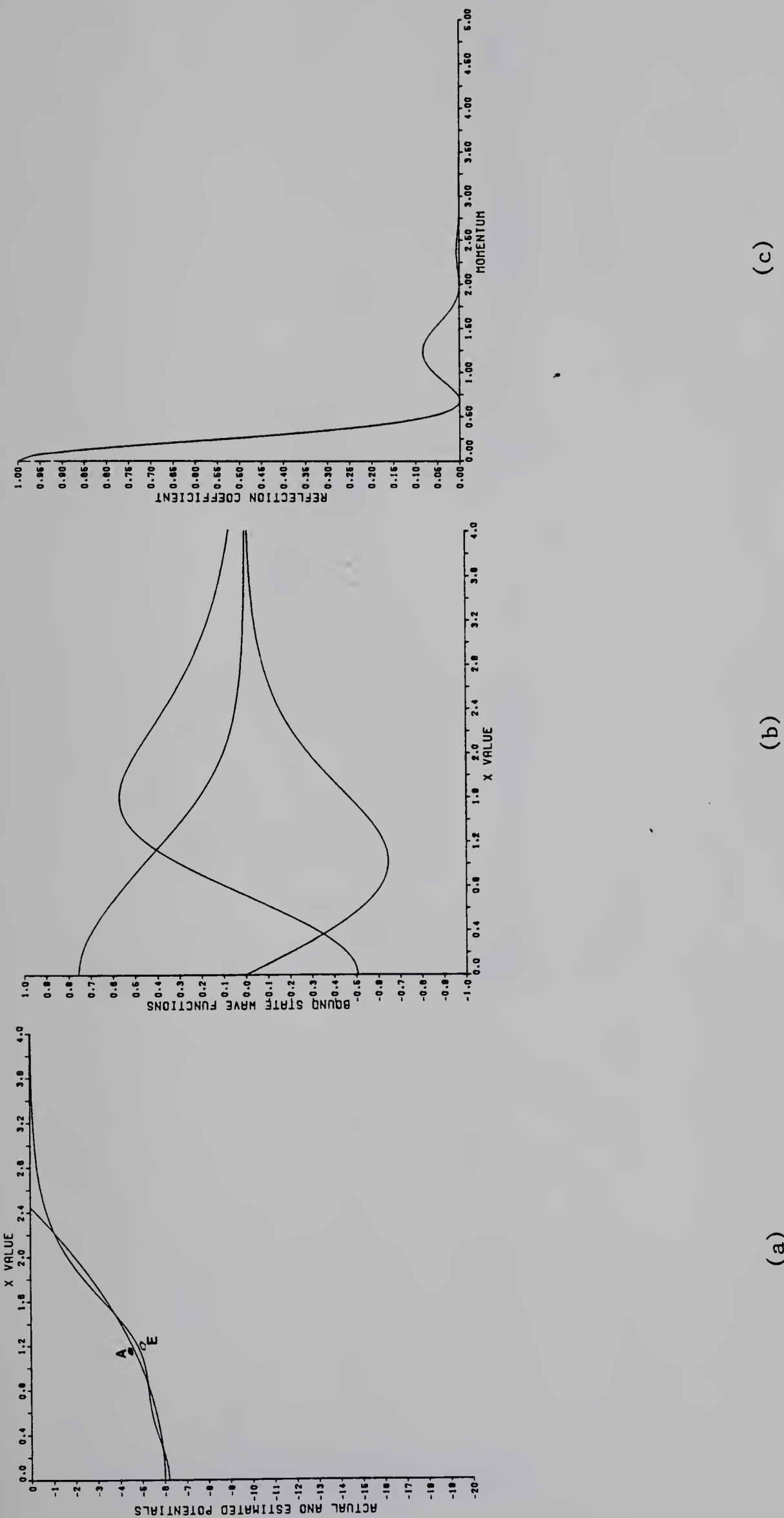
Fig. 3.16. Results for the Harmonic Oscillator Well (E_o = 6.0):
(a) Actual (A) and reflectionless (E) potentials.
(b) Bound-state wavefunctions of the reflectionless potential.
(c) The reflection coefficient.

(a)

(b)

(c)
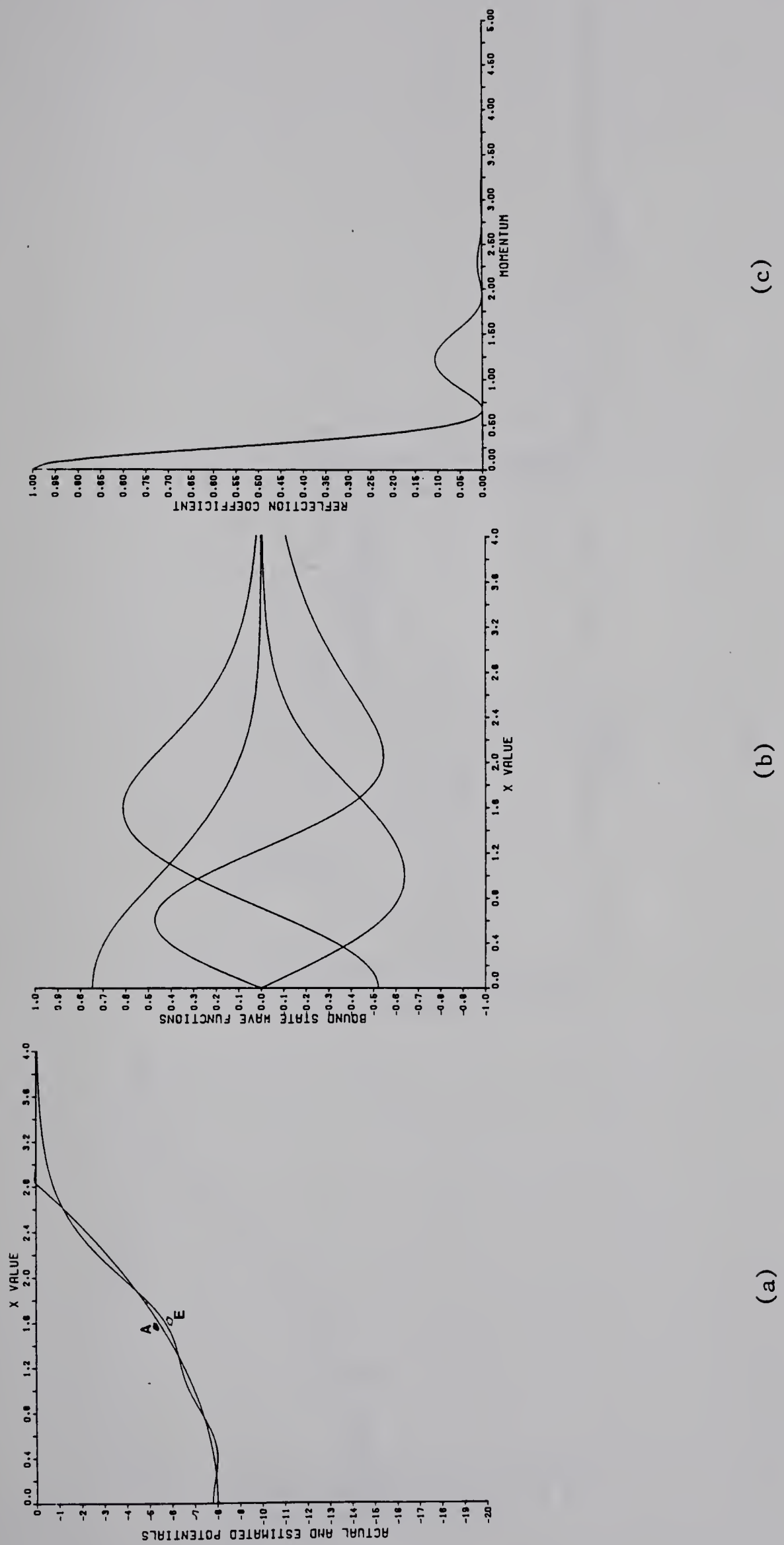
Fig. 3.17. Results for the Harmonic Oscillator Well ($E_o = 8.0$):
(a) Actual (A) and the reflectionless (E) potentials.
(b) Bound-state wavefunctions for the reflectionless potential.
(c) The reflection coefficient.

(a)   (b)   (c)
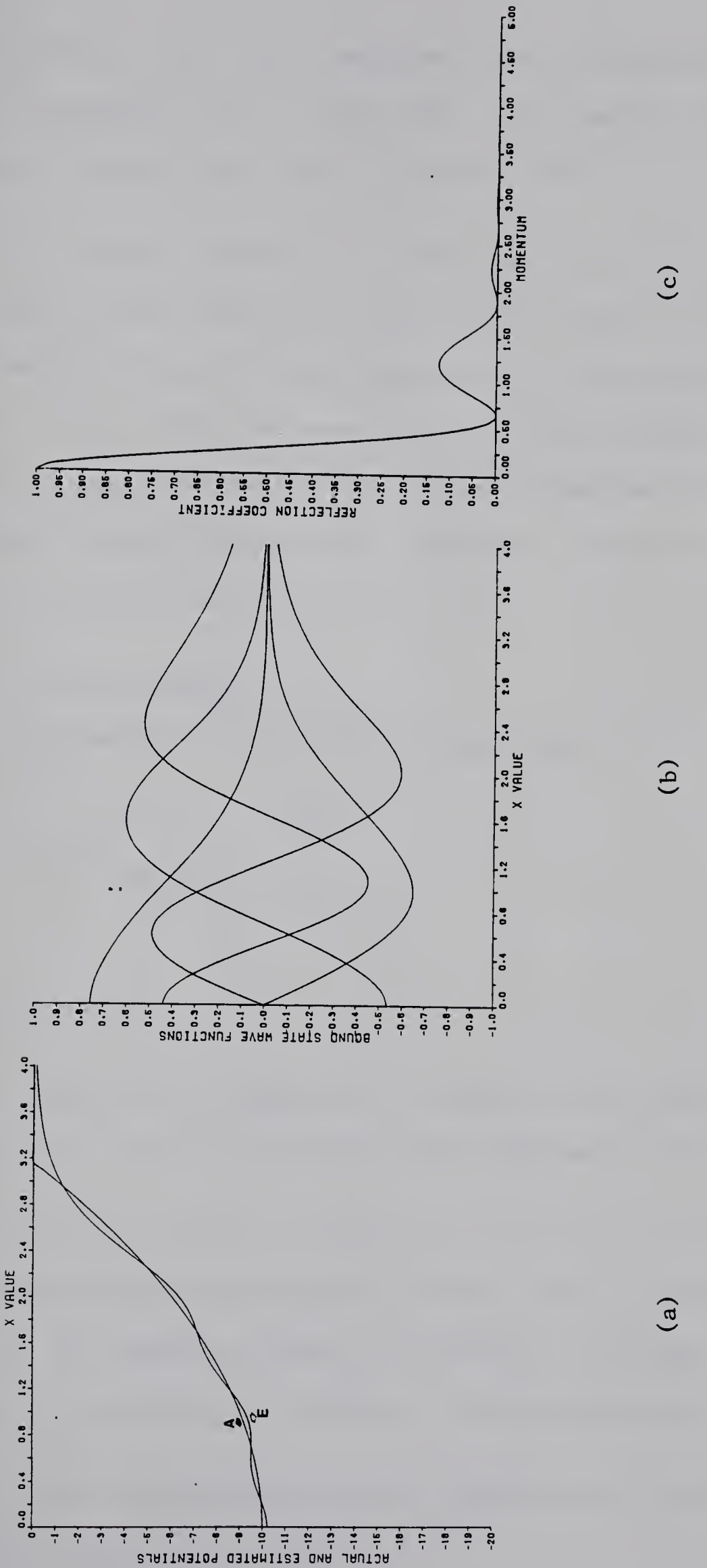
Fig. 3.18. Results for the Harmonic Oscillator Well ($E_O = 10.0$):
(a) Actual (A) and reflectionless (E) potentials.
(b) Bound-state wavefunctions of the reflectionless potential.
(c) The reflection coefficient.

coefficient get higher as E_o increases. The successive zeros, however, seem to be getting closer to each other. The change in the first zero is nominal but the others seem to cluster faster.

The inverse reconstructions show that the reflectionless potentials tend to settle down to a stable pattern, which is not very close to the actual potential, with increase in E_o. This observation is, of course, limited to the five cases which we have considered. There is, however, no suggestion either that the reflectionless potential will eventually diverge from the actual potential. So, we will still classify this case as a favourable one.

3.1.4. The Linear Well.

We consider the potential well given by

$$V(x) = \begin{cases} 0 & ; \ |x| \geq \alpha \\ -E_o + |x| & : \ |x| \leq \alpha \end{cases} . \tag{3.10}$$

Here

$$E_o = \alpha . \tag{3.11}$$

Again, a change in E_o changes both the depth and the range of the potential well. Five such potentials with different E_o were considered.

Our first concern, as usual, is to calculate the exact eigenvalues and reflection coefficient of each of these potential wells. In this case, the numerical methods of Appendix B were used. Table 3.5 and Table 3.6 summarize the results of these calculations.

Inverse calculations and the reflection coefficients have been plotted in Figure 3.19 to Figure 3.23.

Table 3.5 Eigenvalues of the Linear Well

$$V(x) = \begin{cases} 0 & ; |x| \geq \alpha \\ -E_o + |x| & ; |x| \leq \alpha \end{cases} \quad \text{with } E_o = \alpha$$

E_o \ Eigenvalues in Ascending order	$E_1 = -\kappa_1^2$	$E_2 = -\kappa_2^2$	$E_3 = -\kappa_3^2$	$E_4 = -\kappa_4^2$	$E_5 = -\kappa_5^2$
1.67845019	$(-0.692)^*$ $(-0.691)^\dagger$				
2.79315249	$(-1.775)^*$ $(-1.775)^\dagger$	$(-0.491)^*$ $(-0.490)^\dagger$			
3.66807351	$(-2.649)^*$ $(-2.649)^\dagger$	$(-1.332)^*$ $(-1.332)^\dagger$	$(-0.454)^*$ $(-0.454)^\dagger$		
4.45402433	$(-3.435)^*$ $(-3.435)^\dagger$	$(-2.116)^*$ $(-2.116)^\dagger$	$(-1.209)^*$ $(-1.209)^\dagger$	$(-0.402)^*$ $(-0.402)^\dagger$	
5.17032952	$(-4.152)^*$ $(-4.151)^\dagger$	$(-2.832)^*$ $(-2.832)^\dagger$	$(-1.922)^*$ $(-1.922)^\dagger$	$(1.086)^*$ $(1.086)^\dagger$	$(-0.386)^*$ $(-0.385)^\dagger$

Table 3.6   Zeros of the Reflection Coefficient: The Linear Well

$$V(x) = \begin{cases} 0 & ; \quad |x| \geq \alpha \\ -E_o + |x| & ; \quad |x| \leq \alpha \end{cases} \quad \text{with } E_o = \alpha$$

Momentum at which R is zero / E_o	1st	2nd	3rd	4th	5th	6th	7th	8th	9th	10th	11th	12th
1.67845019	1.044	1.923	3.44	3.79								
2.79315249	0.5365	1.633	2.125	2.996	3.307	4.22	4.45					
3.66807351	0.5411	1.315	1.989	2.355	3.01	3.276	3.954	4.17	4.87			
4.45402433	0.4467	1.2644	1.7062	2.242	2.542	3.076	3.312	3.86	4.06	4.62	4.79	
5.17032952	0.44985	1.1427	1.657	1.9953	2.452	2.709	3.167	3.38	3.848	4.03	4.51	4.67
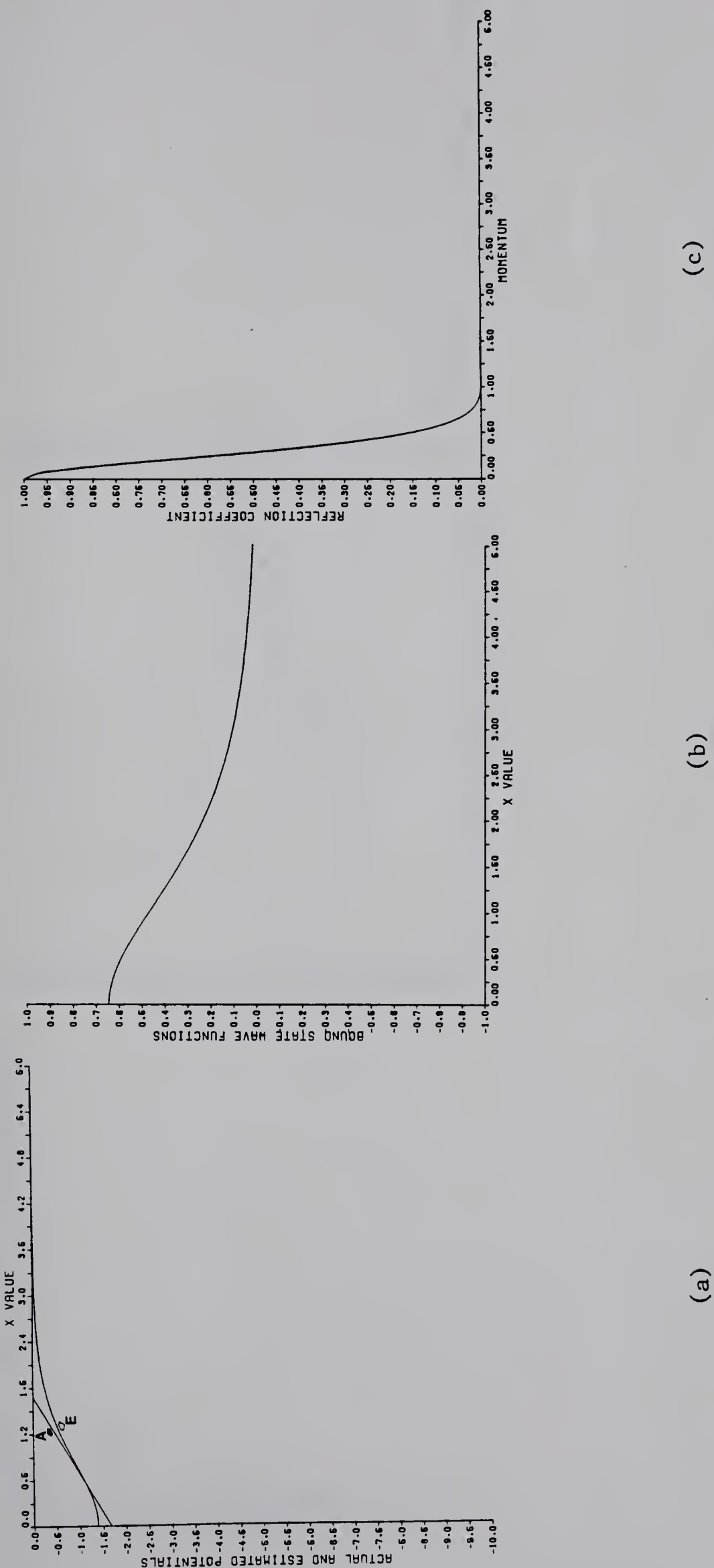
Fig. 3.19. Results for the Linear Well (E_O = 1.67845019):
(a) Actual (A) and reflectionless (E) potentials.
(b) Bound-state wavefunction of the reflectionless potential.
(c) The reflection coefficient.

(a)

(b)

(c)

(a)

(b)

(c)
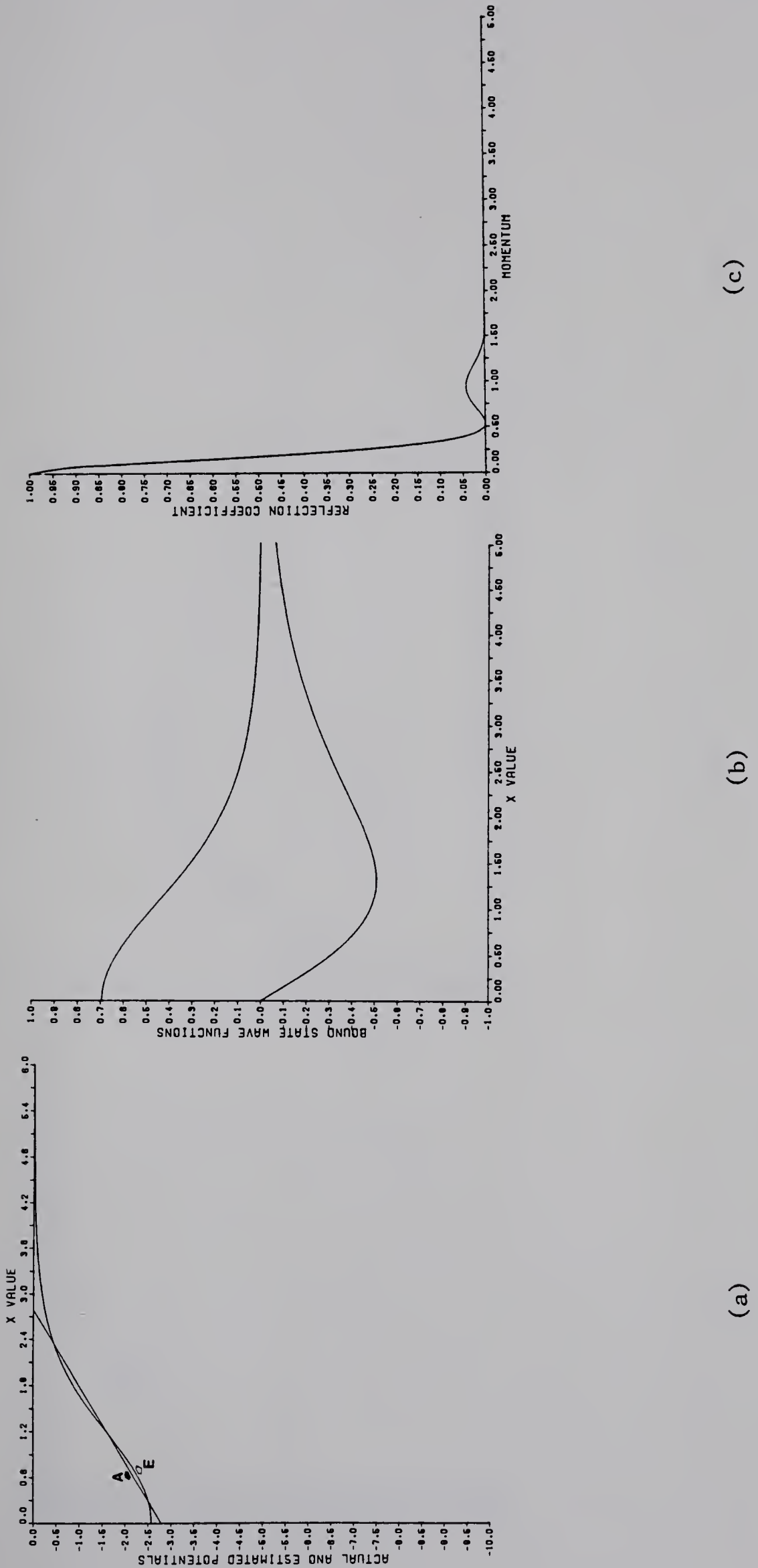
Fig. 3.20. Results for the Linear Well ($E_0 = 2.79315249$):
(a) Actual (A) and reflectionless (E) potentials.
(b) Bound-state wavefunctions of the reflectionless potential.
(c) The reflection coefficient.

(a)

(b)

(c)
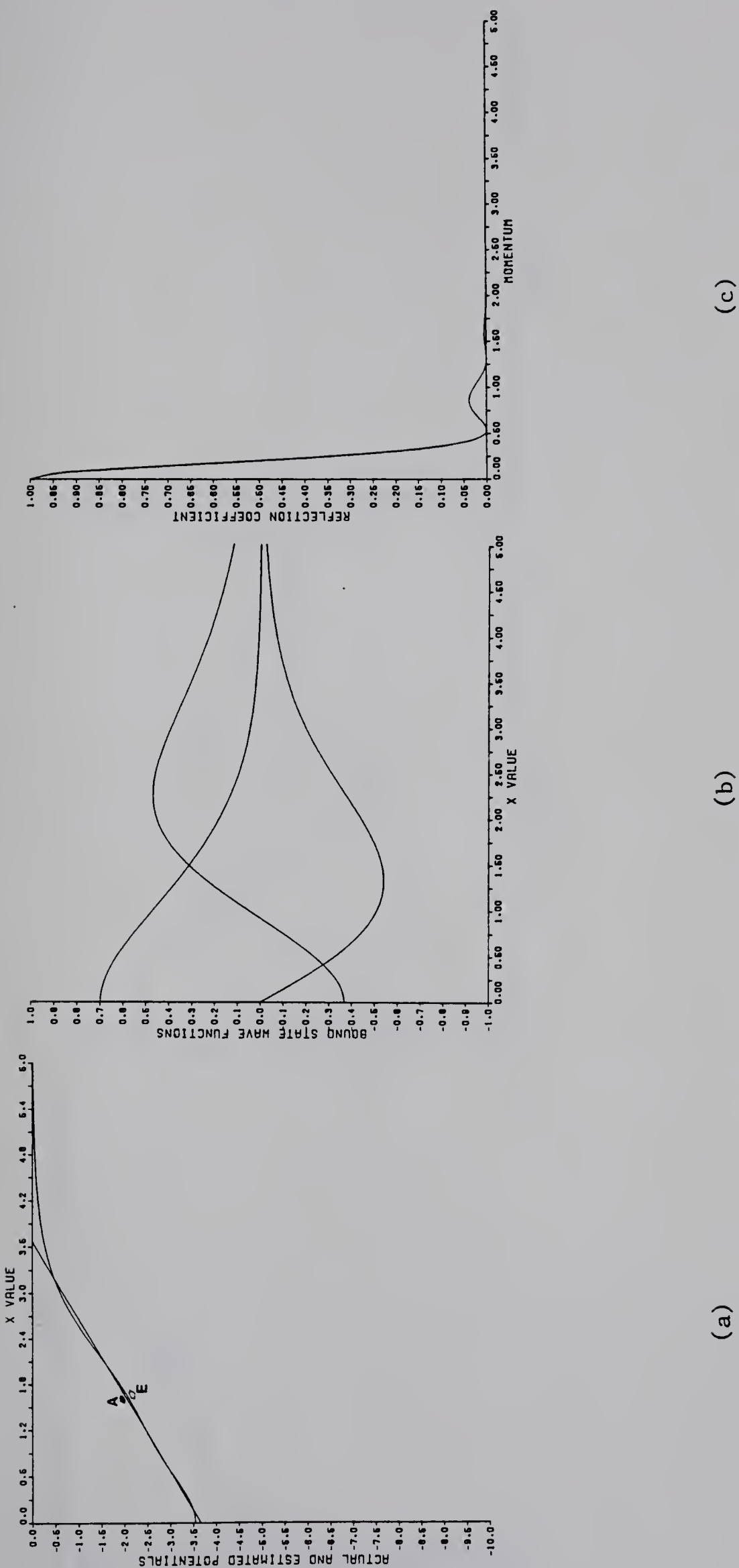
Fig. 3.21. Results for the Linear Well (E_0 = 3.66807351):
(a) Actual (A) and reflectionless (E) potentials.
(b) Bound-state wavefunctions of the reflectionless potential.
(c) The reflection coefficient.

(a)

(b)

(c)
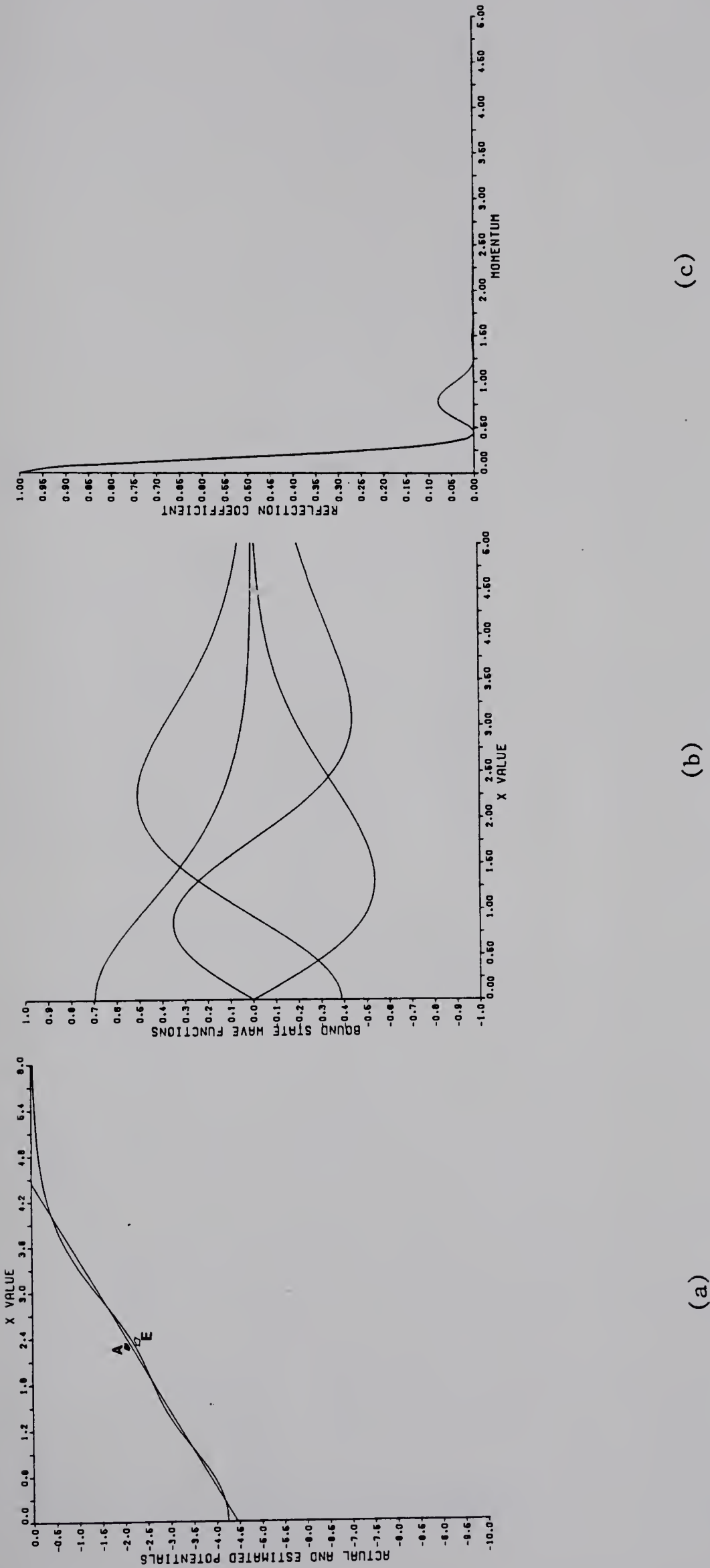
Fig. 3.22. Results for the Linear Well (E_0 = 4.45402433):
(a) Actual (A) and reflectionless (E) potentials.
(b) Bound-state wavefunctions of the reflectionless potential.
(c) The reflection coefficient.

(a)

(b)

(c)
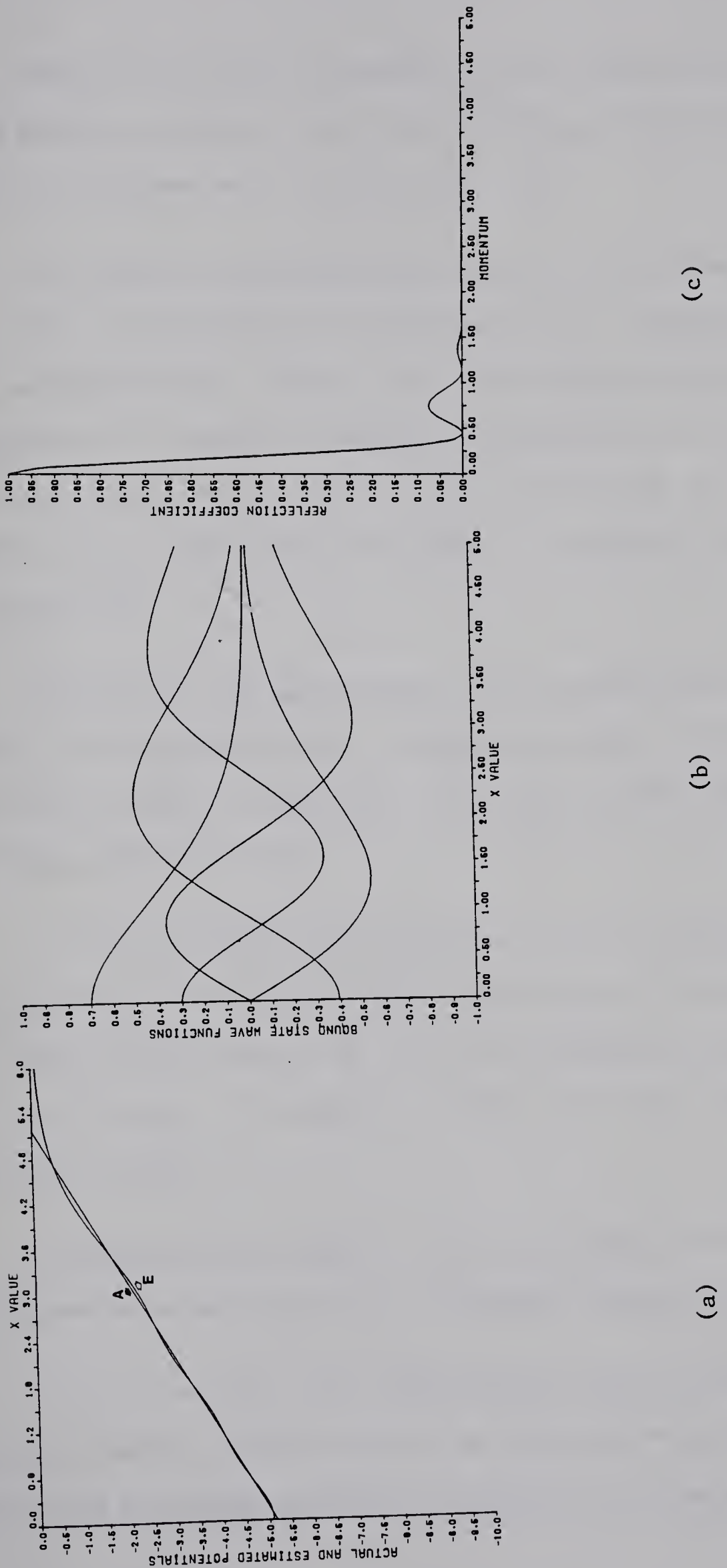
Fig. 3.23. Results for the Linear Well (E_O = 5.17032952):
(a) Actual (A) and reflectionless (E) potentials.
(b) Bound-state wavefunctions of the reflectionless potential.
(c) The reflection coefficient.

Despite its overall resemblance to the reflection coefficient of the harmonic oscillator well, the reflection coefficient of the linear well has some very distinctive features.

The number of observable peaks (up to five decimal places) shows a fast proliferation with increase in E_o in contrast to the harmonic oscillator well. However, the rate of decay of the reflection coefficient as a function of momentum is much faster in this case as compared to the harmonic oscillator well. With these two features together, as one would expect, the peaks are narrower in the case of the linear well.

For each E_o, the gaps between the successive zeros, in the case of the harmonic oscillator well, steadily decreased. In this case, they show some kind of periodicity. The first gap is larger, the second is smaller and so on.

The corresponding gaps in the zeros for two different E_o's are again periodic. With $E_o = 1.67845019$, for instance, the first is smaller, the second is larger and so on. For $E_o = 2.79315249$, on the other hand, the first is larger, the second is smaller and so on. This cycle alternates with each E_o.

The peaks do get narrower with increasing E_o but not necessarily in the same order because of the alternating behaviour described above.

Now, if we look at the reflectionless approximation we can immediately discern a better agreement in this case between the reflectionless and the actual potential as compared to the agreement in the

case of the harmonic oscillator well. First obvious reason seems to be the fact that the reflection coefficient decays much faster in this case.

Narrow peaks seem to favour the agreement. This was also obvious in the case of the harmonic oscillator well in a benign way. It is much more pronounced here as the overall decay does not seem to slow down appreciably with increase in E_o.

The periodicity in the behaviour of the reflection coefficient with increasing E_o seems to be reflected in the periodicity of the agreement between the two potentials. The dependence is curious but it cannot be unravelled by such a numerical exercise.

This potential seems to be much more promising than the harmonic oscillator well from the point of view of this approximation.

3.1.5. The Finite Square Well.

We now come back to the most familiar potential of elementary quantum mechanics, viz., the finite square well

$$V(x) = \begin{cases} 0 & ; \quad x < -a \\ -E_o & ; \quad -a < x < a \\ 0 & ; \quad x > a \end{cases} \tag{3.12}$$

For $E < 0$, we get bound states. Defining

$$k^2 = (E + E_o) \equiv (E_o - |E|) \tag{3.13}$$

$$\kappa^2 = -E \equiv |E| \tag{3.14}$$

the eigenvalue equation for the even-parity levels is given by [61]

$$k \tan ka = \kappa \tag{3.15}$$

and for the odd-parity levels is

$$k \cot ka = -\kappa \quad . \tag{3.16}$$

The even eigenfunctions are given by

$$\psi_{en}(x) = \begin{cases} A_+ \cos k_n x & ; \ 0 \le x \le a \\[2em] A_+ \cos k_n a \ e^{\kappa_n(a-x)} & ; \ x > a \\[2em] \psi_{en}(-x) = \psi_{en}(+x) & . \end{cases} \tag{3.17}$$

Similarly, the odd eigenfunctions are given by

$$\psi_{on}(x) = \begin{cases} A_- \sin k_n x & ; \ 0 \le x \le a \\[2em] A_- \sin k_n a \ e^{\kappa_n(a-x)} & ; \ x > a \\[2em] \psi_{on}(-x) = -\psi_{on}(x) & . \end{cases} \tag{3.18}$$

The normalization constants are given by

$$\frac{1}{A_\pm^2} = a + \frac{1}{\kappa_n} \tag{3.19}$$

for both cases.

For $E > 0$, we get the continuum states. The reflection for this case is well-known [64]

$$R = \left[1 + \frac{4|E|(|E| + E_0)}{E_0^2 \sin^2 \{2\sqrt{\frac{|E| + E_0}{\Delta}}\}} \right]^{-1} \tag{3.20}$$

where

$$\Delta = \frac{1}{a^2} \quad . \tag{3.21}$$

Five such potential wells were considered. All had the same width, viz., $a = \frac{\pi}{2}$. They were, however, of different depths. Eigenvalues were calculated by solving eqn. (3.15) and eqn. (3.16) numerically by the Newton-Raphson method [63]. Reflection coefficients were found by using eqn. (3.20). Table 3.7 and Table 3.8 list the eigenvalues and the zeros of the reflection coefficients respectively.

The results of the inverse calculations and the reflection coefficients are plotted in Figure 3.24 to Figure 3.28.

This is a highly reflecting potential. For smaller depths, the reflection coefficient is relatively smaller, but still higher than the harmonic oscillator well, or the linear well. With an increase in E_o, the peaks get wider and higher. In fact, the reflectionless approximation, though tolerable for wells of smaller depths, disagrees considerably with the actual potential as E_o is increased. There is no indication, whatsoever, that it converges to the actual potential. It does not even seem to settle down to a stable pattern; thus, exhibiting a diverging trend. We, therefore, classify this potential among the unfavourable ones for our approximation.

3.1.6. The Secant-Square Well.

Finally, we consider a potential well of the type

$$V(x) = \begin{cases} 0 & ; \ |x| \geq \alpha \\ \dfrac{8}{\cos^2 2x} - E_o & ; \ |x| \leq \alpha \end{cases} \qquad . \qquad (3.22)$$

Obviously the range α and E_o are related by

Table 3.7 Eigenvalues of the Finite Square Well

$$V(x) = \begin{cases} 0 & ; \ x < -\pi/2 \\ -E_o & ; \ -\pi/2 < x < \pi/2 \\ 0 & ; \ x > \pi/2 \end{cases}$$

Eigenvalues in Ascending Order E_o	$E_1 = -\kappa_1^2$	$E_2 = -\kappa_2^2$	$E_3 = -\kappa_3^2$	$E_4 = -\kappa_4^2$	$E_5 = -\kappa_5^2$	$E_6 = -\kappa_6^2$
2.5	-2.002 (-2.002)*	-0.680 (-0.680)*				
6.5	-5.864 (-5.864)*	-4.017 (-4.017)*	-1.257 (-1.257)*			
12.5	-11.784 (-11.784)*	-9.664 (-9.664)*	-6.250 (-6.250)*	-1.904 (-1.904)*		
20.5	-19.732 (-19.732)*	-17.446 (-17.446)*	-13.693 (-13.693)*	-8.606 (-8.606)*	-2.594 (-2.594)*	
30.5	-29.697 (-29.697)*	-27.296 (-27.296)*	-23.330 (-23.330)*	-17.863 (-17.863)*	-11.043 (-11.043)*	-3.315 (-3.315)*

Note: Numbers without the parentheses correspond to an exact solution by a numerical search technique.

Table 3.8 Zeros of the Reflection Coefficient: The Finite Square Well

$$V(x) = \begin{cases} 0 & ; \quad x < -\pi/2 \\ -E_o & ; \quad -\pi/2 < x < \pi/2 \\ 0 & ; \quad x > \pi/2 \end{cases}$$

Momentum at which R is zero E_o	1st	2nd	3rd	4th
2.5	1.22474	2.54951	3.67423	4.74342
6.5	1.58114	3.08221	4.30116	
12.5	1.87083	3.53553	4.84768	
20.5	2.12132	3.93700		
30.5	2.34521	4.30116		

(a)   (b)

(c)
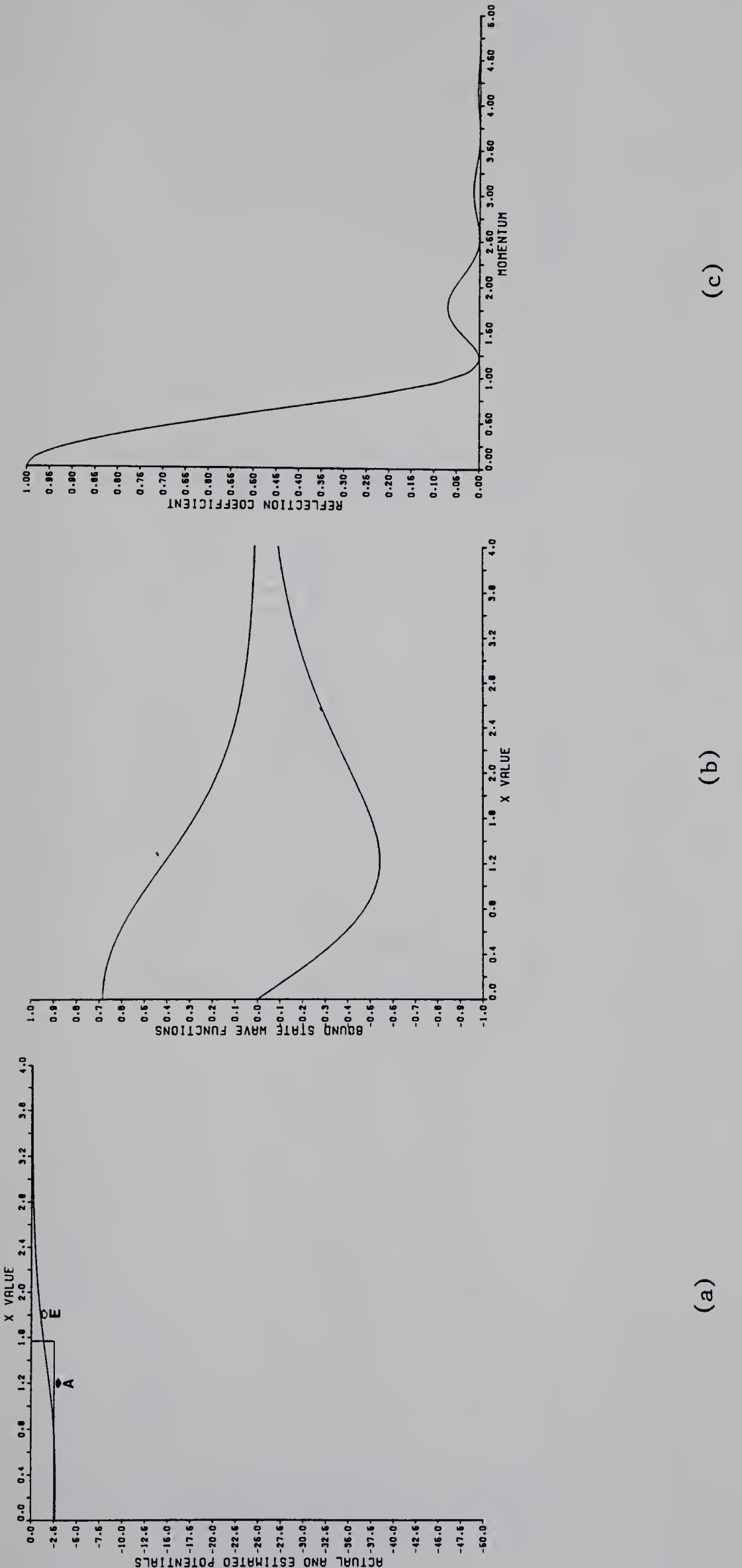
Fig. 3.24. Results for the Finite Square Well ($E_0 = 2.5$):
   (a) Actual (A) and reflectionless (E) potentials.
   (b) Bound-state wavefunctions of the reflectionless potential.
   (c) The reflection coefficient.

(a)

(b)

(c)
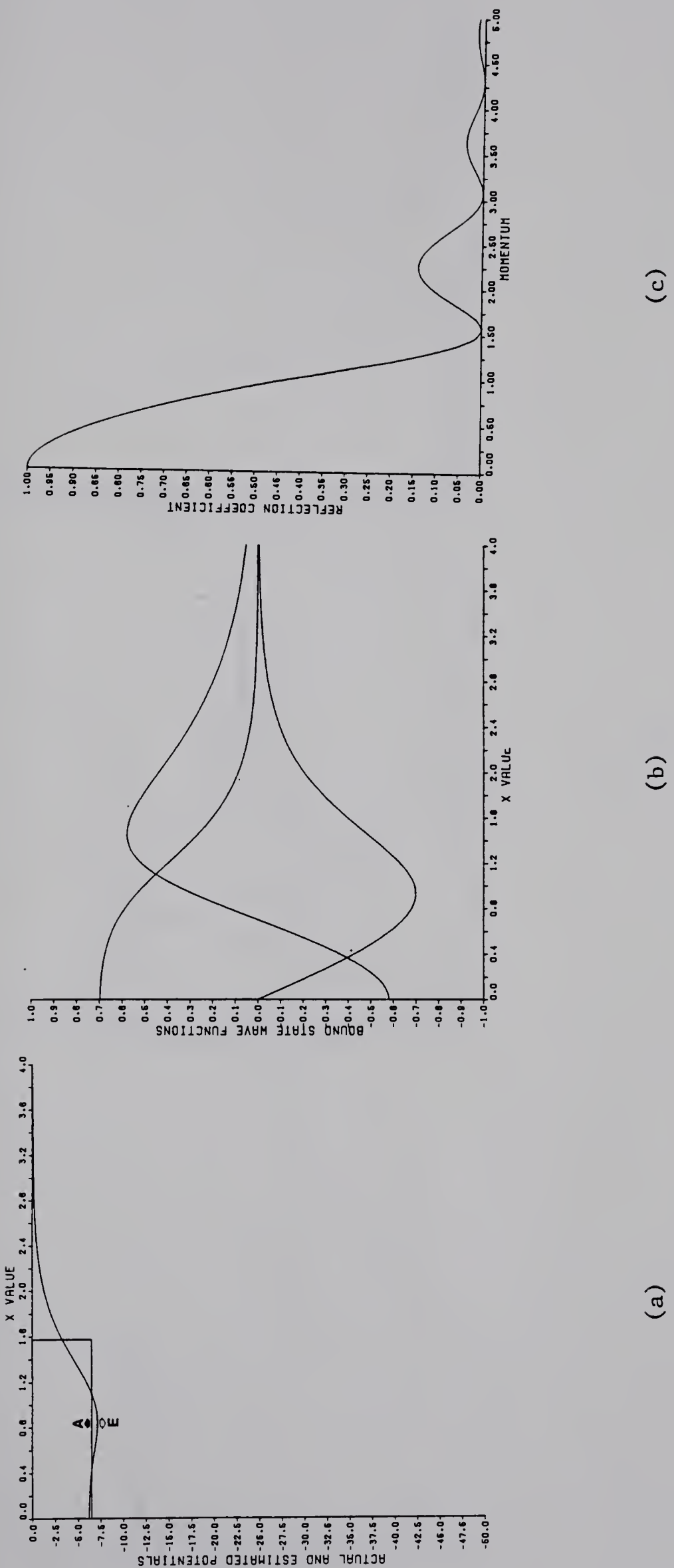
Fig. 3.25. Results for the Finite Square Well ($E_O = 6.5$):
(a) Actual (A) and reflectionless (E) potentials.
(b) Bound-state wavefunctions of the reflectionless potential.
(c) The reflection coefficient.
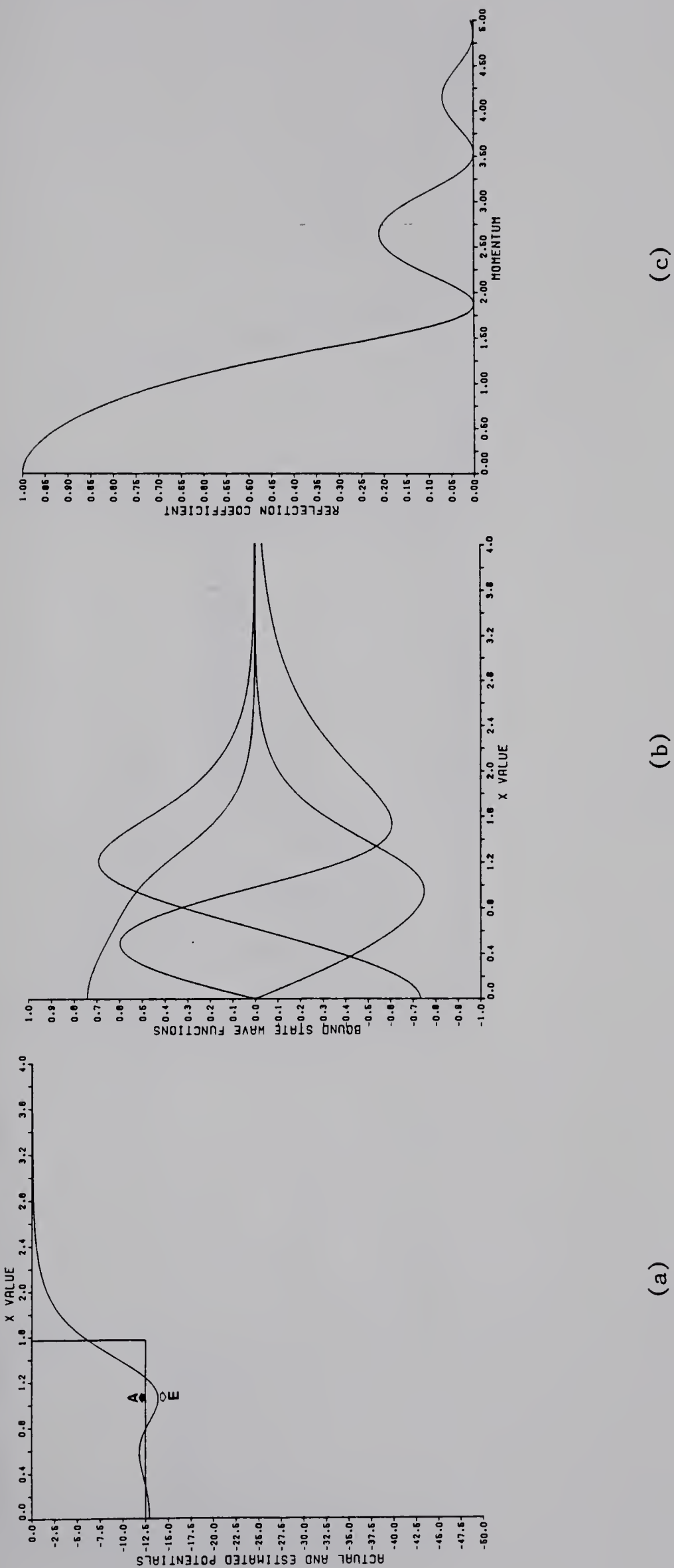
Fig. 3.26. Results for the Finite Square Well ($E_0 = 12.5$):
(a) Actual (A) and reflectionless (E) potential.
(b) Bound-state wavefunctions of the reflectionless potential.
(c) The reflection coefficient.
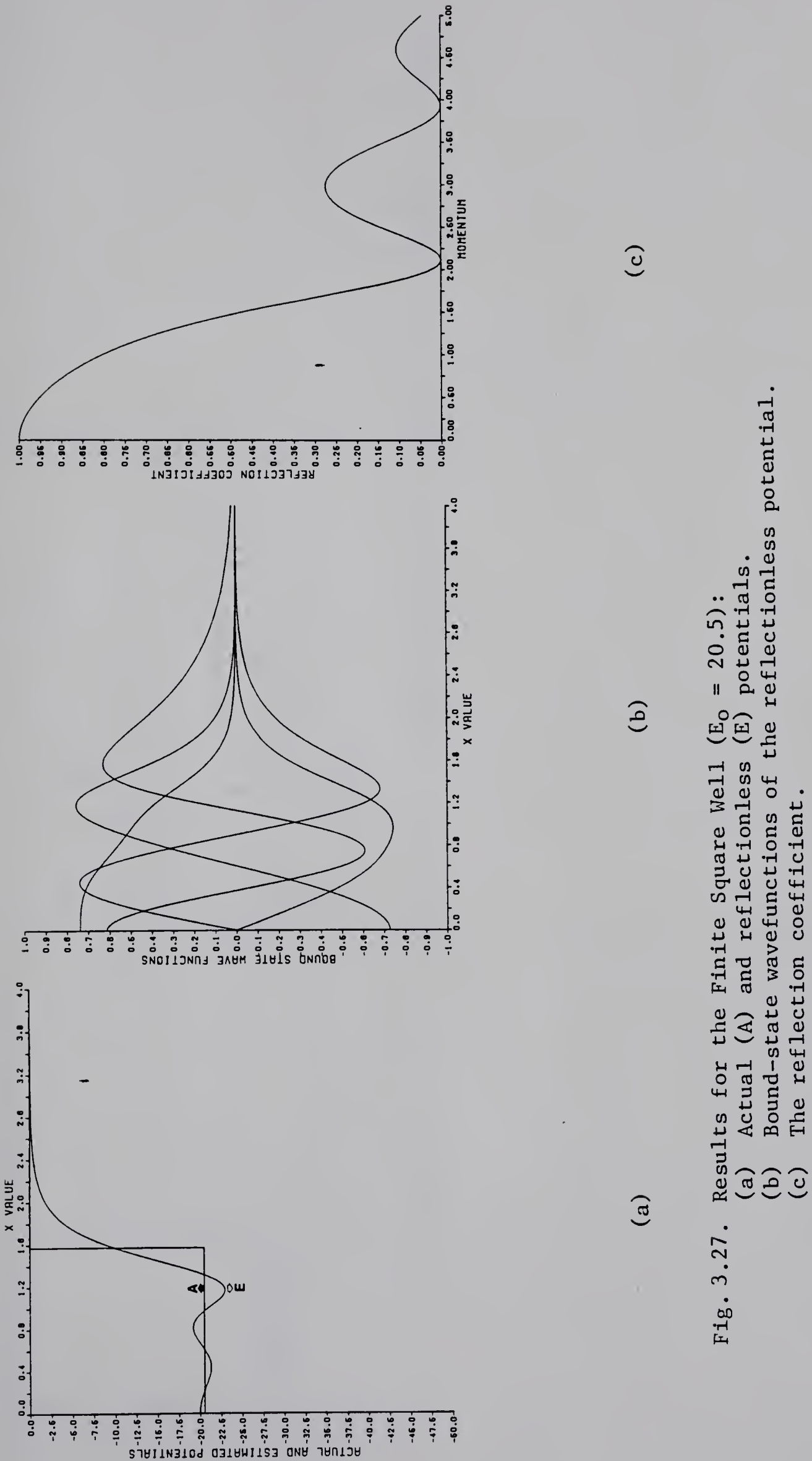
Fig. 3.27. Results for the Finite Square Well (E_O = 20.5):
(a) Actual (A) and reflectionless (E) potentials.
(b) Bound-state wavefunctions of the reflectionless potential.
(c) The reflection coefficient.

(a)   (b)   (c)

(a)

(b)

(c)
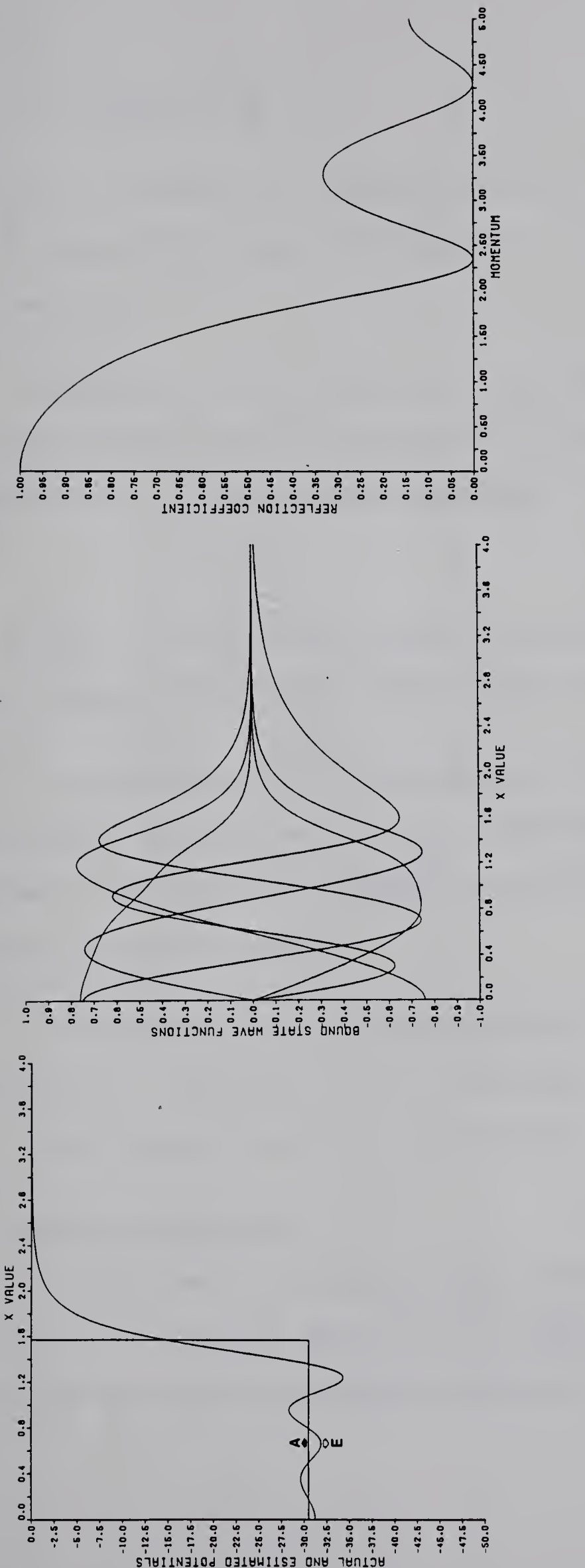
Fig. 3.28. Results for the Finite Square Well ($E_o = 30.5$).
(a) Actual (A) and reflectionless (E) potentials.
(b) Bound-state wavefunctions of the reflectionless potential.
(c) The reflection coefficient.

$$\alpha = \pm \frac{1}{2} \cos^{-1} \sqrt{\frac{8}{E_o}} \ . \tag{3.23}$$

Again, as in the case of the harmonic oscillator well and the linear well, a change in E_o changes the range α, too. Five different depths were considered.

Eigenvalues and the reflection coefficient were calculated by using the numerical methods of Appendix B. Eigenvalues and the zeros of the reflection coefficient are summarized in Table 3.9 and Table 3.10.

Results of the inverse calculations and the reflection coefficients are plotted in Figure 3.29 to Figure 3.33.

The behaviour of the reflection coefficient is rather complex in this case. The potential is highly reflecting. Finally, with an increase in depth ($E_o = 80.0$ onwards) the peaks of the reflection coefficient seem to get broader.

The reflectionless approximation seems to get worse with an increase in E_o. There is no sign of convergence to the actual potential, in much the same way as the square well.

3.2 Confining Potentials

As discussed in the introduction, the symmetric confining potentials in one-dimension form a class of their own for the application of the inverse scattering technique developed so far because of the

Table 3.9 Eigenvalues of the Secant-Square Well

$$V(x) = \begin{cases} 0 & ; \ |x| \geq \alpha \\ \dfrac{8}{\cos^2 2x} - E_o; & |x| \leq \alpha \end{cases} \quad \text{with } E_o = \pm \frac{1}{2} \cos^{-1} \sqrt{\frac{8}{E_o}}$$

Eigenvalues in ascending order E_o	$E_1 = -\kappa_1^2$	$E_2 = -\kappa_2^2$	$E_3 = -\kappa_3^2$	$E_4 = -\kappa_4^2$	$E_5 = -\kappa_5^2$
24.0	$(-9.328)^*$ $(-9.327)^\dagger$				
48.0	$(-32.402)^*$ $(-32.401)^\dagger$	$(-14.883)^*$ $(-14.883)^\dagger$			
80.0	$(-64.174)^*$ $(-64.174)^\dagger$	$(-45.160)^*$ $(-45.160)^\dagger$	$(-20.679)^*$ $(-20.679)^\dagger$		
120.0	$(-104.092)^*$ $(-104.091)^\dagger$	$(-84.589)^*$ $(-84.589)^\dagger$	$(-58.196)^*$ $(-58.196)^\dagger$	$(-26.657)^*$ $(-26.658)^\dagger$	
168.0	$(-152.054)^*$ $(-152.054)^\dagger$	$(-132.341)^*$ $(-132.341)^\dagger$	$(-105.228)^*$ $(-105.228)^\dagger$	$(-71.449)^*$ $(-71.450)^\dagger$	$(-32.779)^*$ $(-32.781)^\dagger$

Table 3.10 Zeros of the Reflection Coefficient: The Secant-Square Well

$$V(x) = \begin{cases} 0 & ; \ |x| \geq \alpha \\ \dfrac{8}{\cos^2 2x} - E_o & ; \ |x| \leq \alpha \end{cases} \quad \text{with } E_o = \pm \frac{1}{2} \cos^{-1} \sqrt{\frac{8}{E_o}}$$

Momentum at which R is zero / E_o	1st	2nd	3rd	4th
24.0	1.335	6.712	10.486	14.02
48.0	1.273	6.814	10.302	13.443
80.0	1.263	7.23	10.75	13.838
120.0	1.269	7.696	11.328	14.453
168.0	1.2831	8.162	11.933	

105
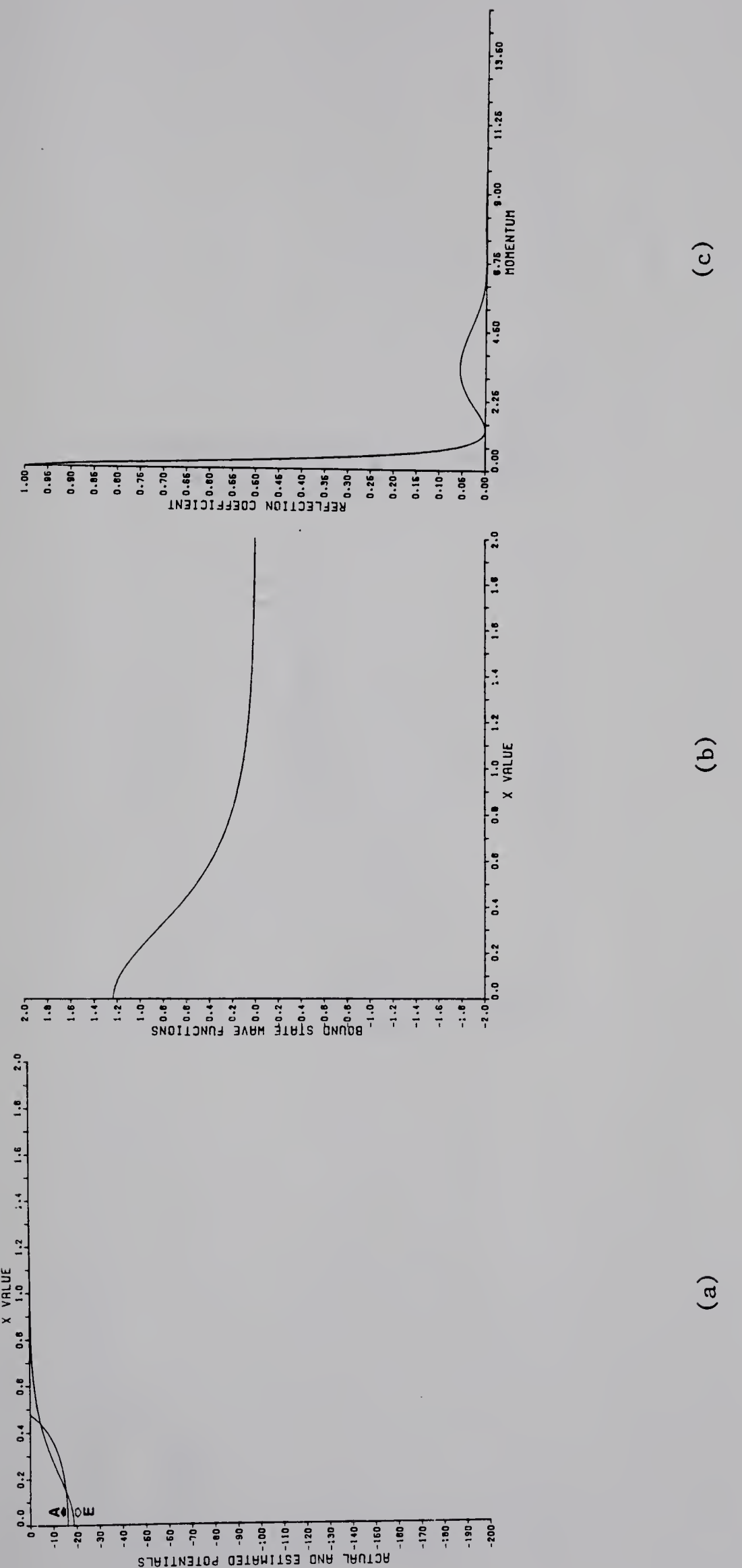
Fig. 3.29. Results for the Secant-Square Well (E_0 = 24.0):
(a) Actual (A) and reflectionless (E) potentials.
(b) Bound-state wavefunction of the reflectionless potential.
(c) The reflection coefficient.
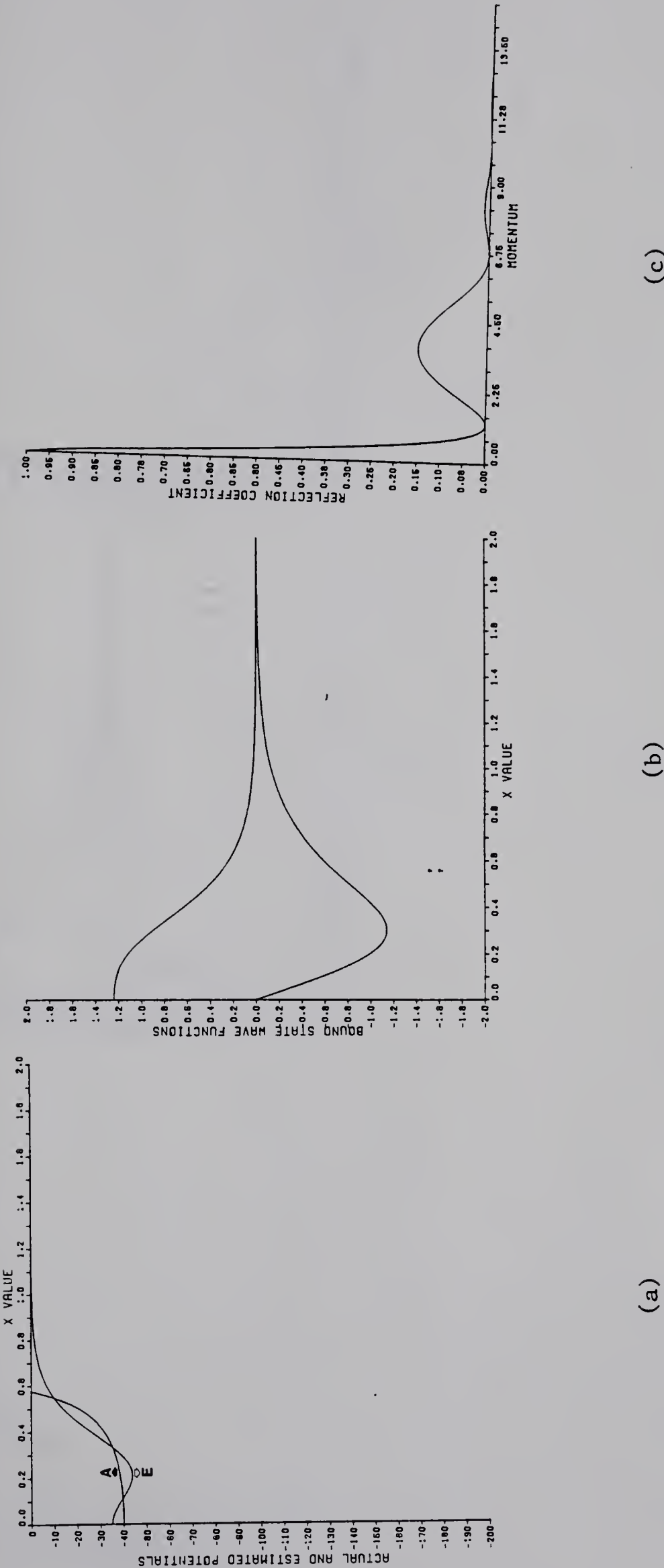
Fig. 3.30. Results for the Secant-Square Well (E_0 = 48.0):
(a) Actual (A) and reflectionless (E) potentials.
(b) Bound-state wavefunctions of the reflectionless potential.
(c) The reflection coefficient.

(a)

(b)

(c)
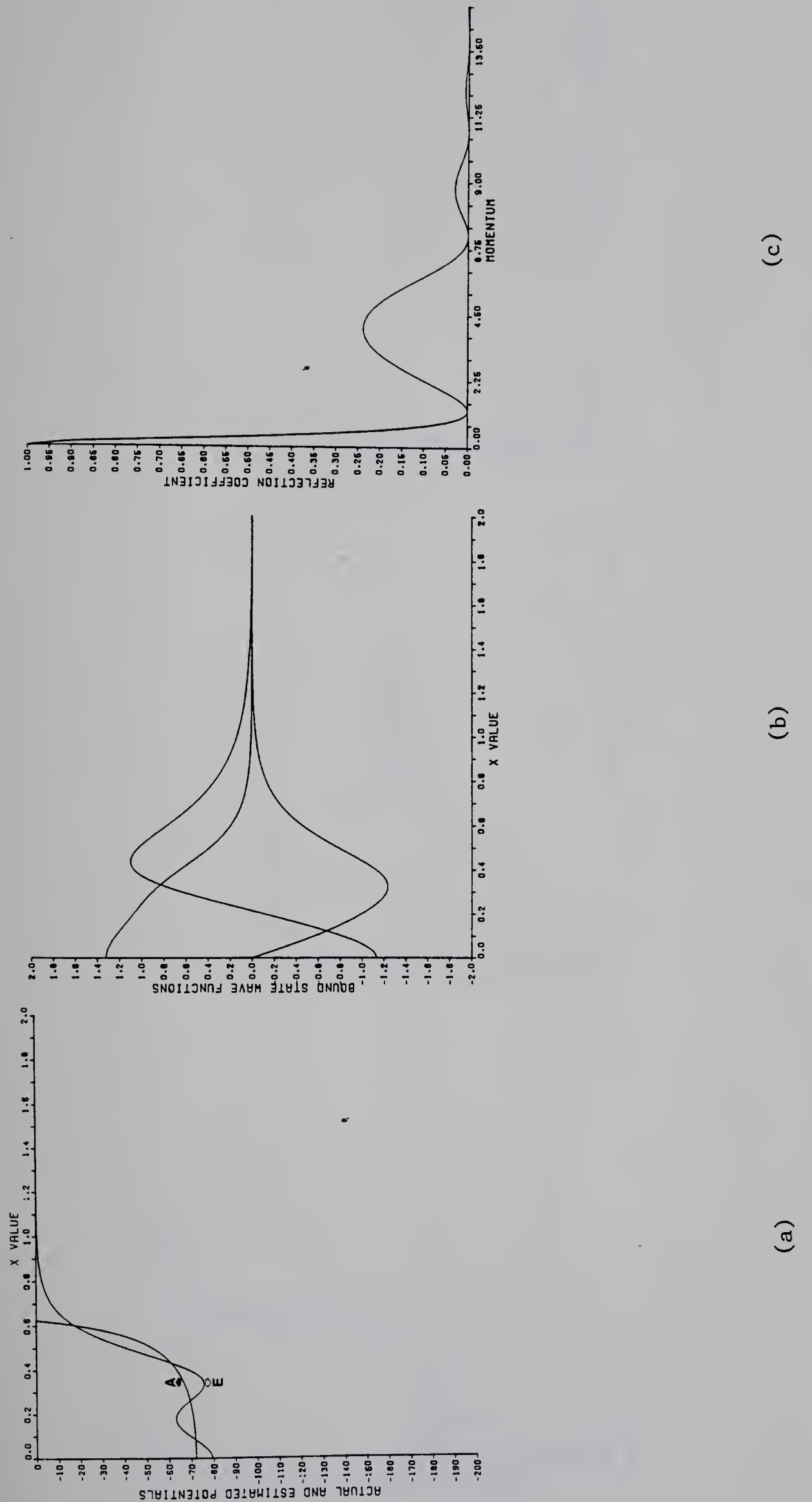
Fig. 3.31. Results for the Secant-Square Well ($E_0 = 80.0$):
(a) Actual (A) and reflectionless (E) potentials.
(b) Bound-state wavefunctions of the reflectionless potential.
(c) The reflection coefficient.

(a)

(b)

(c)
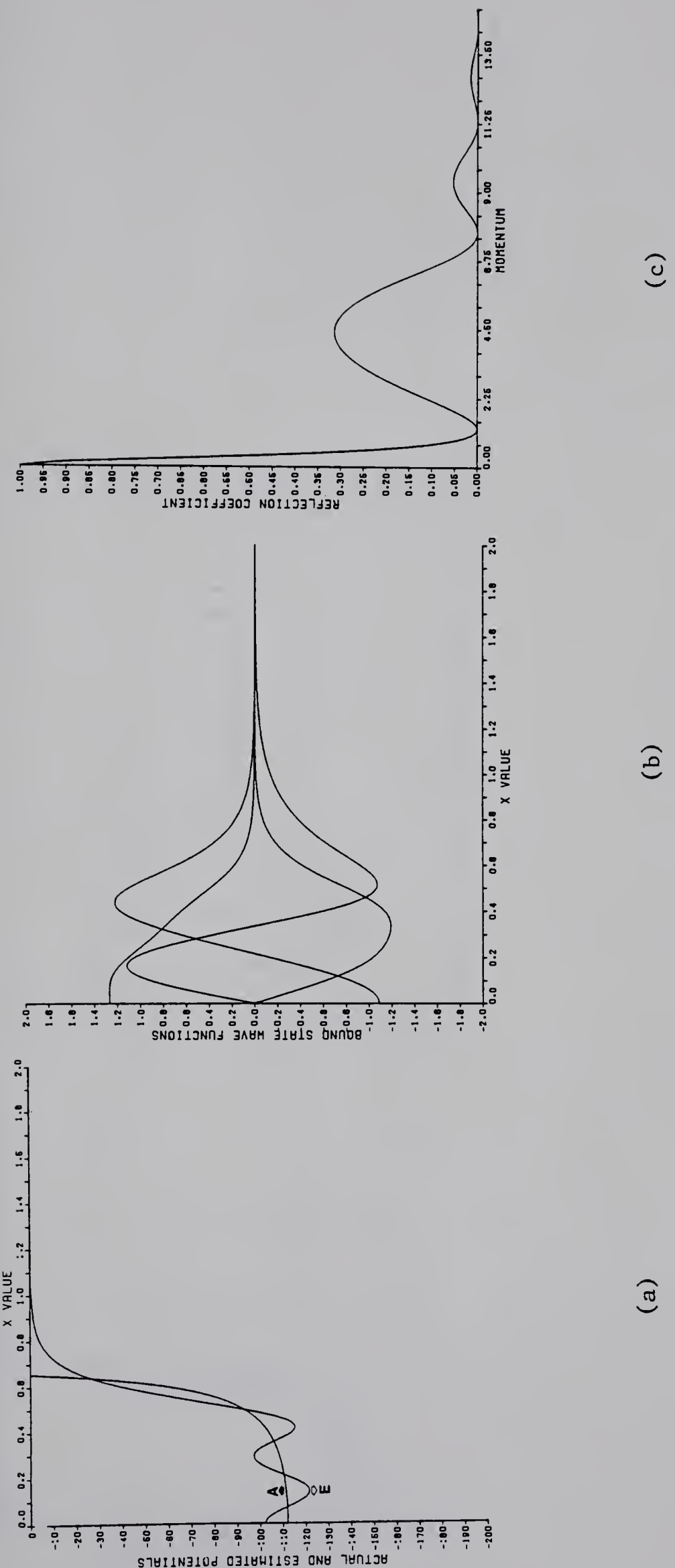
Fig. 3.32. Results for the Secant-Square Well (E_O = 120.0):
(a) Actual (A) and reflectionless (E) potentials.
(b) Bound-state wavefunctions of the reflectionless potential.
(c) The reflection coefficient.

(a)

(b)

(c)
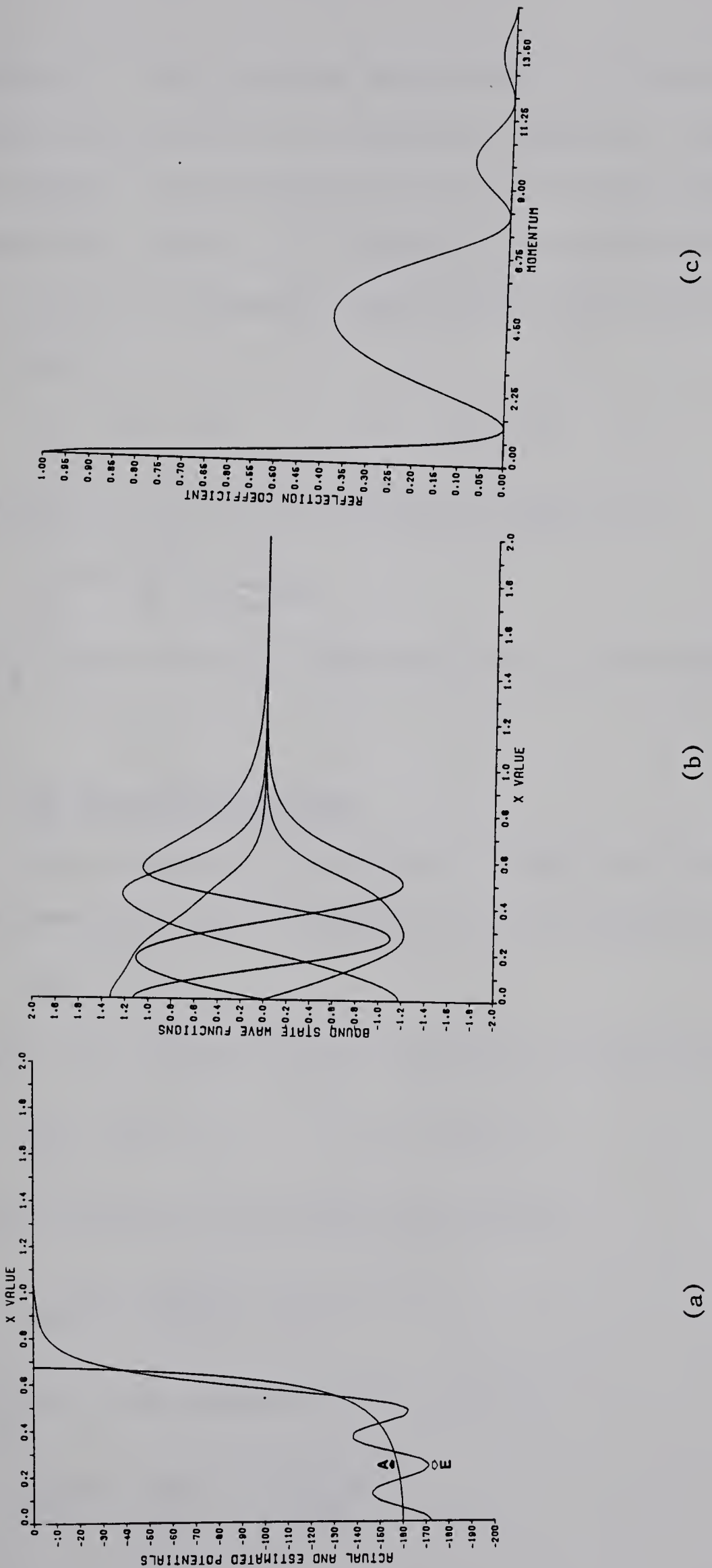
Fig. 3.33. Results for the Secant-Square Well (E_O = 168.0):
(a) Actual (A) and reflectionless (E) potentials.
(b) Bound-state wavefunctions of the reflectionless potential.
(c) The reflection coefficient.

'E_o-ambiguity'. This parameter entered during the translation of the
pure bound-state problem of a confining potential to a suitable scat-
tering problem. To reiterate our plans, we will approximate a confining
potential $V(x)$, locally, by a N-bound-state approximation $V_N(x)$, where
$[V_N(x) - E_o(N)]$ is a symmetric reflectionless potential supporting N
bound-states at

$$-\kappa_n^2 = -E_o + E_n \qquad ; \; n = 1,2,\ldots,N \qquad . \tag{3.24}$$

The parameter $E_o(N)$ will be consistently chosen to be

$$E_o(N) = \frac{1}{2}(E_N + E_{N+1}) \tag{3.25}$$

where E_n stands for the nth bound-state energy of the confining poten-
tial.

3.2.1.   The Harmonic Oscillator.

`   This is one of the most favourite symmetric confining potentials
in one dimension [45,65]. Choosing the parameterization as,

$$V(x) = x^2 \tag{3.26}$$

the bound-state energies of this potential are known to be

$$E_{n+1} = 2n + 1 \qquad ; \; n = 0,1,2,\ldots \tag{3.27}$$

and the bound-state wavefunctions are given by

$$\psi_{n+1}(x) = \frac{\pi^{-1/4}}{\sqrt{2^n \, n!}} \, H_n(x) \, e^{-x^2/2} \tag{3.28}$$

where $H_n(x)$ is the Hermite polynomial given by

$$H_n(x) = (-1)^n \, e^{x^2} \, (\frac{d^n}{dx^n}) e^{-x^2} \, . \tag{3.29}$$

111
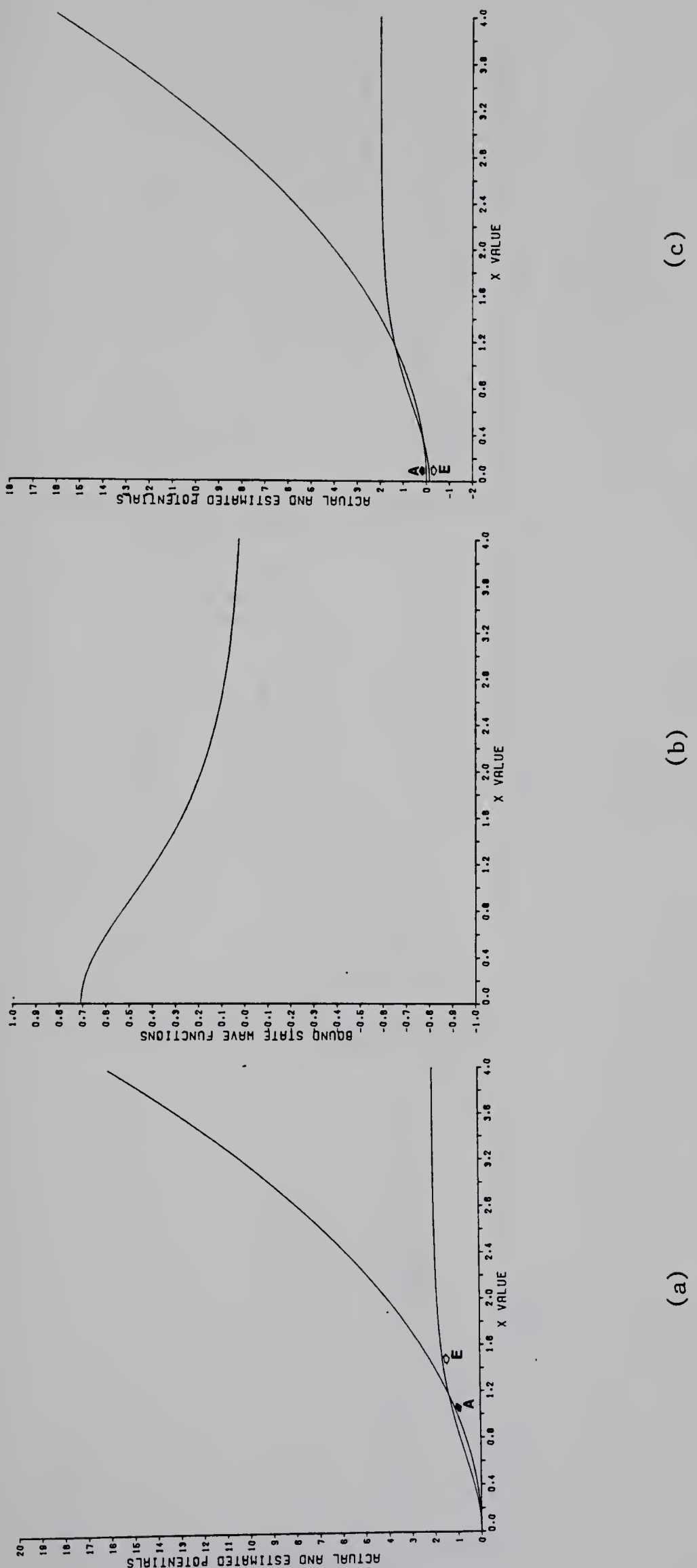
Fig. 3.34. Results for the Harmonic Oscillator:
(a) Actual potential (A) and the N = 1 reflectionless approximation (E).
(b) Bound-state wavefunction of the reflectionless potential.
(c) The corresponding 'exact reconstruction'. (cf. Section 3.3.2)

(a)   (b)   (c)
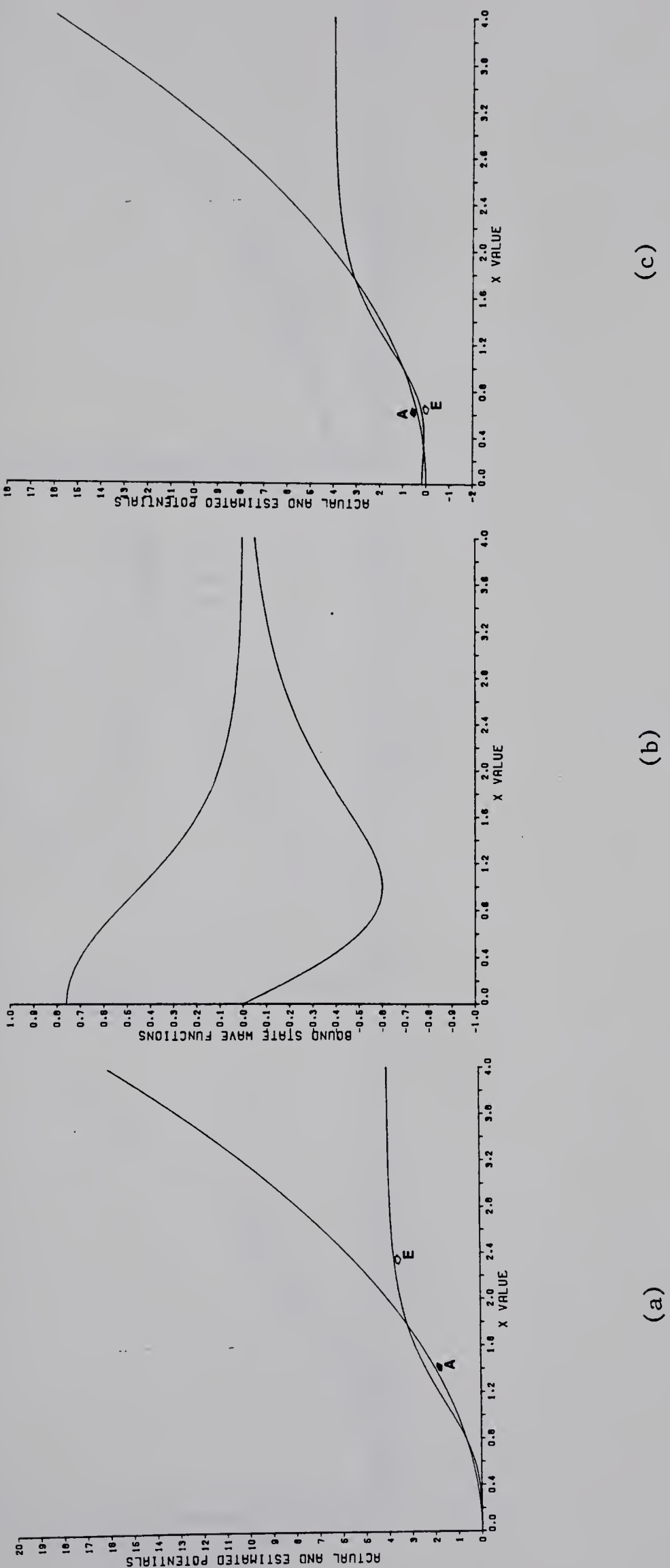
Fig. 3.35. Results for the Harmonic Oscillator:
(a) Actual potential (A) and the N=2 reflectionless approximation (E).
(b) Bound-state wavefunctions of the reflectionless potential.
(c) The corresponding 'exact reconstruction'. (cf. Section 3.3.2)

113
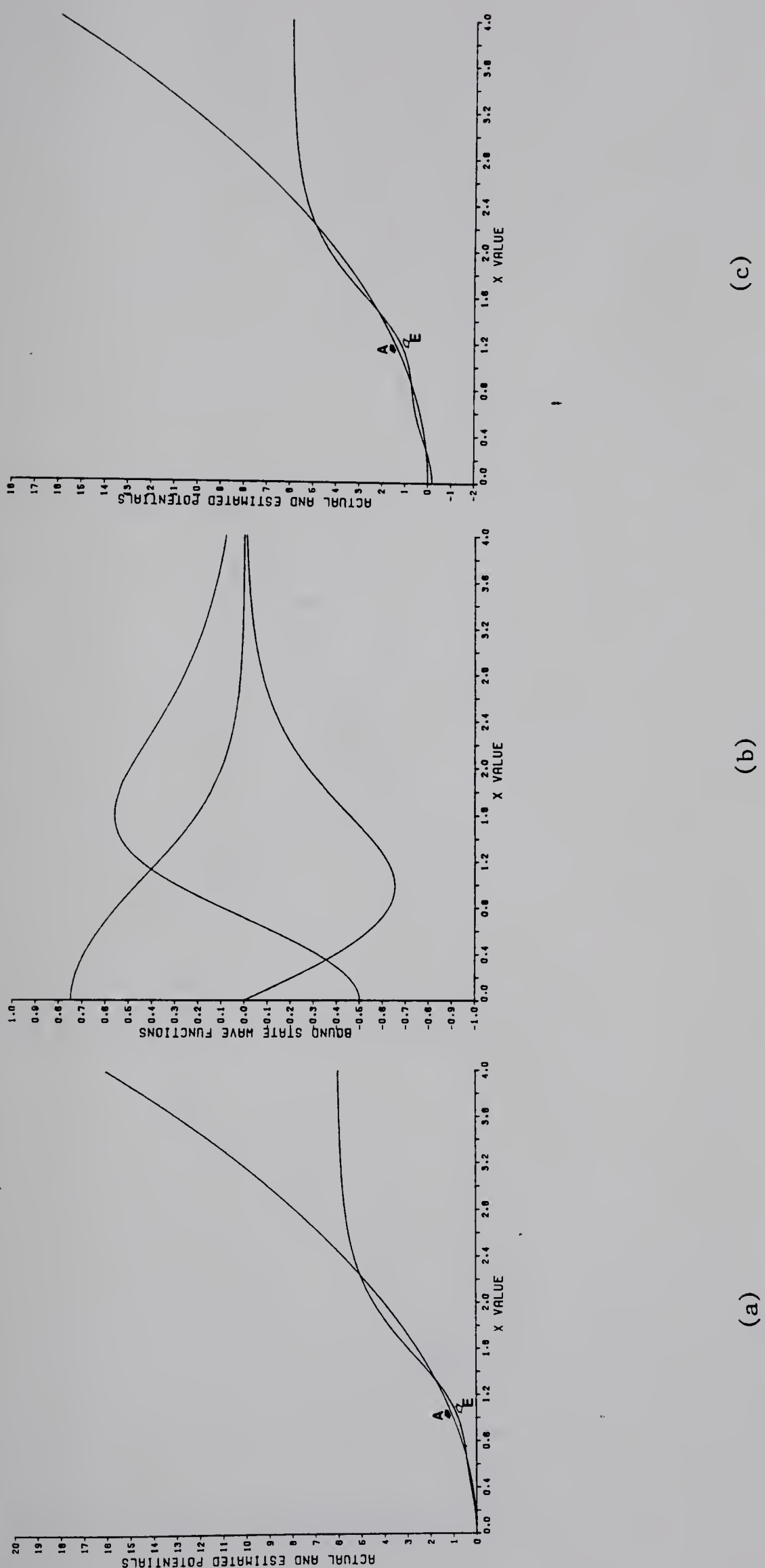
Fig. 3.36. Results for the Harmonic Oscillator:
(a) Actual potential (A) and the N = 3 reflectionless approximation (E).
(b) Bound-state wavefunctions of the reflectionless potential.
(c) The corresponding 'exact reconstruction'. (cf. Section 3.3.2)

(a)

(b)

(c)
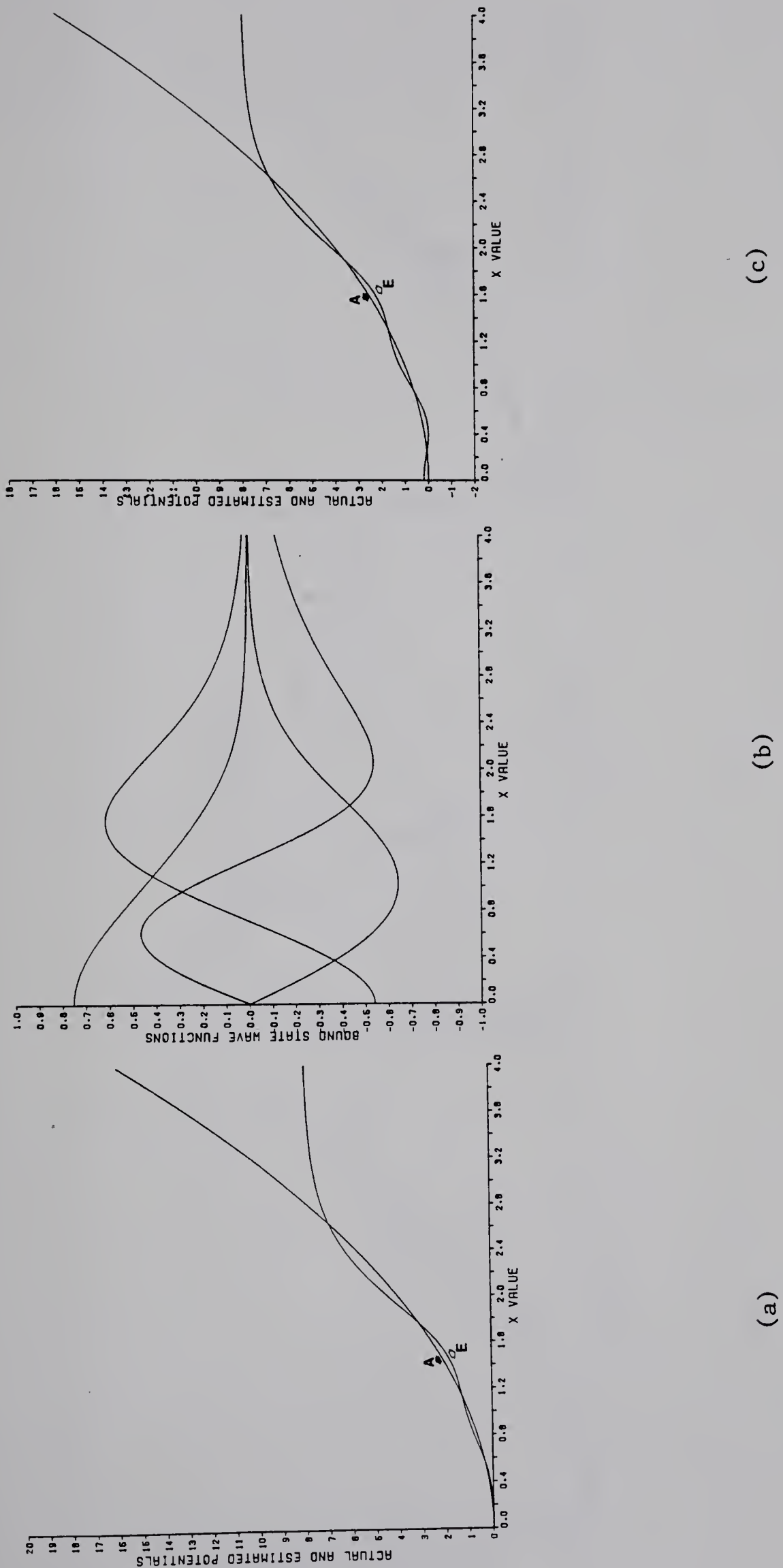
Fig. 3.37. Results for the Harmonic Oscillator:
(a) Actual potential (A) and the N=4 reflectionless approximation (E).
(b) Bound-state wavefunctions of the reflectionless potential.
(c) The corresponding 'exact reconstruction'. (cf. Section 3.3.2).
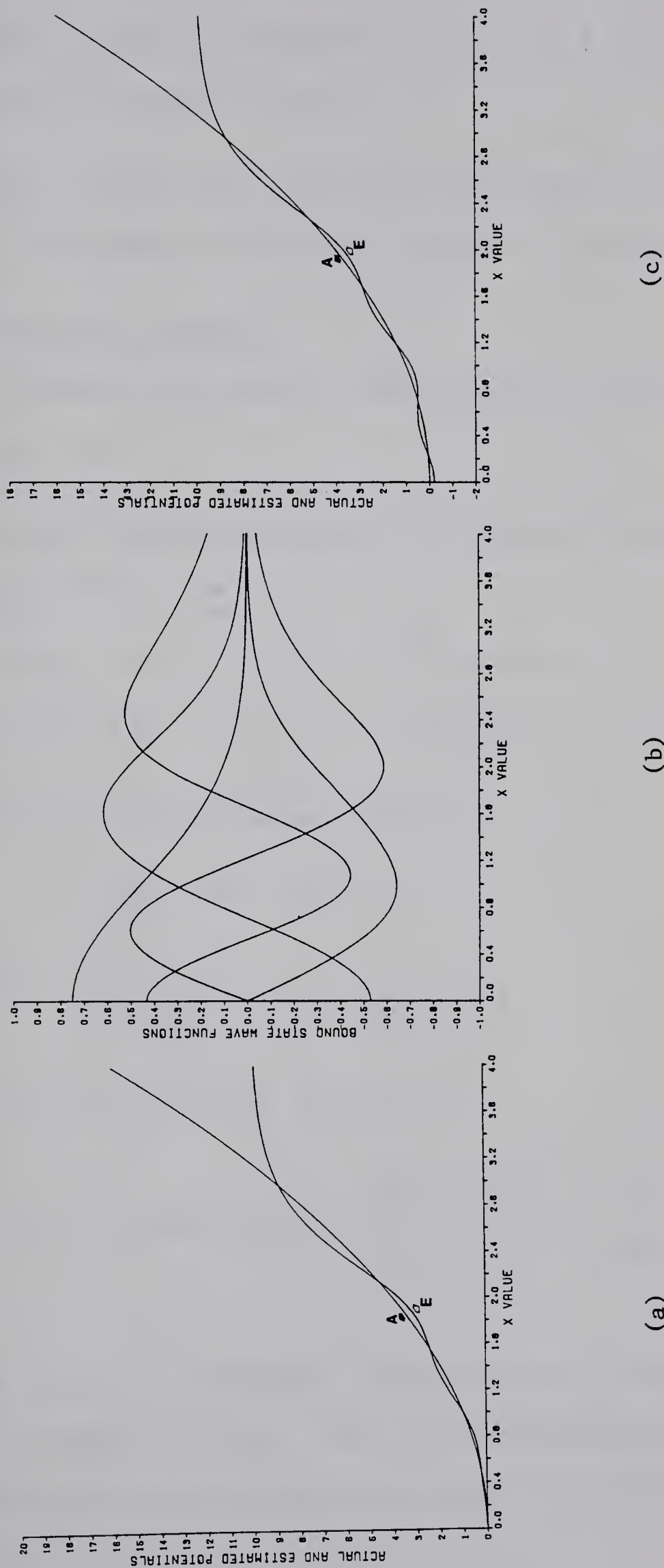
Fig. 3.38. Results for the Harmonic Oscillator:
(a) Actual potential (A) and the N=5 reflectionless approximation (E).
(b) Bound-state wavefunctions of the reflectionless potential.
(c) The corresponding 'exact reconstruction'. (cf. Section 3.3.2)

The successive approximations with $N = 1,2,3,4$ and 5 are plotted in Figure 3.34(a,b) to Figure 3.38(a,b).

Even a casual look at the five cases reveals an impressive tendency of convergence to the actual potential with increase in N.

3.2.2. The Linear Potential.

We consider the symmetric linear potential given by [20,45]

$$V(x) = |x| \quad . \tag{3.30}$$

The bound-state energies are known to be given by the zeros of the Airy functions [62]

$$Ai'(-E_n) = 0 \qquad\qquad ; \; n = 1,3,5,\ldots$$

$$Ai(-E_n) = 0 \qquad\qquad ; \; n = 2,4,6,\ldots \quad . \tag{3.31}$$

The bound-state wavefunctions are given by

$$\psi_n(x) = \begin{cases} \dfrac{1}{\sqrt{N_n}} \; Ai(x - E_n) \quad ; \; x > 0 \\[3mm] \dfrac{(-1)^{n-1}}{\sqrt{N_n}} \; Ai(-x - E_n) \; ; \; x < 0 \end{cases} \tag{3.32}$$

The normalization constant N_n is given by

$$N_n = 2 \int_o^\infty dx [Ai(x - E_n)]^2 = \begin{cases} 2E_n [Ai(-E_n)]^2 \; ; \; n = 1,3,5,\ldots \\[3mm] 2[Ai'(-E_n)]^2 \; ; \; n = 2,4,6,\ldots \end{cases} \quad . \tag{3.33}$$

We display the successive approximations up to $N = 5$ in Figure 3.39(a,b) to Figure 3.43(a,b). There is a strong evidence that the local reflectionless approximation converges to the actual one as N gets larger.
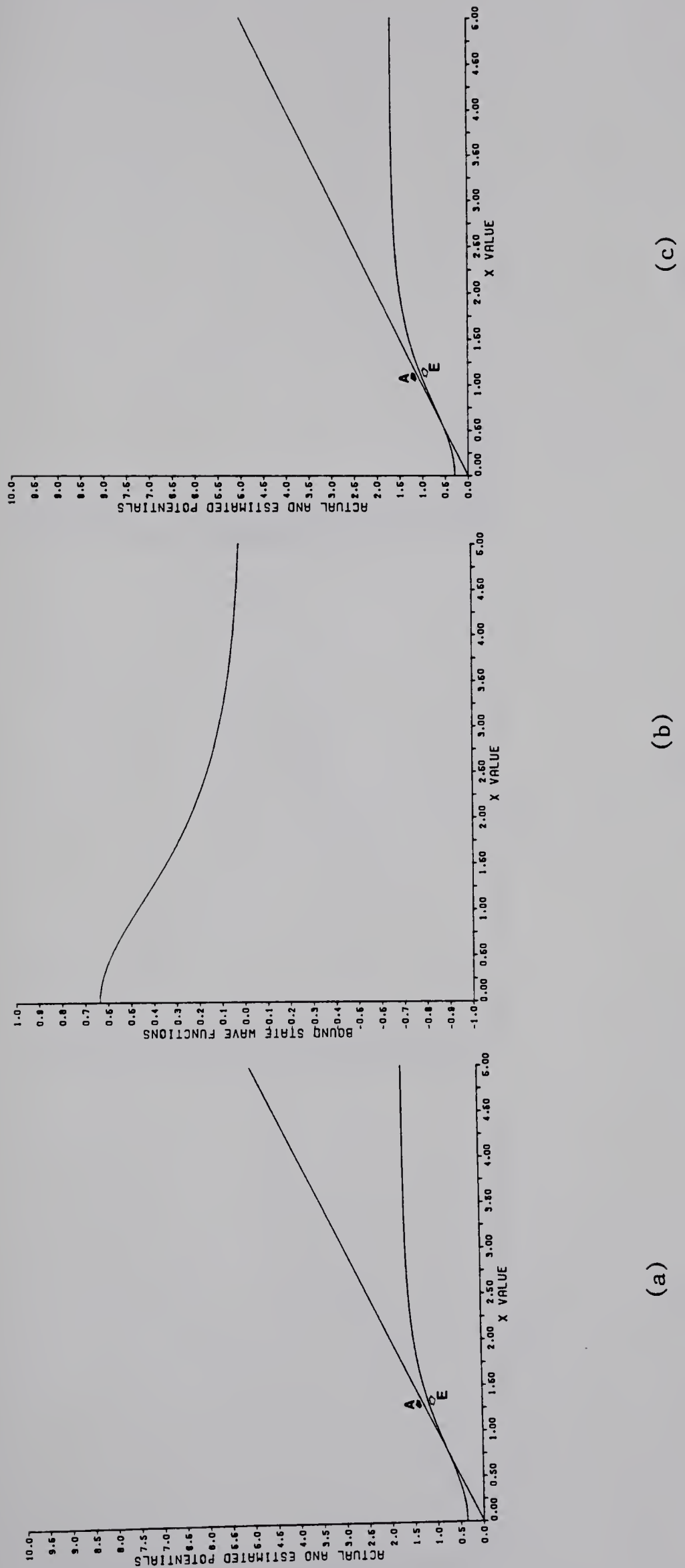
Fig. 3.39. Results for the Linear Potential:
(a) Actual potential (A) and the N = 1 reflectionless approximation (E).
(b) Bound-state wavefunction of the reflectionless potential.
(c) The corresponding 'exact reconstruction'. (cf. Section 3.3.2)
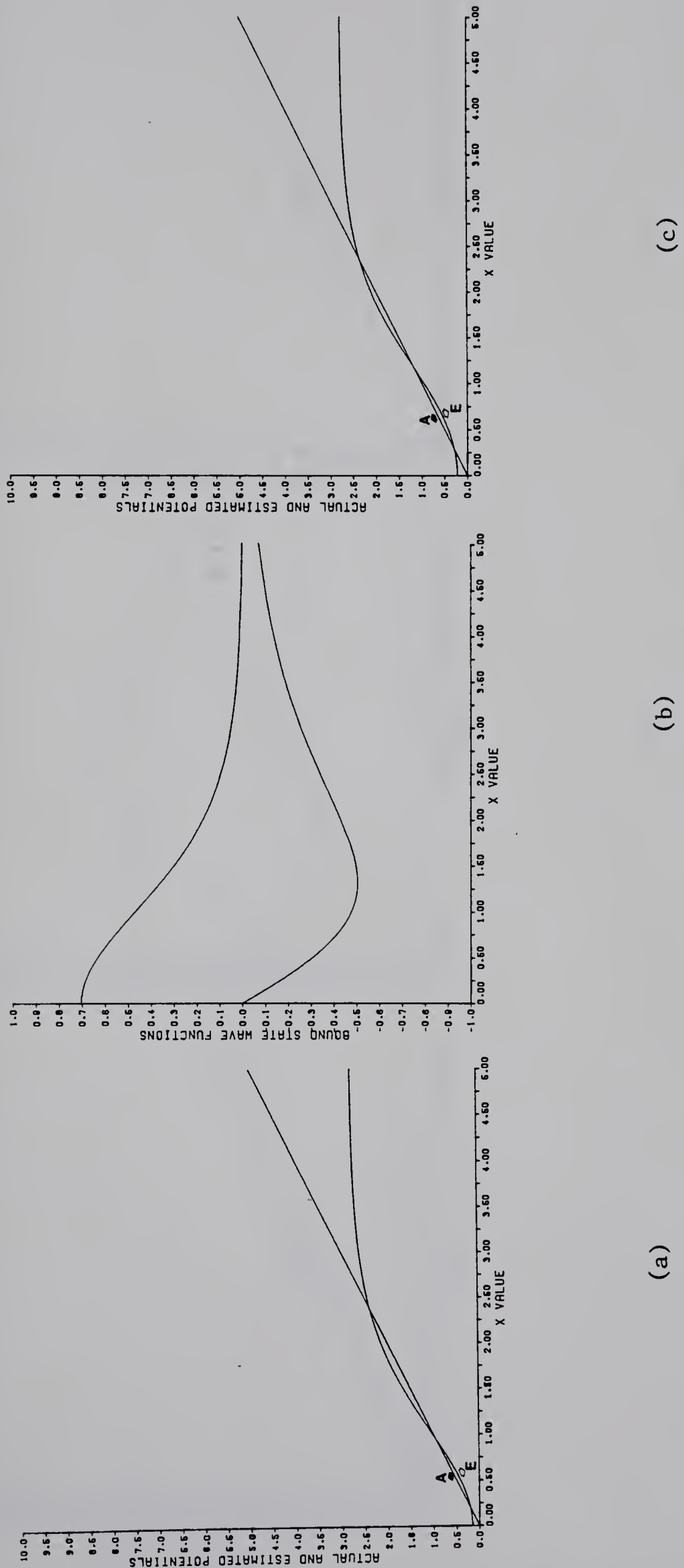
Fig. 3.40. Results for the Linear Potential:
(a) Actual potential (A) and the N = 2 reflectionless approximation (E).
(b) Bound-state wavefunctions of the reflectionless potential.
(c) The corresponding 'exact reconstruction'. (cf. Section 3.3.2)

(a)   (b)   (c)
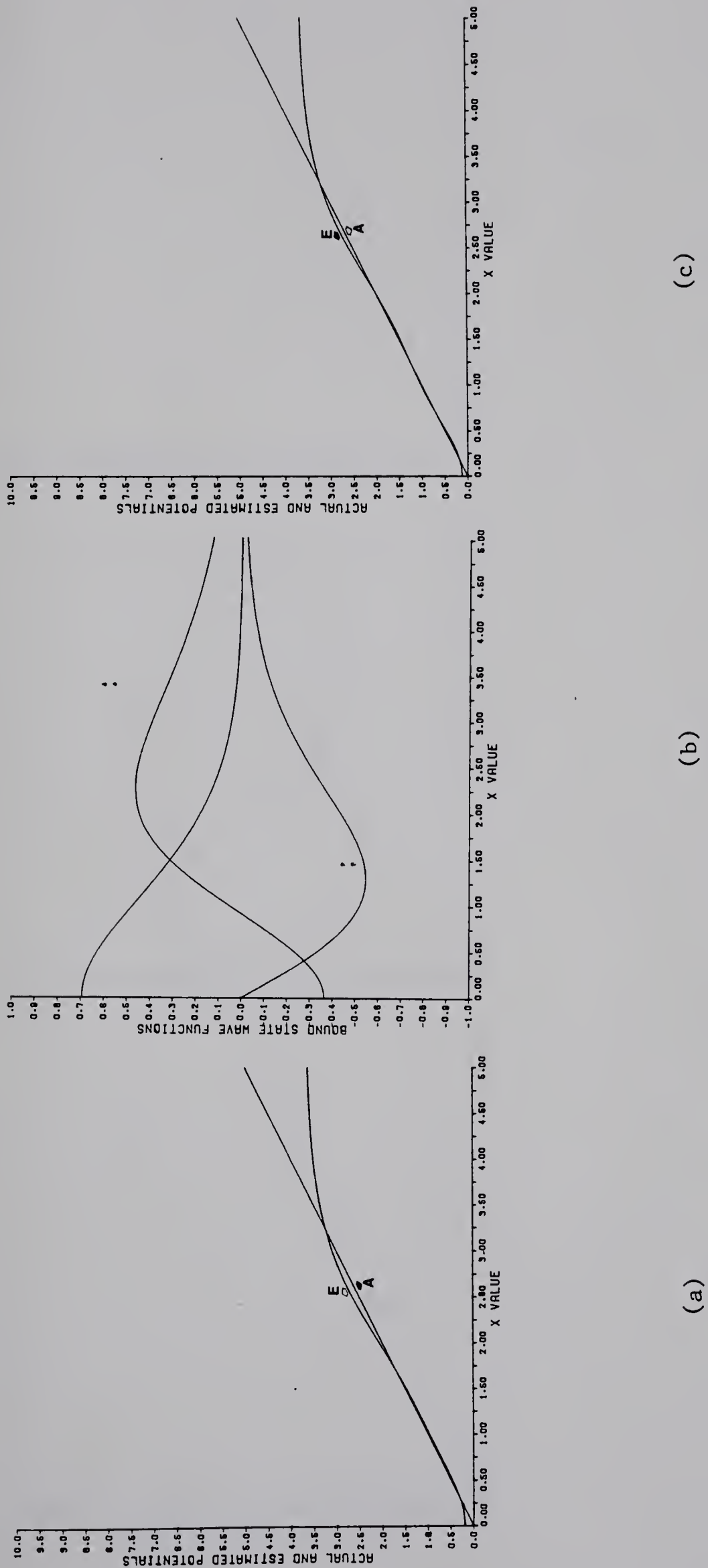
Fig. 3.41. Results for the Linear Potential:
(a) Actual potential (A) and the N = 3 reflectionless approximation (E).
(b) Bound-state wavefunctions of the reflectionless potential.
(c) The corresponding 'exact reconstruction'. (cf. Section 3.3.2)
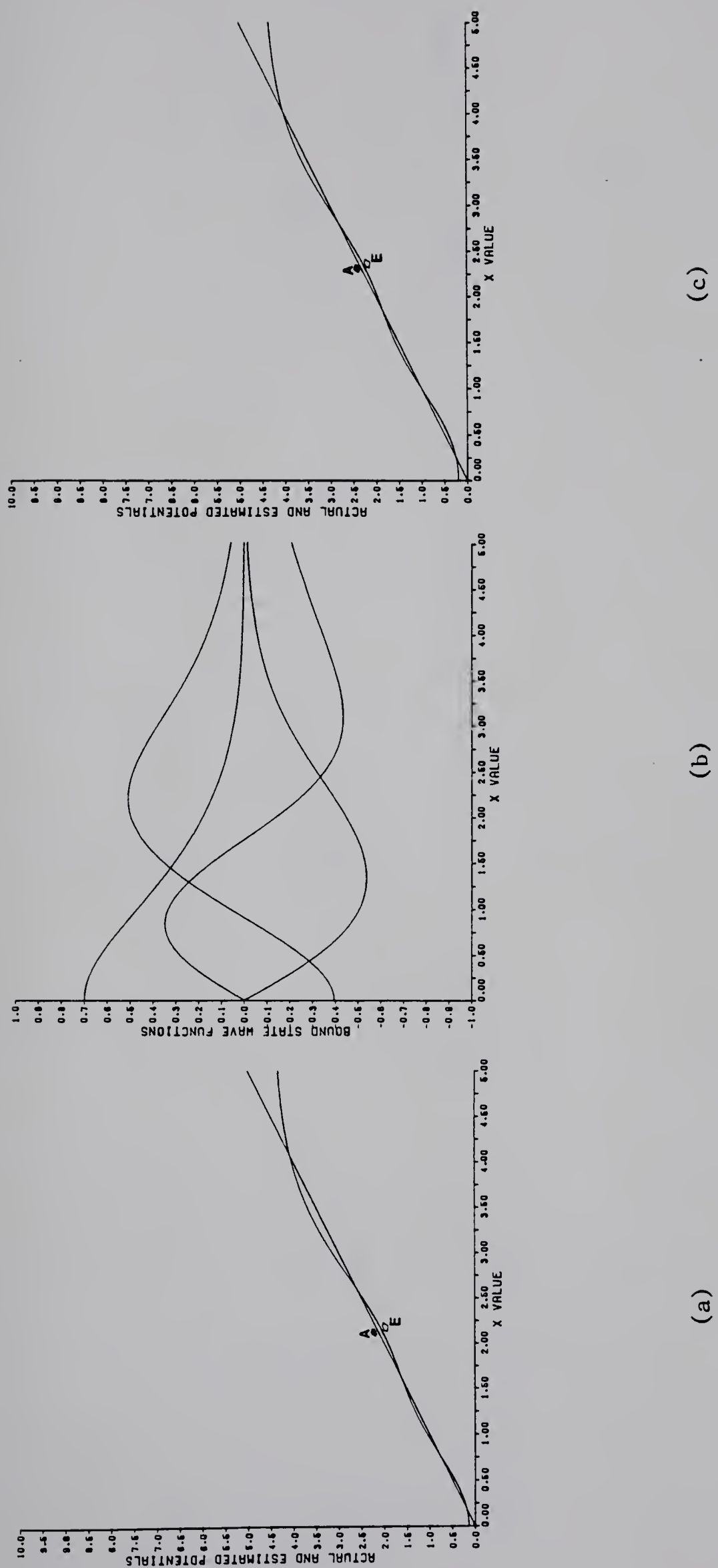
Fig. 3.42. Results for the Linear Potential:
(a) Actual potentials (A) and the N = 4 reflectionless approximation (E).
(b) Bound-state wavefunctions of the reflectionless potential.
(c) The corresponding 'exact reconstruction'. (cf. Section 3.3.2)

(a)

(b)

(c)
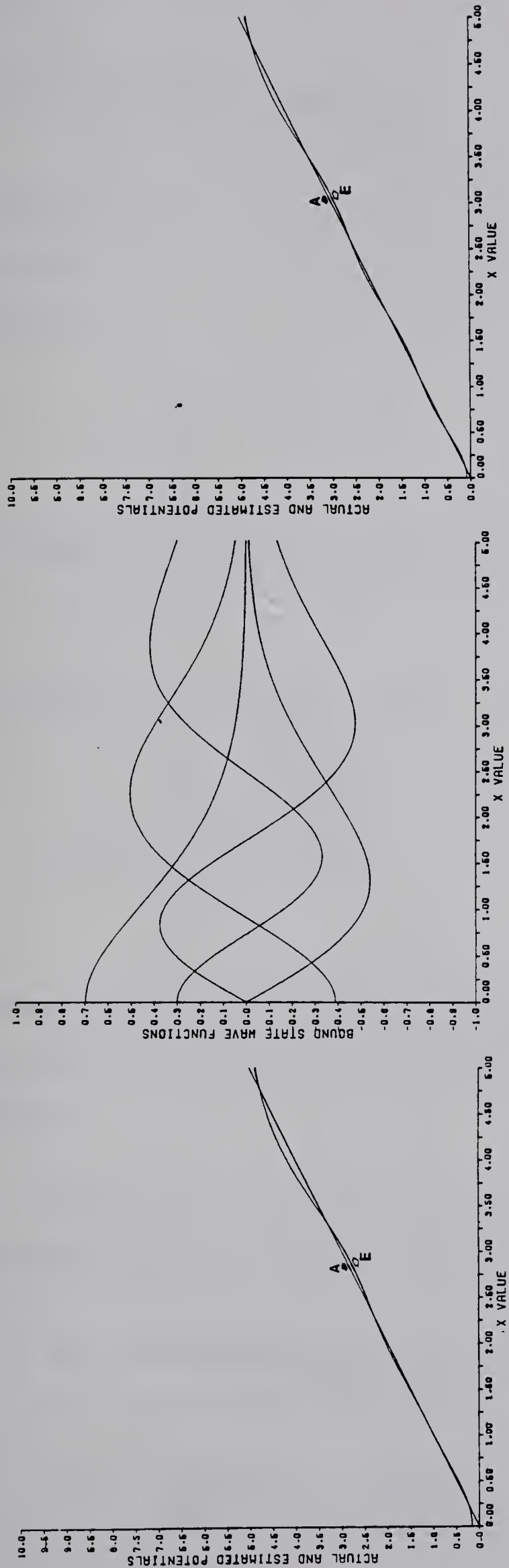
Fig. 3.43. Results for the Linear Potential:
(a) Actual potential (A) and the $N = 5$ reflectionless approximation (E).
(b) Bound-state wavefunctions of the reflectionless potential.
(c) The corresponding 'exact reconstruction'. (cf. Section 3.3.2)

3.2.3. The Infinite Square Well.

This is again one of the most common examples in elementary quantum mechanics. This depicts a particle trapped between two impenetrable walls. In the wave picture, this illustrates the standing waves [45,61]

$$
V(x) = \begin{cases} 0 & ; \ |x| < \pi/2 \\ \infty & ; \ |x| > \pi/2 \end{cases} \quad . \tag{3.34}
$$

The bound-state energies of this potential are known to be

$$
E_n = n^2 \qquad\qquad ; \ n = 1,2,3,\ldots \quad . \tag{3.35}
$$

The bound-state wavefunctions are

$$
\psi_n(x) = \begin{cases} \begin{bmatrix} \pi^{-1/2} \cos nx & ; \ n = 1,3,\ldots \\ \pi^{-1/2} \sin nx & ; \ n = 2,4,\ldots \end{bmatrix} & ; \ |x| < \pi/2 \\ 0 & ; \ |x| > \pi/2 \end{cases} \quad . \tag{3.36}
$$

Starting with $N = 1$, the successive approximations to the infinite square well up to $N = 5$ have been plotted in Figure 3.44(a,b) to Figure 3.48(a,b).

Apart from an oscillatory stability at $x = 0$, the reflectionless approximation does not seem to converge to the actual potential.

3.2.4. The Confining Pöschl-Teller Potential.

Let us now consider the potential

$$
V(x) = \left[\frac{\kappa(\kappa - 1)}{\sin^2(x - \frac{\pi}{4})} + \frac{\lambda(\lambda - 1)}{\cos^2(x - \frac{\pi}{4})} \right] \quad . \tag{3.37}
$$

(a)

(b)

(c)
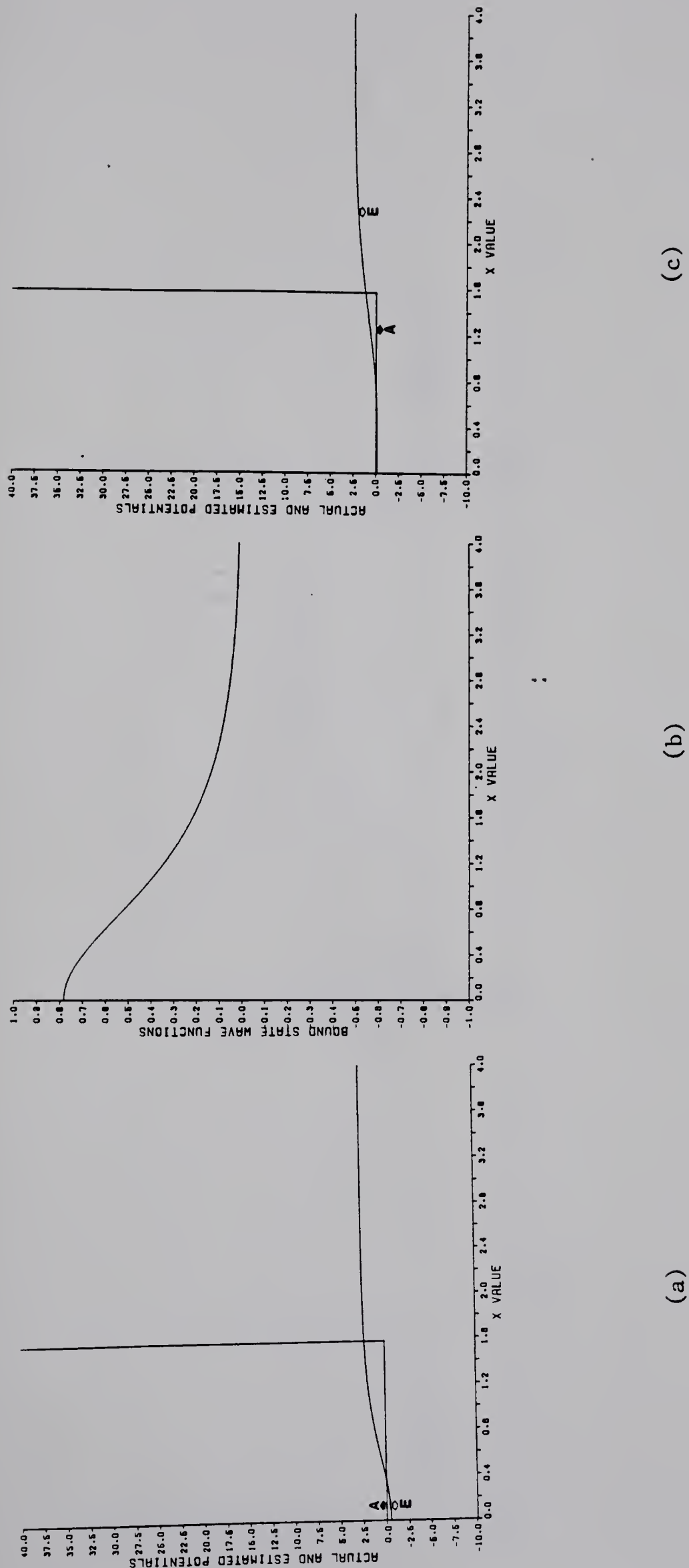
Fig. 3.44. Results for the Infinite Square Well:
(a) Actual potential (A) and the N = 1 reflectionless approximation (E).
(b) Bound-state wavefunction of the reflectionless potential.
(c) The corresponding 'exact reconstruction'. (cf. Section 3.3.2)

(a)

(b)

(c)
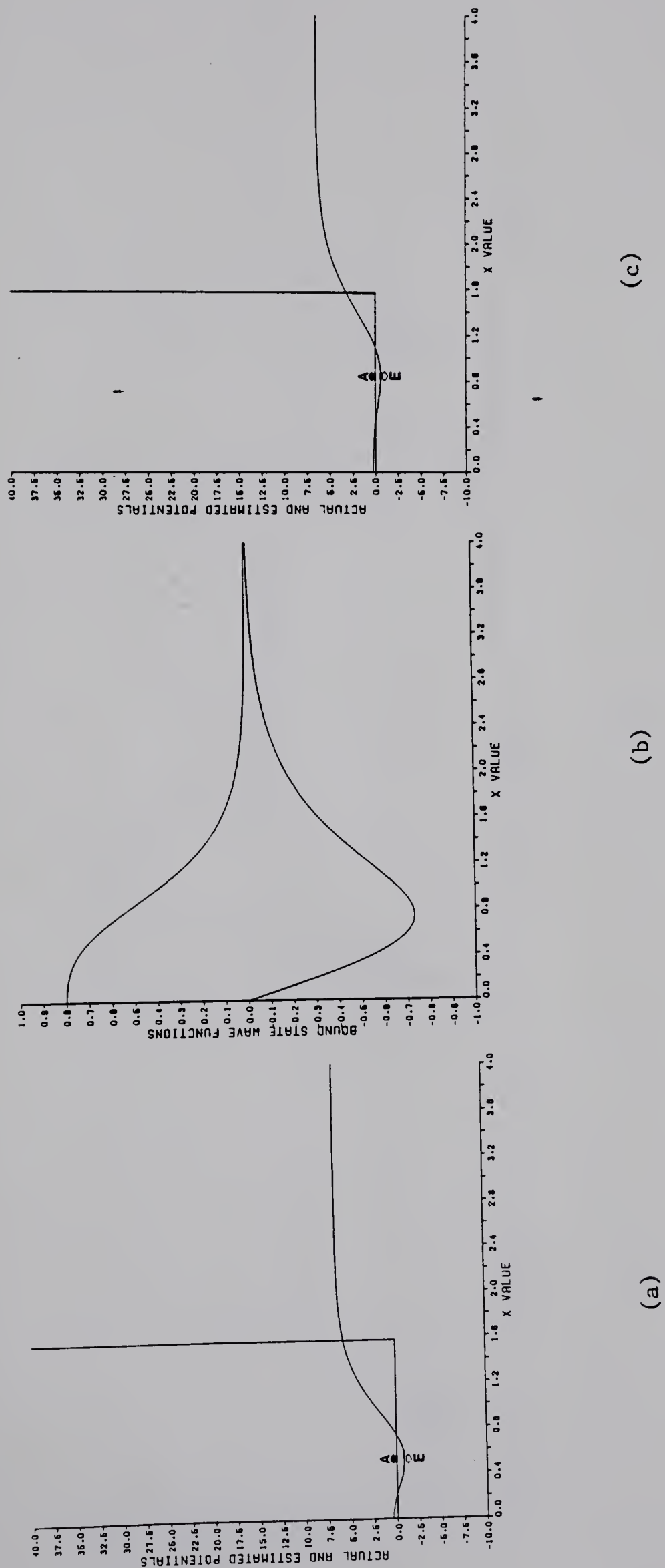
Fig. 3.45. Results for the Infinite Square Well:
(a) Actual potential (A) and the N = 2 reflectionless approximation (E).
(b) Bound-state wavefunctions of the reflectionless potential.
(c) The corresponding 'exact reconstruction'. (cf. Section 3.3.2)

(a)

(b)

(c)
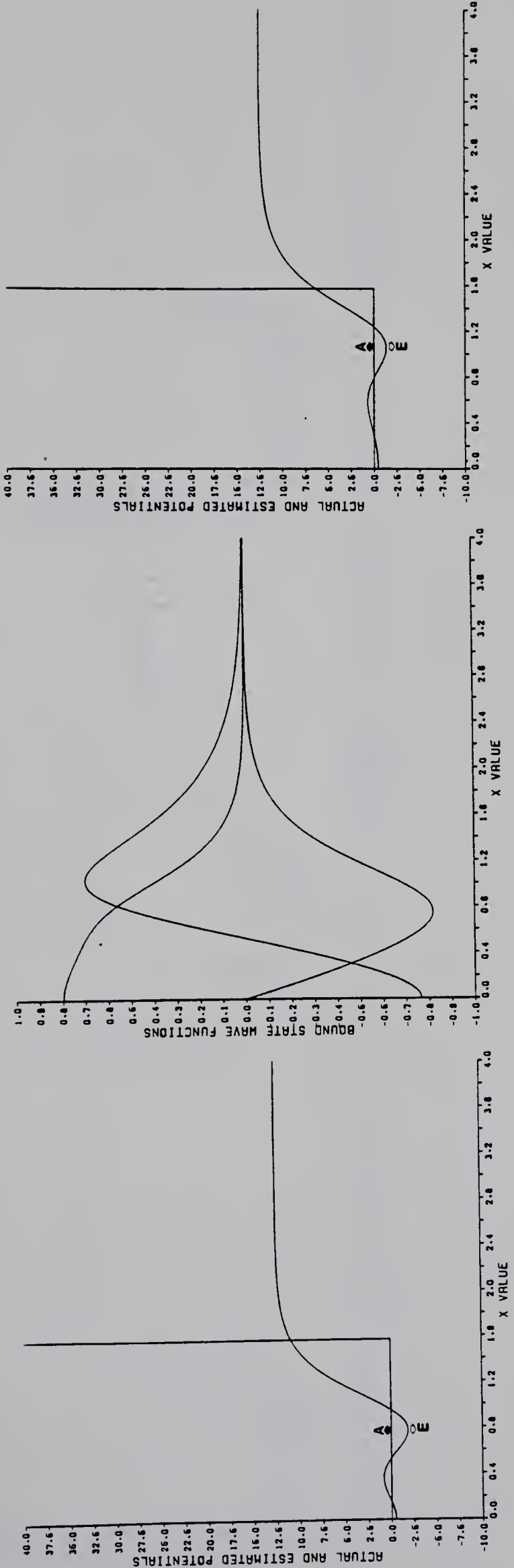
Fig. 3.46. Results for the Infinite Square Well:
(a) Actual potential (A) and the N = 3 reflectionless approximation (E).
(b) Bound-state wavefunctions of the reflectionless potential.
(c) The corresponding 'exact reconstruction'. (cf. Section 3.3.2)

(a)

(b)

(c)
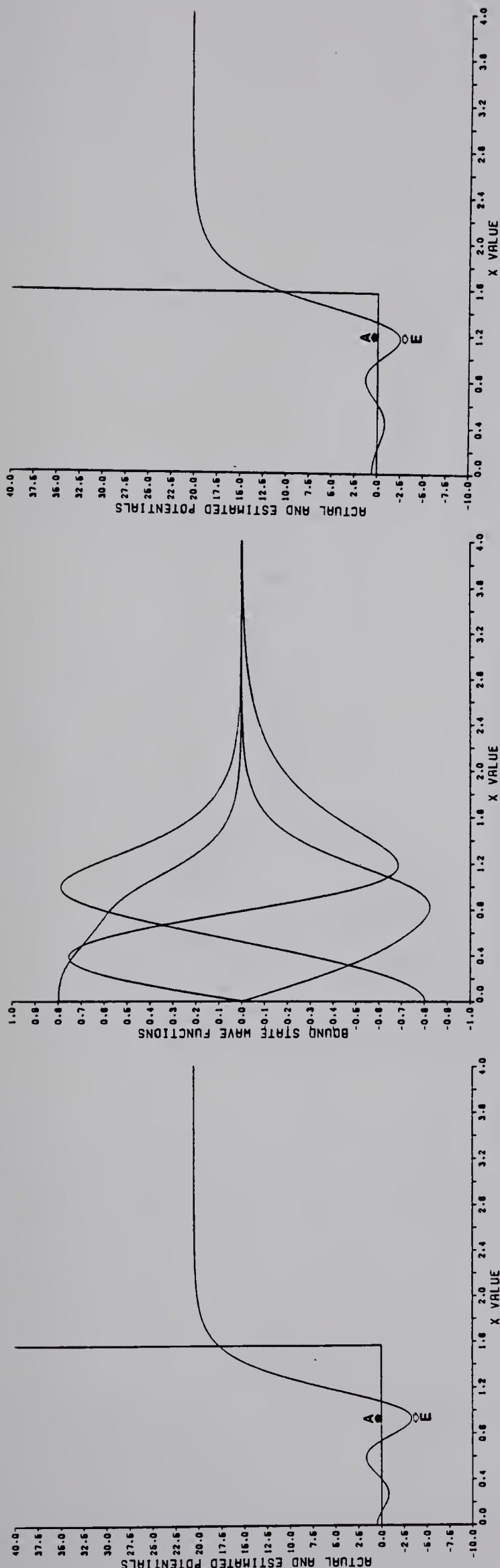
Fig. 3.47. Results for the Infinite Square Well:
(a) Actual potential (A) and the N = 4 reflectionless approximation (E).
(b) Bound-state wavefunctions of the reflectionless potential.
(c) The corresponding 'exact reconstruction'. (cf. Section 3.3.2)
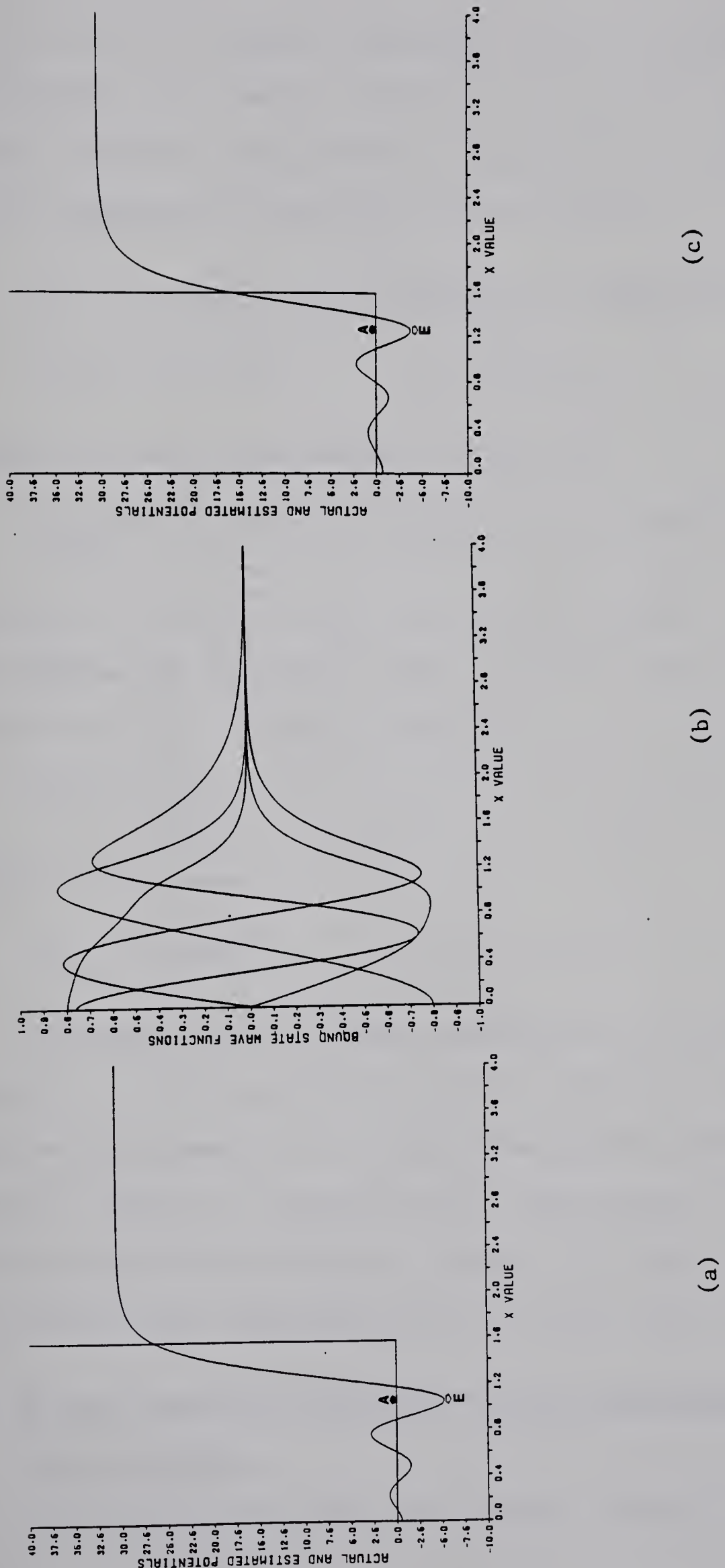
Fig. 3.48. Results for the Infinite Square Well:
(a) Actual potential (A) and the N = 5 reflectionless approximation (E).
(b) Bound-state wavefunctions of the reflectionless potential.
(c) The corresponding 'exact reconstruction'. (cf. Section 3.3.2)

For $\kappa = \lambda$, this is a symmetric potential. This is, obviously, a perio-dic potential. We, however, consider it only between $-\frac{\pi}{4} \leq x \leq \frac{\pi}{4}$. The barriers put by the singularities are impenetrable. So, this suffices for the confinement of a particle in this potential.

The eigenvalues for this potential are known to be [61]

$$E_{n+1} = (\kappa + \lambda + 2n)^2 \qquad ; \; n = 0,1,2,\ldots \qquad (3.38)$$

and the unnormalized wavefunctions are given by

$$\psi_{n+1}(z) = C_1 \sin^\kappa z \, \cos^\lambda z \; {}_2F_1(-n,\kappa+\lambda+n,\kappa+\tfrac{1}{2};\sin^2 z) \qquad (3.39)$$

where $z = x - \pi/4$, and C_1 is the normalization constant. We consider this potential for one specific value of κ and λ, viz. $\kappa = \lambda = 2$. In this case eqn. (3.37) takes the simple form

$$V(x) = \frac{8}{\cos^2 2x} \qquad (3.40)$$

and eqn. (3.38) becomes

$$E_{n+1} = (4 + 2n)^2 \qquad ; \; n = 0,1,2,\ldots \; . \qquad (3.41)$$

Successive reflectionless approximations to this confining potential up to $N = 5$ are plotted in Figure 3.49(a,b) to Figure 3.53(a,b). Except for an agreement at $x = 0$, the reflectionless approximation does not seem to exhibit a converging trend. The behaviour is similar to the infinite square well which is, perhaps, not unexpected. Both of them have the sharp impenetrable walls at certain values of x.

3.3. On the Convergence of the Reflectionless Approximation to the

Actual Potential.

Our investigations have left us with a veriety of results. We

(a)

(b)

(c)
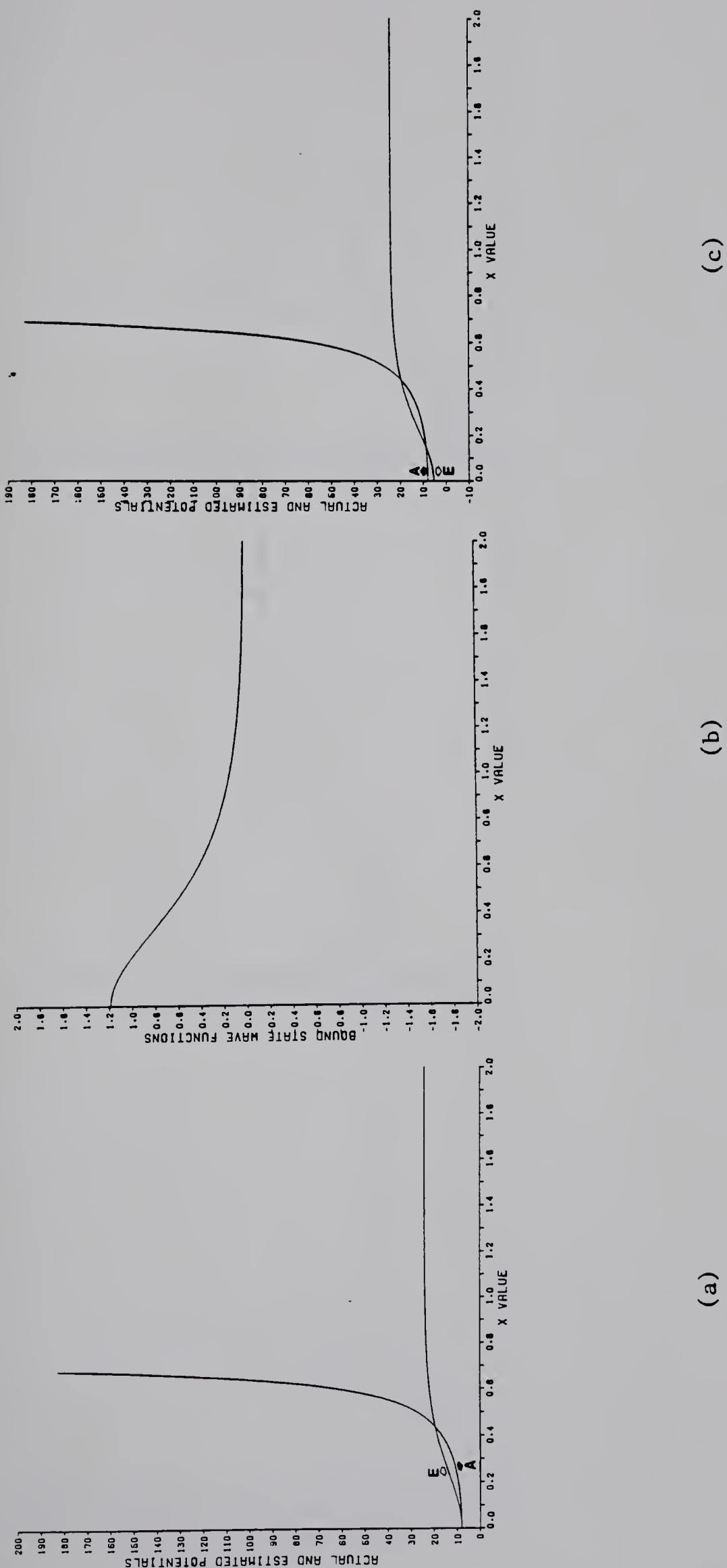
Fig. 3.49. Results for the Confining Pöschl-Teller Potential:

(a) Actual potential (A) and the N = 1 reflectionless approximation (E).

(b) Bound-state wavefunction of the reflectionless potential.

(c) The corresponding 'exact reconstruction'. (cf. Section 3.3.2)

(a)

(b)

(c)
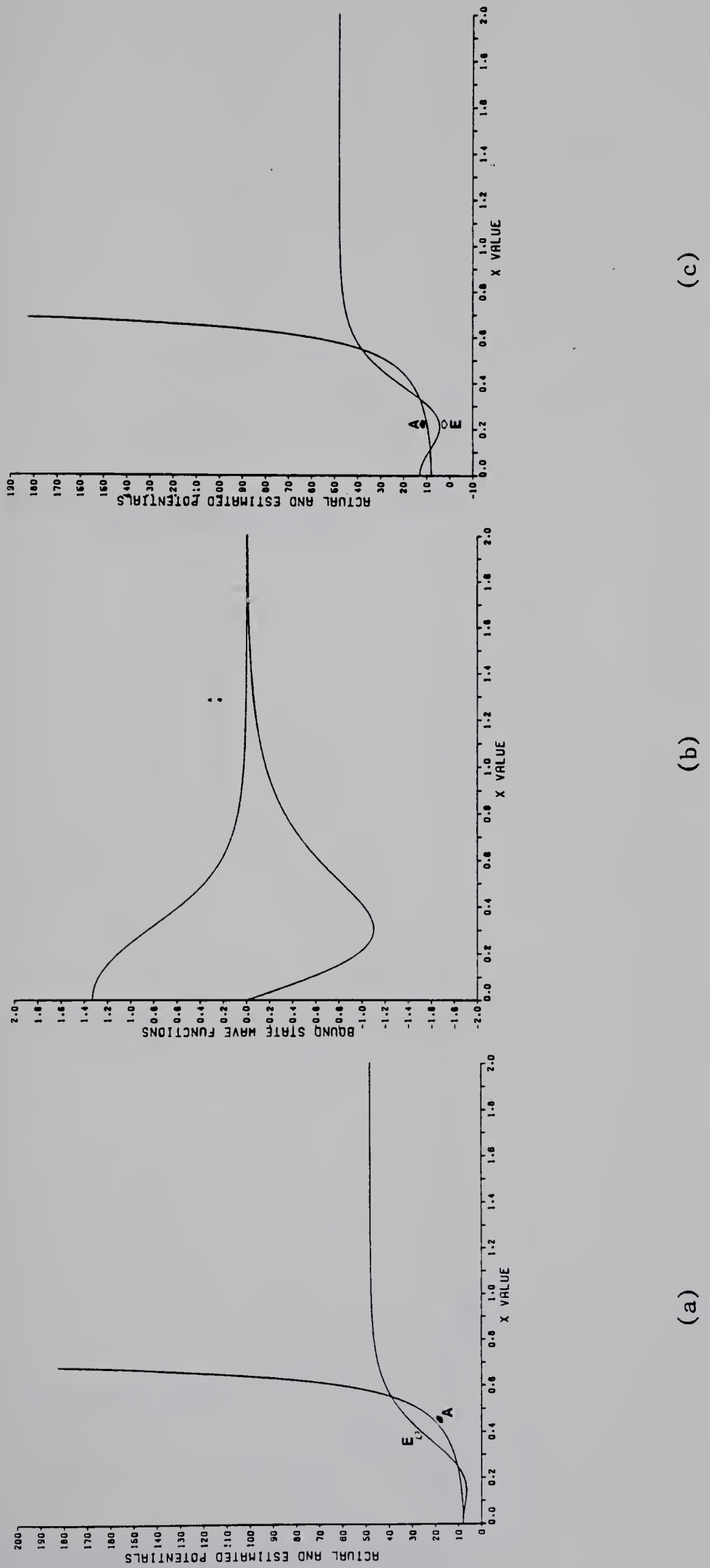
Fig. 3.50. Results for the Confining Pöschl-Teller Potential:
(a) Actual potential (A) and the N=2 reflectionless approximation (E).
(b) Bound-state wavefunctions of the reflectionless potential.
(c) The corresponding 'exact reconstruction'. (cf. Section 3.3.2)

(a)

(b)

(c)
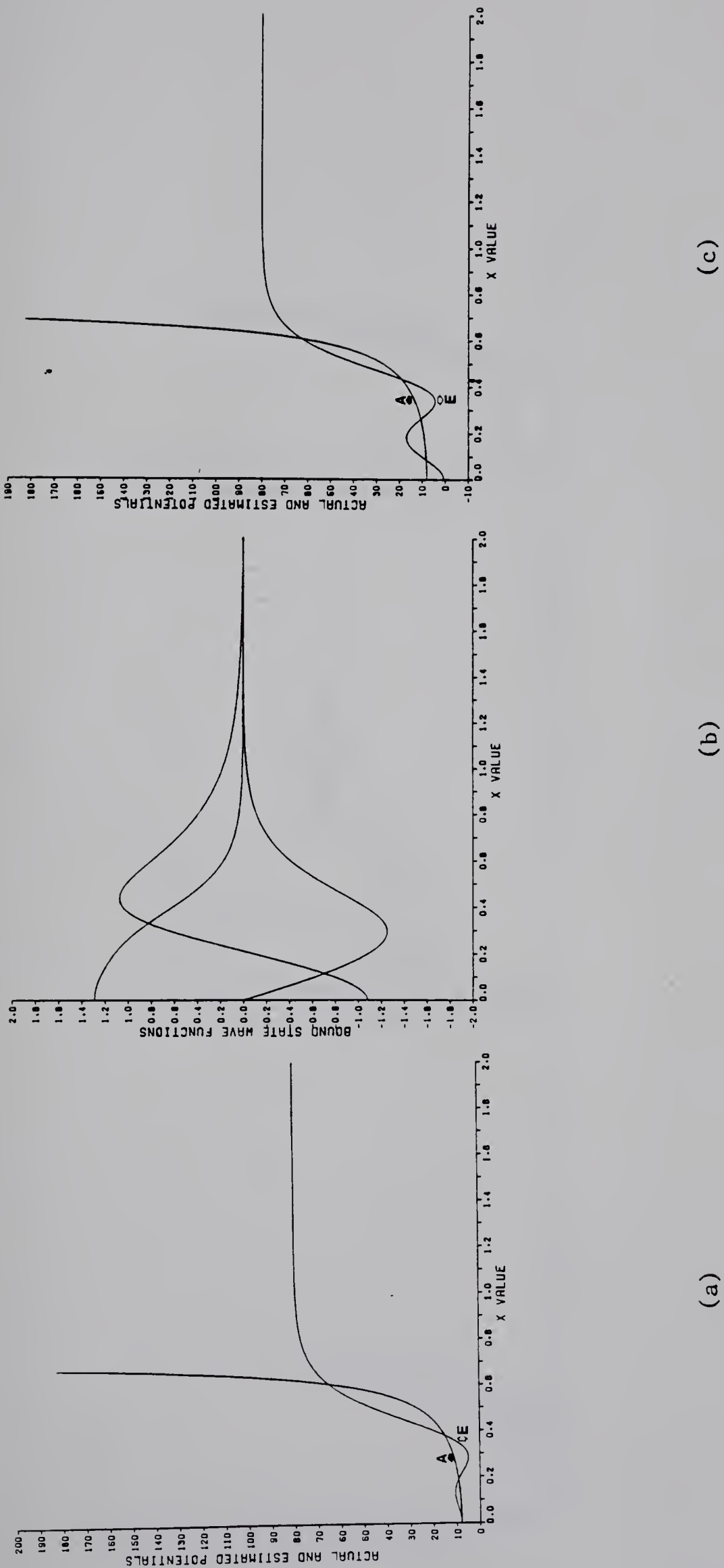
Fig. 3.51. Results for the Confining Pöschl-Teller Potential:
  (a) Actual potential (A) and the N = 3 reflectionless approximation (E).
  (b) Bound-state wavefunctions of the reflectionless potential.
 (c) The corresponding 'exact reconstruction'. (cf. Section 3.3.2)

(a)

(b)

(c)
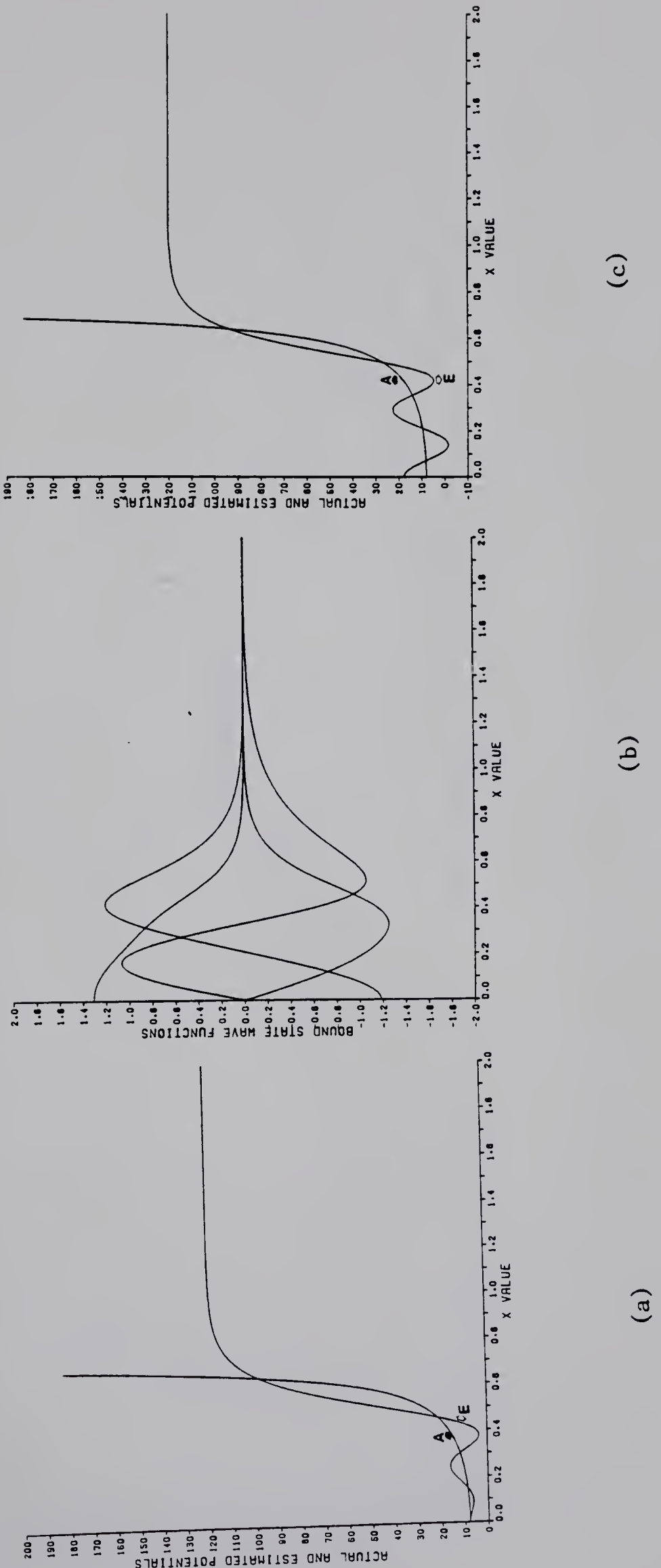
Fig. 3.52. Results for the Confining Pöschl-Teller Potential:
(a) Actual potential (A) and the N=4 reflectionless approximation (E).
(b) Bound-state wavefunctions of the reflectionless potential.
(c) The corresponding 'exact reconstruction'. (cf. Section 3.3.2)
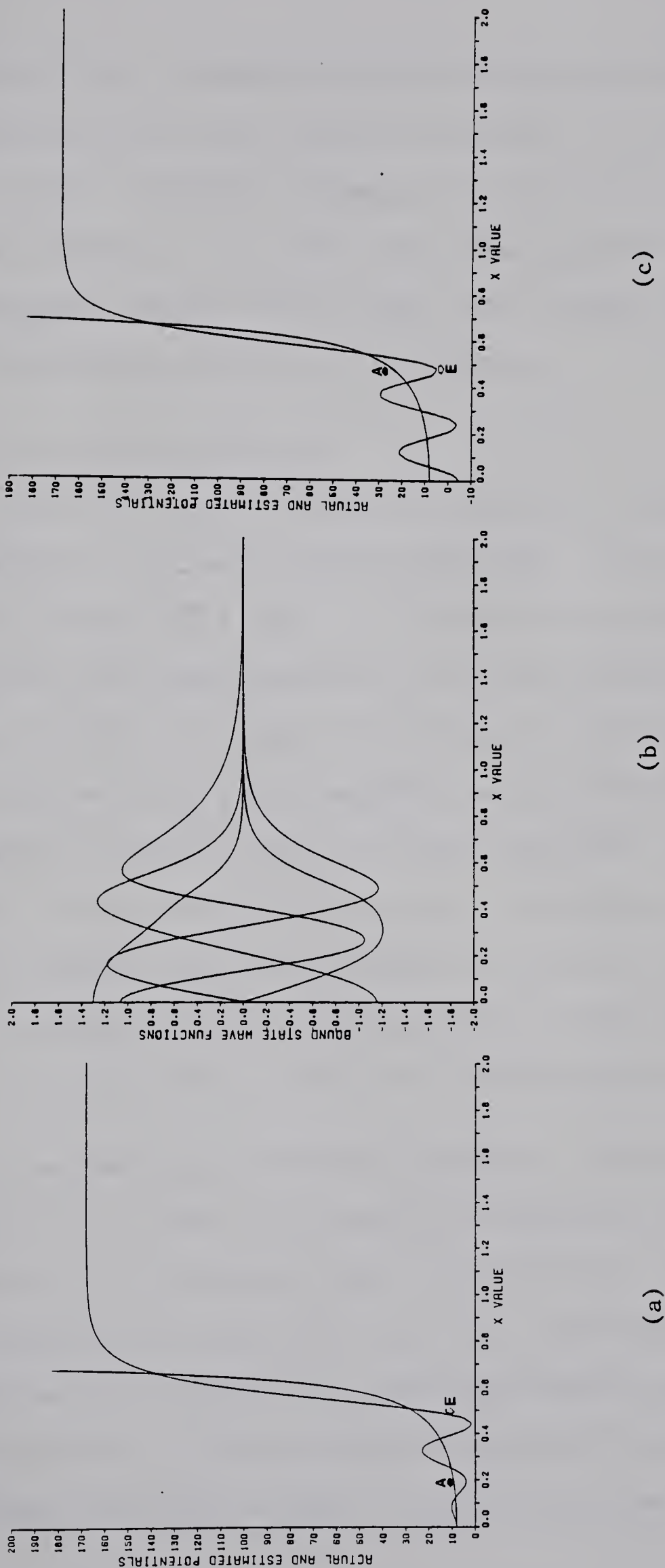
Fig. 3.53. Results for the Confining Pöschl-Teller Potential:
(a) Actual potential (A) and the N = 5 reflectionless approximation (E).
(b) Bound-state wavefunctions of the reflectionless potential.
(c) The corresponding 'exact reconstruction'. (cf. Section 3.3.2)

have observed cases of excellent agreement between the reflectionless

approximation and the actual symmetric potential. At the same time,

however, we have encountered instances of catastrophic divergences from

the actual potential. Do we have, then, some suggestions regarding

the convergence? We shall try to answer this question, within the

scope of the results obtained, in this section.

3.3.1. Non-confining Potential.

Things are relatively simple for potentials belonging to this

class because of the absence of the E_o-ambiguity. We have approximated

the actual potential by a symmetric, reflectionless potential having

bound-states at the same energies as the actual potential. Exact

bound-state energies were used in the inverse reconstruction. This

cannot, then, be a source of disagreement between the two. The rele-

vant quantity to observe is the reflection coefficient. This was the

motivation for calculating the reflection coefficient as a function of

momentum or energy. The reflectionless approximation is unique - so,

unless the actual potential is reflectionless, the two cannot be the

same. The question, then, is that how close the agreement is?

We saw one case of fantastic agreement - the Pöschl-Teller

potential with $\lambda = 3.0001$. The reflection coefficient was equal to

unity at $k = 0$ and, practically, zero everywhere else. This suggests

that if the actual potential has a reflection coefficient which decays

extremely fast with increase in k, the reflectionless approximation

should be excellent. This was further vindicated in the case of other

Pöschl-Teller potentials and some of the Gaussians, too.

All other potentials except these two had sharp 'corners' and they exhibited pronounced resonances in their spectrum. We have been able to obtain two, rather primitive, suggestions. First, if the re-flection coefficient, when plotted as a function of momentum, decays quickly then, despite the presence of 'sharp' resonances, the approxi-mation is tolerable. Second, if the reflection coefficient decays very slowly and has broad resonances, the approximation is disappoin-ting.

Based on these experiences, we can 'qualitatively' define two classes of reflection coefficients. If the reflection coefficient decays quickly and its peaks, if any, are narrow then we will call such a reflection coefficient to be exhibiting a *favourable behaviour*. On the other hand, the reflection coefficient which decays slowly and whose peaks, if any, are broad will be said to exhibit an *unfavourable behaviour*.

3.3.2. Confining Potentials.

A convergence of the reflectionless potential to the actual confining one at $x = 0$ [47] does not necessarily guarantee any tendency towards convergence even in the 'local' sense put forward by Schonfeld et. al. and QRT [45,47]. A glaring example of such a failure is the Confining Pöschl-Teller Potential where the approximation diverges despite its agreement at $x = 0$ with the actual potential. What is im-perative is to obtain evidences of "overall" convergence in the desired region - if possible, some criteria in support of such a behaviour.

Our investigations in the case of non-confining wells, which

are bonafide members of the class of scattering potentials, have prompted us to expect that if the bound-state energies used in the inverse method are correct and if the reflection coefficient behaves in a 'favourable' way, then the reflectionless approximation is satisfactorily close to the actual potential. Our numerical studies do not, in totality, define the 'favourable' class of reflection coefficients. However, as discussed in the earlier section, we have evidence for a few in this class. Undoubtedly, it is beyond controversy that the two quantities of interest in investigating the problem of convergence are the bound-state energies and the reflection coefficients.

When we get down to the confining potentials, there is an inherent artificiality involved in translating this purely bound-state problem into a scattering problem. As per QRT's prescriptions, we introduce a zero of energy E_o, half-way between the Nth and $(N+1)^{th}$ bound-states. We then approximate the confining potential $V(x)$, 'locally', by a potential $V_N(x)$, where $[V_N(x) - E_o]$ is the reflectionless potential supporting bound-states at the scaled 'confining energies' (i.e. bound-state energies corresponding to the confining potential, viz., E_n) $-\kappa_n^2 = -E_o + E_n$. We will call this - the *QRT approximation*. As far as the reconstruction of confining potentials is concerned, this prescription is sufficient because the only informations we have are the bound-state energiesof the confining potential. However, when we want to talk about convergence, we need to carefully define the scattering counterpart of the confining potential, corresponding to a specific E_o, which we hope to simulate. That will, then, give us some information regarding the various factors affecting the convergence.

To put QRT's prescription the other way round we scale down the actual potential by E_o and try to approximate the negative part of the scaled potential by a reflectionless potential having bound-states at $-\kappa_n^2 = -E_o + E_n$, as shown in Figure 3.54(a) and Figure 3.54(b). If we recall the properties of the reflectionless potentials that they are always negative and go to zero exponentially as $x = \pm\infty$, we realize that what we can hope to reconstruct, in the best of events, is the following scattering potential

$$V^{scatt.}(x) = \begin{cases} V(x) - E_o & ; \ |x| \leq \alpha \\ 0 & ; \ |x| \geq \alpha \end{cases} \qquad (3.42)$$

with the obvious equality

$$V(\pm\alpha) - E_o = 0 \quad . \qquad (3.43)$$

This is the truncated potential shown in Figure 3.54(c). This is the actual scattering counterpart of the confining potential $V(x)$ corresponding to a specific E_o. The successive approximations to the confining potential with increasing E_o or N then become approximations to the wells of the kind (3.42) with increasing depth.

At the very outset, it is clear that bound-state energies of the scattering counterpart are not the same as the scaled confining energies. The boundary conditions are to be imposed at $x = \pm\alpha$ rather than at $x = \pm\infty$. We can expect the lower bound-states to be close to the assumed value, if the potential is deep enough, but the upper ones will be very different. Moreover, the discrepancy between the two is highly dependent on the potential and forbids one to draw any general conclusion.
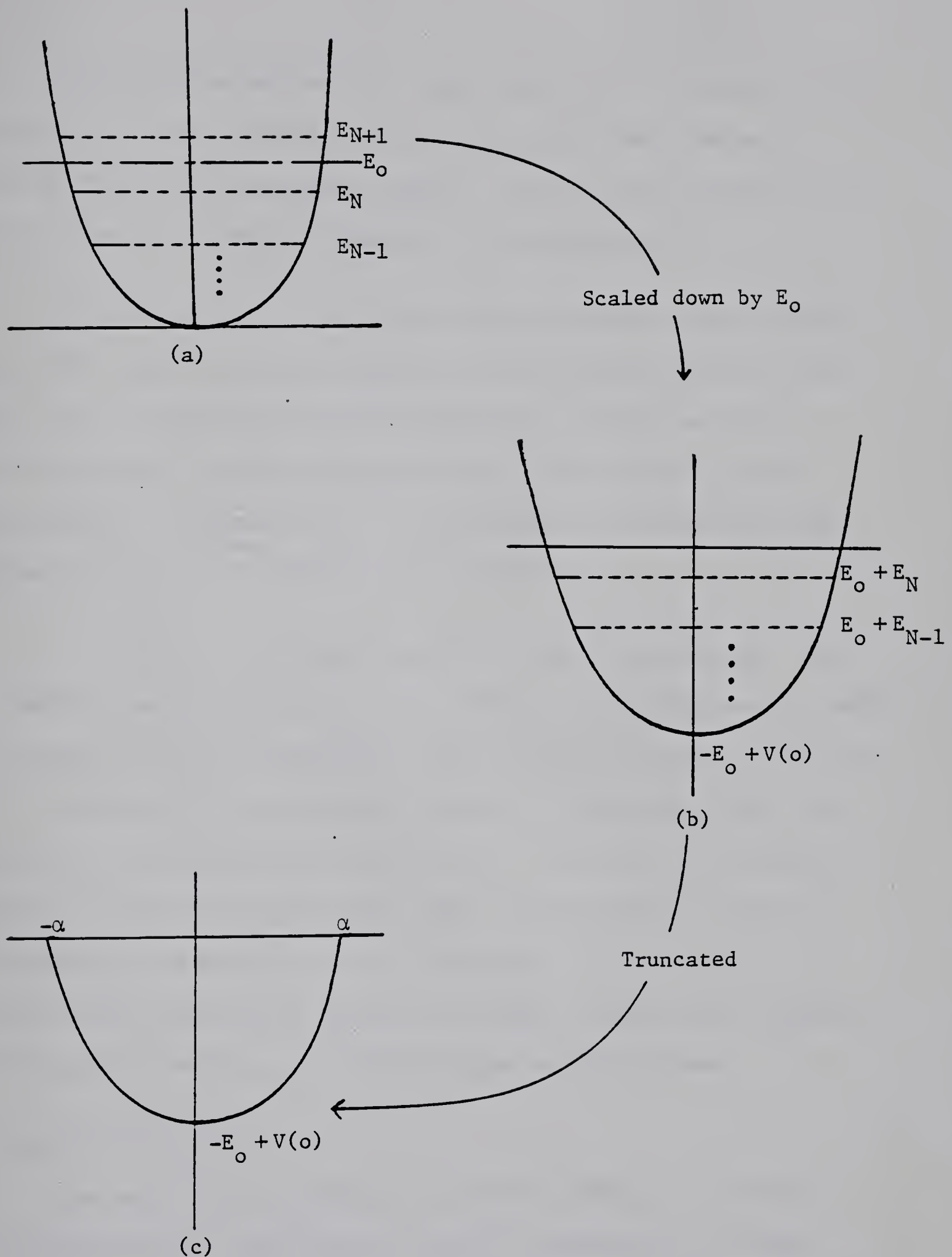
Fig. 3.54.   Scattering counterpart of a confining potential corresponding
to a specific E_o.

In the QRT reconstruction, then, one tries to simulate a potential with the reflectionless potential supporting bound-states at slightly (hopefully!) different energies. What is the contribution of this towards the convergence features of the approximation?

The obvious way to check this is to reconstruct wells of the kind (3.42) with desired V(x) and E_o using the true bound-state energies. We call this the *exact reconstruction*. Now that we have a carefully defined scattering counterpart of the confining potential corresponding to a specific E_o, we can calculate its reflection coefficient and watch its behaviour as E_o increases.

In fact, we have already carried out such a calculation. The non-confining wells in Section 3.1.3 - Section 3.1.6 are precisely wells of the type (3.42) corresponding to the confining potentials in Section 3.2.1 - Section 3.2.4 respectively, precisely in the same order. We have scaled up the results in Section 3.1.3 - Section 3.1.6 by the relevant E_o and then displayed those 'exact reconstructions' with the corresponding 'QRT reconstructions' in Section 3.2.1 - Section 3.2.4. The reflection coefficients for such wells have already been discussed in the previous section. We will make some remarks on them.

The Harmonic Oscillator.

Looking at Figure 3.34(a,c) to Figure 3.38(a,c), we realize that the encouraging convergence of the QRT reconstruction has disappeared in the exact case. The agreement in the exact case is, however, tolerable and does not seem to diverge.

The reflection coefficients in this case have already been seen to get favourable with an increase in E_o.

The Linear Potential.

A comparison between the exact and the QRT reconstruction can be drawn from Figure 3.39(a,c) to Figure 3.43(a,c). The overwhelming convergence of the QRT reconstruction has again gotten subdued in the exact one. However, the exact one shows some explicit tendency towards convergence unlike in the case of the harmonic oscillator.

As we have already seen in Section 3.1.4, the reflection co-efficient in this case behaves more favourably than in the case of the harmonic oscillator.

The Infinite Square Well.

It is interesting to note that the actual scattering counter-parts in this case have not only different eigenvalues but they have an additional bound-state as compared to the numbers assumed in the QRT construction.

Figure 3.44(a,c) – Figure 3.48(a,c) immediately suggest an enhanced diverging trend in the exact reconstructions. The reflection coefficient in this case, with its broad peaks and slow decay, has already been classified as unfavourable.

The Confining Pöschl-Teller Potential.

Figure 3.49(a,c) – Figure 3.53(a,c) confirm that the behaviour in this case is similar to the behaviour in the case of the infinite square well. With its unfavourable reflection coefficient, it shows a

definite divergence from the actual potential. The divergence is much more pronounced in the exact reconstructions.

This numerical exercise suggests that unless the reflection coefficient of the actual scattering counterpart of the confining potential with a specific E_o behaves 'favourably' with an increase in E_o, the convergence of the reflectionless approximation to the confining potential, even in the local sense, is doubtbul. The encouraging convergence observed in the QRT reconstruction seems to be a result of the fact that one uses the scaled confining energies there instead of the exact bound-state energies of the scattering counterpart which one is trying to simulate. This discrepancy leads to a scaling of the upper levels in the N bound-state approximation relative to the lower ones. The reconstruction seems to be quite sensitive to this scaling.

4. DISCUSSION

As proposed in the introduction, the purpose of this thesis was to investigate the reliability of the reflectionless approximation to a symmetric potential in one dimension by applying it to various known potentials of this kind. Our results have confirmed that the reliability of this approximation is highly potential-dependent. This is not unexpected as one is trying to simulate a reflecting potential by a reflectionless one. Our calculations have unfolded some systematics in the behaviour of the reflection coefficient of the actual potential, as a function of momentum (or energy), which indicate an agreement (or a disagreement) between the two.

The question of convergence of the reflectionless approximation to the actual potential is, again, a potential-dependent query. An agreement between the two at a specific point may be highly misleading - it does not necessarily guarantee even a converging trend. What is desired is an 'overall' agreement between the two. The only, obvious, way to obtain this is to solve the Gel'fand-Levitan equation using the reflection and the transmission coefficients of the actual potential and to show that, indeed, the difference between the resulting potential and the reflectionless approximation is small. This is a highly non-trivial job as one needs the detailed analytic structure of the reflection and the transmission coefficients in the complex k-plane.

The problem of convergence of the local, N-bound state approximation to the confining potential, with increasing N, is still more formidable. This approximation to the confining potential is actually

an approximation to a 'scattering counterpart' with a certain depth.
This was brought into light in Chapter 3. The scaled confining-energies
used in the QRT reconstruction are not the eigenvalues of the scatter-
ing counterpart which one is trying to simulate. In fact, they differ
considerably. In some cases even the number of eigenvalues of the
'scattering counterpart' is different from the number of scaled con-
fining-energies - in contrast to the assumption implicit in QRT's
prescription. We observed that the effect of these discrepancies is
quite substantial. So, there are two crucial factors which govern the
convergence in this case: (i) a discrepancy in the number and values
of the scaled confining-energies which are used in the QRT reconstruc-
tion; and (ii) the scattering counterpart is, in general, a reflecting
potential. The eigenvalue dependence of the reflectionless potential
is rather involved and forbids us from making any comment. Our inves-
tigations, however, show that the successive 'local' reflectionless
approximations to the confining potential, as per QRT's prescription,
do not show an 'overall' convergence unless the reflection coefficient
of the scattering counterpart behaves in a 'favourable' way with an
increase in depth.

From a practical point of view, the problem of convergence of
the local N bound-state reflectionless approximation to a confining
potential with an increase in N, is not very demanding. The method
has computational limitations, anyway, for large N. The numbers invol-
ved become too large or too small to command a faith in themselves. The
exact limiting value of N is again dependent on the potenatial. How-
ever, it is enough to realize that there is a practical cut-off to N.

The important practical concerns are, then: (i) Does it show a converging trend or a diverging trend?; (ii) How fast is the convergence or divergence?. If the reflectionless approximation converges very fast or diverges very slowly then the usefulness of this technique is retained. On the other hand, if it converges very slowly or diverges very fast then it is of no real use.

To make a comment on the overall performance of this technique, one needs to recall the kind of job it was supposed to do. We knew very few energy levels of a symmetric potential in one dimension. That was all. From that *bit* of information, this method was supposed to generate the scattering potential for us. Even a mild cynicism towards this technique will accede to the fact that the input information is too meagre to expect a grand result. Within this limitation, the performance of this technique has been satisfactory. For a small number of eigenvalues, which is its actual domain of application, it simulates the rough 'qualitative' features of the potential quite well. Even in the worst cases which we encountered, it showed at least this much promise. Any 'quantitative' expectation from this technique is, perhaps, highly ambitious. This is, indeed, beyond the scope of any such naive technique.

REFERENCES

1. J.J. Aubert et. al.; Phys. Rev. Lett. 33 (1974) 1404.

2. J.E. Augustin et. al.; Phys. Rev. Lett. 33 (1974) 1406.

3. G.S. Abrams et. al.; Phys. Rev. Lett. 34 (1974) 1453.

4. G.H. Trilling; Phys. Rep. 75 (1981) 57.

5. E.D. Bloom and G.J. Feldman; Scientific American 246 (1982) 66.

6. S. Gasiorowicz and J.L. Rosner; Am. J. Phys. 49 (1981) 954.

7. R.F. Schwitters, Scientific American 237 (1977) 56.

8. S.W. Herb,et. al.; Phys. Rev. Lett. 39 (1977) 252.

9. L.M. Lederman; Scientific American 239 (1978) 72.

10. W.R. Innes et. al.; Phys. Rev. Lett. 39 (1977) 1240, 1640 (E).

11. P. Franzini and J. Lee-Franzini; Phys. Rep. 81 (1982) 239.

12. K. Gottfried; Comments Nucl. Part. Phys. 9 (1981) 141.

13. E. Eichten et. al.; Phys. Rev. Lett. 34 (1975) 369.

14. E. Eichten and K. Gottfried; Phys. Lett. 66B (1977) 286.

15. M. Machacek and Y. Tomozawa; Annals of Phys. 110 (1978) 407.

16. J.L. Richardson; Phys. Lett. 82B (1979) 272.

17. G. Bhanot and S. Rudaz; Phys. Lett. 78B (1978) 119.

18. H. Kraseman and S. Ono; Nucl. Phys. B154 (1979) 283.

19. A. Martin; Phys. Lett. 93B (1980) 338.

20. C. Quigg and J.L. Rosner; Phys. Rep. 56C (1979) 167.

21. H. Grosse and A. Martin; Phys. Rep. 60 (1980) 341.

22. T. Sterling; Nucl. Phys. B141 (1978) 272.

23. G. Feldman, T. Fulton and A. Devoto; Nucl. Phys. B154 (1979) 441.

24. A. Martin; Phys. Lett. 67B (1977) 330.

25. H. Grosse; Phys. Lett. 68B (1977) 343.

26. R. Bertlmann, H. Grosse and A. Martin; Phys. Lett. 81B (1979) 59.

27. H. Grosse and A. Martin; Phys. Lett. 79B (1978) 103.

28. A. Martin; Phys. Lett. 70B (1977) 192.

29. H. Grosse and A. Martin; Nucl. Phys. B132 (1978) 125.

30. C.N. Leung and J.L. Rosner; J. Math. Phys. 20 (1979) 1435.

31. J.L. Rosner, C. Quigg and H.B. Thacker; Phys. Lett. 74B (1978) 350.

32. C. Quigg and J.L. Rosner; Phys. Lett. 71B (1977) 153.

33. C. Quigg and J.L. Rosner; Comments Nucl. Part. Phys. 8 (1978) 11.

34. C. Quigg and J.L. Rosner; Phys. Rev. D17 (1978) 2364.

35. C. Quigg and J.L. Rosner; Phys. Lett. 72B (1978) 462.

36. A.L.G. Rees; Proc. Phys. Soc. 59 (1947) 998.

37. W.G. Richards and R.F. Barrow; Proc. Phys. Soc. 83 (1964) 1045.

38. F.J. Zeleznik; J. Chem. Phys. 42 (1965) 2836.

39. W.H. Miller; J. Chem. Phys. 51 (1969) 3631.

40. E.A. Mason and L. Monchick; Adv. Chem. Phys. 12 (1967) 351.

41. W.H. Miller; J. Chem. Phys. 54 (1971) 4174.

42. J.A. Wheeler in Studies in Math. Phys., edited by E.H. Lieb, B. Simon, A.S. Wightman, Princeton University Press, 1976, p. 351.

43. I.I. Goldman and V.D. Krichenkov; Problems in Quantum Mechanics, Addison-Wesley.

44. Problems in Quantum Mechanics, ed. D. ter Haar; Pion Ltd. (1975).

45. H.B. Thacker, C. Quigg and J.L. Rosner; Phys. Rev. D18 (1978) 274.

46. H.B. Thacker, C. Quigg and J.L. Rosner; Phys. Rev. D18 (1978) 287.

47. J.F. Schonfeld, W. Kwong, J.L. Rosner, C. Quigg and H.B. Thacker; Ann. of Phys. 128 (1980) 1.

48. C. Quigg, H.B. Thacker and J.L. Rosner; Phys. Rev. D21 (1980) 234.

49. I. Kay and H.E. Moses; J. App. Phys. 27 (1956) 1503.

50. V.E. Zakharov and A.B. Shabat; Sov. Phys. -JETP 34 (1972) 62.

51. I. Kay and H.E. Moses; Nuovo Cimento 2 (1955) 917.

52. I. Kay and H.E. Moses; Nuovo Cimento 3 (1956) 66.

53. I. Kay and H.E. Moses; Nuovo Cimento 3 (1956) 276.

54. I. Kay and H.E. Moses; Nuovo Cimento Suppl. 5 (1957) 230.

55. L.D. Faddeev; J. Sov. Math. 5 (1976) 334.

56. G.L. Lamb, Jr.; Elements of Soliton Theory, John Wiley & Sons, 1980.

57. J.W. Dettman; Mathematical Methods in Physics & Engineering, McGraw-Hill Book Company Inc., 1962.

58. F.B. Hildebrand; Methods of Applied Maths., Prentice-Hall Inc., 1952.

59. A. Messiah; Quantum Mechanics, vol. I, North-Holland Pub. Co, 1961.

60. I. Kay; Comm. on Pure & App. Math. 13 (1960) 371.

61. S. Flügge; Practical Quantum Mechanics, Springer-Verlag, 1974.

62. M. Abramowitz and I.A. Stegun; Handbook of Mathematical Functions, Dover Pub., New York.

63. Carl-Erik Fröberg; Introduction to Numerical Analysis, Addison-Wesley Pub. Co. Inc., 1965.

64. P.M. Mathews and K. Venkatesan; A Test Book of Quantum Mechanics, Tata-McGraw-Hill Pub. Co. Ltd., 1977.

65. A.K. Ghatak and S. Loknathan; Quantum Mechanics, the Macmillan Co. of India Ltd., 1977.

APPENDIX A. SOME IMPORTANT LEMMAS

Lemma 1. The determinant of the matrix $\left\| \dfrac{1}{\kappa_n + \kappa_\nu} \right\|$ is given by

$$\Delta_N = \det \left\| \frac{1}{\kappa_n + \kappa_\nu} \right\| = \left\{ \prod_{n=1}^{N} \left(\frac{1}{2\kappa_n} \right) \right\} \frac{\prod\limits_{j>1}^{N} (\kappa_1 - \kappa_j)^2 \prod\limits_{j>2}^{N} (\kappa_2 - \kappa_j)^2 \cdots \prod\limits_{j>N-1}^{N} (\kappa_{N-1} - \kappa_j)^2}{\prod\limits_{j>1}^{N} (\kappa_1 + \kappa_j)^2 \prod\limits_{j>2}^{N} (\kappa_2 + \kappa_j)^2 \cdots \prod\limits_{j>N-1}^{N} (\kappa_{N-1} + \kappa_j)^2}$$

with $n = \nu = 1, 2, \ldots, N$.

Proof. Let us define

$$\Delta_p = \det \left\| \frac{1}{\kappa_n + \kappa_\nu} \right\| \qquad ; \quad n = \nu = 1, \ldots, p \quad . \tag{A.1}$$

We will then prove this lemma by induction on p. For $p = 1$,

$$\Delta_1 = \left| \frac{1}{\kappa_1 + \kappa_1} \right| = \frac{1}{2\kappa_1} \quad . \tag{A.2}$$

For $p = 2$,

$$\Delta_2 = \begin{vmatrix} \dfrac{1}{\kappa_1 + \kappa_1} & \dfrac{1}{\kappa_1 + \kappa_2} \\[2mm] \dfrac{1}{\kappa_2 + \kappa_1} & \dfrac{1}{\kappa_2 + \kappa_2} \end{vmatrix} \quad . \tag{A.3}$$

Subtracting the first row from the other

$$\Delta_2 = \frac{(\kappa_1 - \kappa_2)}{(\kappa_1 + \kappa_1)(\kappa_1 + \kappa_2)} \begin{vmatrix} 1 & 1 \\[2mm] \dfrac{1}{\kappa_2 + \kappa_1} & \dfrac{1}{\kappa_2 + \kappa_2} \end{vmatrix} \quad . \tag{A.4}$$

Subtracting the first column from the others

$$\Delta_2 = \left(\frac{1}{2\kappa_1} \right) \left(\frac{1}{2\kappa_2} \right) \frac{(\kappa_1 - \kappa_2)^2}{(\kappa_1 + \kappa_2)^2} = \left\{ \prod_{n=1}^{2} \left(\frac{1}{2\kappa_n} \right) \right\} \frac{\prod\limits_{j>1}^{2} (\kappa_1 - \kappa_j)^2}{\prod\limits_{j>1}^{2} (\kappa_1 + \kappa_j)^2} \quad . \tag{A.5}$$

If we do exactly the same thing for $p = 3$, we get

$$\Delta_3 = \left\{ \prod_{n=1}^{3} \left(\frac{1}{2\kappa_n}\right) \right\} \frac{\prod\limits_{j>1}^{3} (\kappa_1-\kappa_j)^2 \prod\limits_{j>2}^{3} (\kappa_2-\kappa_j)^2}{\prod\limits_{j>1}^{3} (\kappa_1+\kappa_j)^2 \prod\limits_{j>2}^{3} (\kappa_2+\kappa_j)^2} \quad . \tag{A.6}$$

We assume the result for $p = N-1$, i.e.

$$\Delta_{N-1} = \left\{ \prod_{n=1}^{N-1} \left(\frac{1}{2\kappa_n}\right) \right\} \frac{\prod\limits_{j>1}^{N-1} (\kappa_1-\kappa_j)^2 \prod\limits_{j>2}^{N-1} (\kappa_2-\kappa_j)^2 \cdots \prod\limits_{j>N-2}^{N-1} (\kappa_{N-2}-\kappa_j)^2}{\prod\limits_{j>1}^{N-1} (\kappa_1+\kappa_j)^2 \prod\limits_{j>2}^{N-1} (\kappa_2+\kappa_j)^2 \prod\limits_{j>N-2}^{N-1} (\kappa_{N-2}+\kappa_j)^2} \quad . \tag{A.7}$$

Finally, we prove it for $p = N$

$$\Delta_N = \begin{vmatrix} \dfrac{1}{\kappa_1+\kappa_1} & \dfrac{1}{\kappa_1+\kappa_2} & \cdots\cdots & \dfrac{1}{\kappa_1+\kappa_N} \\[2mm] \dfrac{1}{\kappa_2+\kappa_1} & \dfrac{1}{\kappa_2+\kappa_2} & \cdots\cdots & \dfrac{1}{\kappa_2+\kappa_N} \\[2mm] \vdots & \vdots & & \vdots \\[2mm] \dfrac{1}{\kappa_N+\kappa_1} & \dfrac{1}{\kappa_N+\kappa_2} & & \dfrac{1}{\kappa_N+\kappa_N} \end{vmatrix} \quad .$$

Subtracting the first row from all the others, we get

$$\Delta_N = \frac{\prod\limits_{j>1}^{N} (\kappa_1-\kappa_j)}{2\kappa_1 \prod\limits_{j>1}^{N} (\kappa_1+\kappa_j)} \begin{vmatrix} 1 & \cdots & 1 & \cdots & 1 \\[2mm] \dfrac{1}{\kappa_2+\kappa_1} & \cdots & \dfrac{1}{\kappa_2+\kappa_2} & \cdots & \dfrac{1}{\kappa_2+\kappa_N} \\[2mm] \vdots & & \vdots & & \vdots \\[2mm] \dfrac{1}{\kappa_N+\kappa_1} & \cdots & \dfrac{1}{\kappa_N+\kappa_2} & \cdots & \dfrac{1}{\kappa_N+\kappa_N} \end{vmatrix} \quad . \tag{A.8}$$

Subtracting the first column from all the others, we have

$$\Delta_N = \frac{\prod\limits_{j>1}^{N}(\kappa_1-\kappa_j)^2}{2\kappa_1\prod\limits_{j>1}^{N}(\kappa_1+\kappa_j)^2}
\begin{vmatrix}
1 & 0 & \cdots & 0 \\
1 & \dfrac{1}{\kappa_2+\kappa_2} & \cdots & \dfrac{1}{\kappa_2+\kappa_N} \\
\vdots & \vdots & & \vdots \\
1 & \dfrac{1}{\kappa_N+\kappa_2} & \cdots & \dfrac{1}{\kappa_N+\kappa_N}
\end{vmatrix}$$

(A.9)

$$= \frac{\prod\limits_{j>1}^{N}(\kappa_1-\kappa_j)^2}{2\kappa_1\prod\limits_{j>1}^{N}(\kappa_1+\kappa_j)^2}\ \Delta_{N-1}\ (n,\nu = 2,\ldots,N)$$

$$= \left\{\prod\limits_{n=1}^{N}\left(\frac{1}{2\kappa_n}\right)\right\}\ \frac{\prod\limits_{j>1}^{N}(\kappa_1-\kappa_j)^2\ \prod\limits_{j>2}^{N}(\kappa_2-\kappa_j)^2\cdots\prod\limits_{j>N-1}^{N}(\kappa_{N-1}-\kappa_j)^2}{\prod\limits_{j>1}^{N}(\kappa_1+\kappa_j)^2\ \prod\limits_{j>2}^{N}(\kappa_2+\kappa_j)^2\cdots\prod\limits_{j>N-1}^{N}(\kappa_{N-1}+\kappa_j)^2}$$ (A.10)

QED .

Lemma 2. It can be proved that

$$\prod\limits_{\substack{n=m=1\\n\neq m}}^{N}\left|\frac{\kappa_n-\kappa_m}{\kappa_n+\kappa_m}\right| = \frac{\prod\limits_{j>1}^{N}(\kappa_1-\kappa_j)^2\ \prod\limits_{j>2}^{N}(\kappa_2-\kappa_j)^2\cdots\prod\limits_{j>N-1}^{N}(\kappa_{N-1}-\kappa_j)^2}{\prod\limits_{j>1}^{N}(\kappa_1+\kappa_j)^2\ \prod\limits_{j>2}^{N}(\kappa_2+\kappa_j)^2\cdots\prod\limits_{j>N-1}^{N}(\kappa_{N-1}+\kappa_j)^2}$$

Proof. We define

$$\prod\limits_{(p)} \equiv \prod\limits_{\substack{n,m=1\\n\neq m}}^{p}\left|\frac{\kappa_n-\kappa_m}{\kappa_n+\kappa_m}\right|\ .$$ (A.11)

We will then prove this lemma by induction on p. For p = 1, the equality

of the two products in the statement is obvious. For p = 2;

$$\prod_{\substack{n,m=1 \\ n \neq m}}^{2} \left| \frac{\kappa_n - \kappa_m}{\kappa_n + \kappa_m} \right| = \frac{|\kappa_1 - \kappa_2|}{|\kappa_1 + \kappa_2|} \frac{|\kappa_2 - \kappa_1|}{|\kappa_2 + \kappa_1|} = \frac{\prod\limits_{j>1}^{2} (\kappa_1 - \kappa_j)^2}{\prod\limits_{j>1}^{2} (\kappa_1 + \kappa_j)^2} \quad . \tag{A.12}$$

For $p = 3$;

$$\prod_{\substack{n,m=1 \\ n \neq m}}^{3} \left| \frac{\kappa_n - \kappa_m}{\kappa_n + \kappa_m} \right| = \left\{ \frac{|\kappa_1 - \kappa_2|}{|\kappa_1 + \kappa_2|} \cdot \frac{|\kappa_1 - \kappa_3|}{|\kappa_1 + \kappa_3|} \right\} \times \left\{ \frac{|\kappa_2 - \kappa_1|}{|\kappa_2 + \kappa_1|} \cdot \frac{|\kappa_2 - \kappa_3|}{|\kappa_2 + \kappa_3|} \right\}$$

$$\times \left\{ \frac{|\kappa_3 - \kappa_1|}{|\kappa_3 + \kappa_1|} \cdot \frac{|\kappa_3 - \kappa_2|}{|\kappa_3 + \kappa_2|} \right\}$$

$$= \frac{\prod\limits_{j>1}^{3} (\kappa_1 - \kappa_j)^2 \prod\limits_{j>2}^{3} (\kappa_2 - \kappa_j)^2}{\prod\limits_{j>1}^{3} (\kappa_1 + \kappa_j)^2 \prod\limits_{j>2}^{3} (\kappa_2 + \kappa_j)^2} \quad . \tag{A.13}$$

We assume this result for $p = N-1$, i.e.,

$$\prod_{\substack{n,m=1 \\ n \neq m}}^{N-1} \left| \frac{\kappa_n - \kappa_m}{\kappa_n + \kappa_m} \right| = \frac{\prod\limits_{j>1}^{N-1} (\kappa_1 - \kappa_j)^2 \dots \prod\limits_{j>N-2}^{N-1} (\kappa_{N-2} - \kappa_j)^2}{\prod\limits_{j>1}^{N-1} (\kappa_1 + \kappa_j)^2 \dots \prod\limits_{j>N-2}^{N-1} (\kappa_{N-2} + \kappa_j)^2} \quad . \tag{A.14}$$

Finally, we prove it for $p = N$

$$\prod_{\substack{n,m=1 \\ n \neq m}}^{N} \left| \frac{\kappa_n - \kappa_m}{\kappa_n + \kappa_m} \right| = \left\{ \prod_{\substack{n,m=1 \\ n \neq m}}^{N-1} \left| \frac{\kappa_n - \kappa_m}{\kappa_n + \kappa_m} \right| \right\}$$

$$\times \frac{|\kappa_1 - \kappa_N|}{|\kappa_1 + \kappa_N|} \frac{|\kappa_2 - \kappa_N|}{|\kappa_2 + \kappa_N|} \dots \frac{|\kappa_{N-1} - \kappa_N|}{|\kappa_{N-1} + \kappa_N|}$$

$$\times \frac{|\kappa_N - \kappa_1|}{|\kappa_N + \kappa_1|} \frac{|\kappa_N - \kappa_2|}{|\kappa_N + \kappa_2|} \dots \frac{|\kappa_N - \kappa_{N-1}|}{|\kappa_N + \kappa_{N-1}|}$$

$$= \left\{ \prod_{\substack{n,m=1 \\ n \neq m}}^{N-1} \left| \frac{\kappa_n - \kappa_m}{\kappa_n + \kappa_m} \right| \right\} \frac{(\kappa_1 - \kappa_N)^2}{(\kappa_1 + \kappa_N)^2} \dots \frac{(\kappa_{N-1} - \kappa_N)^2}{(\kappa_{N-1} + \kappa_N)^2}$$

$$= \frac{\prod\limits_{j>1}^{N} (\kappa_1 - \kappa_j)^2 \prod\limits_{j>2}^{N} (\kappa_2 - \kappa_j)^2 \cdots \prod\limits_{j>N-2}^{N} (\kappa_{N-2} - \kappa_j)^2 \prod\limits_{j>N-1}^{N} (\kappa_{N-1} - \kappa_j)^2}{\prod\limits_{j>1}^{N} (\kappa_1 + \kappa_j)^2 \prod\limits_{j>2}^{N} (\kappa_2 + \kappa_j)^2 \cdots \prod\limits_{j>N-2}^{N} (\kappa_{N-2} + \kappa_j)^2 \prod\limits_{j>N-1}^{N} (\kappa_{N-1} + \kappa_j)^2}$$

$$\text{QED} \quad . \tag{A.15}$$

APPENDIX B.   NUMERICAL METHODS FOR CALCULATING THE REFLECTION COEFFICIENT

   AND THE EIGENVALUES OF A SYMMETRIC POTENTIAL IN ONE DIMENSION.

Eigenvalues

Two methods were used to numerically calculate the eigenvalues. The first one is fairly general and does not need the specific assumption of symmetry of the potential. We discuss that first

(i) The Matrix Method: The Schrödinger equation for a potential $V(x)$ in one dimension is

$$\frac{d^2\psi}{dx^2} - V\psi = -E\psi \qquad\qquad ; \; -\infty < x < \infty \qquad\qquad (B.1)$$

where E is the energy of the particle. We have to find those solutions which satisfy the boundary conditions

$$\psi(+\infty) = \psi(-\infty) = 0 \quad . \qquad\qquad (B.2)$$

For numerical computations we need to consider a finite interval $a \leq x \leq b$. We assume the boundary conditions to be $\psi(a) = \psi(b) = 0$. Physically, this means that we are putting infinite impenetrable walls at $x = a$ and $x = b$. We divide this interval $a \leq x \leq b$ into $(n+1)$ fine intervals of width 'h', i.e.

$$h = \frac{b-a}{n+1} \qquad\qquad (B.3)$$

where

$$a + (n+1)h = b \quad . \qquad\qquad (B.4)$$

If we replace the Schrödinger equation (B.1) by its corresponding difference equation, we get

$$\frac{\psi_{r-1} - 2\psi_r + \psi_{r+1}}{h^2} - V_r\psi_r = -E\psi_r \quad . \tag{B.5}$$

Using the boundary conditions at $x = a$ and $x = b$, we get the following

set of equations from (B.5)

$$\begin{bmatrix} \left(\frac{2}{h^2}+V_1\right) & -\left(\frac{1}{h^2}\right) & & & 0 \\ -\left(\frac{1}{h^2}\right) & \left(\frac{2}{h^2}+V_2\right) & -\left(\frac{1}{h^2}\right) & & \\ & & \ddots & \ddots & \ddots & -\left(\frac{1}{h^2}\right) \\ & 0 & & & -\left(\frac{1}{h^2}\right) & \left(\frac{2}{h^2}+V_n\right) \end{bmatrix} \begin{bmatrix} \psi_1 \\ \psi_2 \\ \vdots \\ \psi_n \end{bmatrix} = E \begin{bmatrix} \psi_1 \\ \psi_2 \\ \vdots \\ \psi_n \end{bmatrix} \tag{B.6}$$

where we have multiplied throughout by a minus sign. So, the eigen-

value problem for the Schrödinger equation is now reduced to this

algebraic eigenvalue problem for the tridiagonal matrix in eqn. (B.6).

The lowest negative eigenvalues give us the required bound-state

energies for the Schrödinger equation. These were calculated using

the EQRT1S subroutine from the IMSL Fortran Library.

In practice, the computation goes in two steps. First, one

picks up a particular pair 'a' & 'b' and repeats the calculation of

the eigenvalues by increasing the number of intervals (n + 1) till one

gets a value stabilized to a desired accuracy. Then one increases 'a'

and 'b' and repeats the same procedure. When the stabilized values

for two consecutive 'a' & 'b' agree within a desired tolerance, one

stops.

The advantages of this technique are its simplicity and the

fact that it can be used for any kind of potential. However, the process of stabilizing the eigenvalue, even to a few places, is very tedious. It serves as a method to quickly locate the positions of all the levels at the same time.

(ii) Solving the Eigenvalue Equation for a Symmetric Potential Numerically: Let us consider a symmetric potential of the form

$$V(x) = \begin{cases} 0 & ; \; x \leq -\alpha & \text{(Region I)} \\ V(x) & ; \; -\alpha \leq x \leq \alpha & \text{(Region II)} \\ 0 & ; \; x \geq \alpha & \text{(Region III)} \end{cases} \tag{B.7}$$

and $V(x) = V(-x)$. Also, it is obvious that $V(\pm\alpha) = 0$. We can, then, immediately write down the solutions of the Schrödinger equation, ψ_I, ψ_{II} and ψ_{III}, in region I, II and III, respectively (for $E < 0$):

$$\psi_I = Ae^{kx}$$

$$\psi_{II} = B\psi_e + C\psi_o$$

$$\psi_{III} = De^{-kx} \tag{B.8}$$

where

$$|E| = k^2 \quad . \tag{B.9}$$

Since the potential is symmetric in Region II, the two linearly independent solutions in this region are the odd (ψ_o) and even (ψ_e) solutions. If we now impose the continuity conditions at $x = \pm\alpha$ and use the symmetry properties of ψ_e and ψ_o, we immediately get that the even eigenvalues are the solutions of the equation

$$\psi_e'(x = +\alpha) + k\psi_e(x = +\alpha) = 0 \tag{B.10}$$

and the odd eigenvalues are the solutions of the equation

$$\psi_o'(x = +\alpha) + k\psi_o(x = +\alpha) = 0 \quad . \tag{B.11}$$

These two equations were solved numerically to find out the values of the bound-state energies. Values of ψ_e, ψ_o, ψ_e' and ψ_o' at $x = +\alpha$ were needed in this process. They were calculated using the DVERK subroutine from the IMSL Fortran Library with the obvious conditions

$$\psi_e'(0) = 0$$
$$\psi_o(0) = 0 \quad . \tag{B.12}$$

This subroutine uses the Runge-Kutta method to do this job.

This technique is much more accurate and convenient. <u>Note</u>: For potentials with infinite tails like the Gaussian, the same method was used. Some value of α was assumed to start with. Then it was gradually increased and the calculations were repeated each time. One stopped when two consecutive calculations for the eigenvalues agreed within a desired accuracy.

Reflection Coefficient

We concentrate on a well of the type (B.7). We are now concerned with the continuum solutions $(E = k^2) > 0$. Solutions in the three classified regions are

$$\psi_I = A_+ e^{ikx} + A_- e^{-ikx}$$

$$\psi_{II} = B_+ \psi_e(x) + B_- \psi_o(x)$$

$$\psi_{III} = C_+ e^{ikx} \quad . \tag{B.13}$$

The other solution e^{-ikx} in ψ_{III} is absent because there is no incoming wave in region III. $\psi_e(x)$ and $\psi_o(x)$ are again the even and odd solutions for $E > 0$ in region II. Imposing the continuity conditions at $x = \pm\alpha$ and using the symmetry properties of the solutions $\psi_e(x)$ and $\psi_o(x)$ one immediately gets the reflection coefficient

$$R = \left|\frac{A_-}{A_+}\right|^2 = \frac{\left(\dfrac{\psi_e'(x=+\alpha)\psi_o'(x=+\alpha)}{k} + k\psi_e(x=+\alpha)\psi_o(x=+\alpha)\right)^2}{W^2 + \left(\dfrac{\psi_e'(x=+\alpha)\psi_o'(x=+\alpha)}{k} + k\psi_e(x=+\alpha)\psi_o(x=+\alpha)\right)^2} \quad (B.14)$$

where W is the Wronskian

$$W = \psi_o(x)\psi_e'(x) - \psi_e(x)\psi_o'(x) \quad . \tag{B.15}$$

The Wronskian can be easily evaluated at $x = 0$. For a numerical calculation of R as a function of momentum k, one needs the values of ψ_e, ψ_e', ψ_o, ψ_o' at $x = +\alpha$. These were again calculated using the DVERK subroutine which uses the Runge–Kutta method.

Note: For potentials with infinite tails, one starts with an assumed value for α. It is then gradually increased and the calculations are repeated. Once the value of R stabilizes to a certain desired accuracy one stops.